



**Ernest Orlando Lawrence**  
**Berkeley National Laboratory**  
1 Cyclotron Road, 70R0108B  
Berkeley CA 94720-8168  
(510) 495-2679; fax: (510) 486-4260

Environmental Energy Technologies Division

August 21, 2014

Mr. Tien Q. Duong  
3V/Forrestal Building  
Office of Vehicle Technologies  
U.S. Department of Energy  
1000 Independence Avenue, S.W.  
Washington D.C. 20585

Dear Tien,

Here is the third quarter FY 2014 report for the Batteries for Advanced Transportation Technologies (BATT) Program. This report and prior Program reports can be downloaded from <http://batt.lbl.gov/reports/quarterly-reports/>.

Sincerely,

A handwritten signature in black ink, appearing to be "Venkat Srinivasan", written over a light blue horizontal line.

Venkat Srinivasan  
Acting Head  
BATT Program

edited by: V. Battaglia  
M. Fouré  
S. Lauer  
M. Minamihara

cc: J. Barnes                   DOE/OVT  
P. Davis                   DOE/OVT  
D. Howell                  DOE/OVT  
P. Smith                   DOE/OVT  
J. Muhlestein              DOE-BSO

## Featured Highlights

### ***Electrolytes –***

- ✦ Strand (Wildcat Discovery Technologies) discovered a class of additives for EC-based electrolytes and another for PC-based electrolytes for reducing the first cycle irreversible capacity loss of Si anodes.

### ***Cathodes -***

- ✦ Looney and Wang (BNL) have synthesized a  $\text{CuVO}_3$  with a reversible capacity greater than 300 mAh/g.

### ***Diagnostics -***

- ✦ Meng (UCSD) showed preliminary data indicating that a lithium lanthanum titanium oxide (LLTO) coating on a Mn-rich material results in a lower first cycle irreversible capacity.
- ✦ Somorjai and Ross (LBNL) found that VC forms a different SEI decomposition component upon reduction than FEC and EC which form a similar product on lithiated Si.

### ***Modeling -***

- ✦ Srinivasan (LBNL) provided preliminary evidence that the local polarization across the low surface area single-ion conductor/electrolyte interface may be of the same order of magnitude as that of lithiation into high surface area layered cathode materials.

### Electrode Failure Benchmarking Analysis

**PROJECT OBJECTIVE:** This project is to support the BATT Focus Groups. The emphasis of this work will be on the High-Voltage Cathode Project and the Si Anode Project. If the difference in cycleability of NMO and NCM can be understood through identification of a difference in reaction products, then perhaps the cycleability of NCM at higher voltages can be improved. If differences between the side reactions on graphite and Si can be measured, then perhaps the Si surface can be modified to allow for long-term full cell cycleability comparable to that of cells containing graphite.

**PROJECT IMPACT:** Success with understanding and improving the stability of NCM in the presence of electrolyte at voltages greater than 4.3 V vs. Li/Li<sup>+</sup> will translate to an increase in capacity and voltage and hence a compounding improvement in energy density. Improvement in the passivating effects of SEI on Si that allows for long term cycleability, would result in larger fractions of Si in the anode and improved energy density of high-capacity cathode cells.

**OUT-YEAR GOALS:** The goal of this project is to support the High-Voltage Focus Group, which is to understand the limits of cycleability of NCM as the voltage is increased. This project will provide electrochemical and chemical data to support that effort. The other goal of the project is to support the Si Anode Focus Group, which is to effectively use Si in a battery. This project will provide electrochemical and chemical data to support that effort.

**COLLABORATIONS:** None this quarter.

#### Milestones

- 1) Make a pouch cell with the same cycling behavior as a coin cell. (Dec. 13) **Complete.**
- 2) **Go/No-Go:** Generate measurable levels of soluble reaction products. **Criteria:** Evaluate one of the proposed experimental test set-ups for its ability to generate measurable levels of soluble reaction products. (Mar. 14) **Go**
- 3) Demonstrate a 3-electrode cell where the impedance data of the individual electrodes can be directly assigned to the full cell data. (Jun. 14) **Complete**
- 4) Measure the gas composition of a high-voltage cell. (Sep. 14) **Ongoing**
- 5) Measure the gas composition of a Si-anode cell. (Sep. 14) **Ongoing**

## Progress Report

### Demonstrate a 3-electrode cell where the impedance data of the individual electrodes can be directly assigned to the full cell data.

This quarter the analysis of the 3-electrode cell was completed, which involved a combination of modeling, 3-electrode cell data, and 2-electrode cell data. The problem with 3-electrode cells is with the placement of the electrodes: the reference electrode is placed either within the cell sandwich between electrodes, where it inherently disrupts the current distribution in the cell, or outside the cell, but in close proximity to the edge of the cell. The problem with this second configuration is that it is nearly impossible to align the two working electrodes within the thickness of that of the separator, *ca.* 25  $\mu\text{m}$ , and any misalignment of the electrodes results in a non-symmetric current distribution. This leads to ac impedance data that is not straight forward to interpret.

Through modeling, it was determined that the overlap of one working electrode over the other will distort the response of each electrode to a reference that is in the area where the current distribution is not symmetric. When using the reference to acquire impedance data from each electrode, the sum of the impedance data is equivalent to that recorded for the two electrode cell. However, the response recorded for one electrode will show impedance data that is greater than expected of the electrode alone plus contributions from the opposite electrode; this is the dominant electrode. Contrary to that, the impedance of the opposite electrode will be less than expected from that electrode, plus negative “inductance loop” contributions. All of this was verified with symmetric cells and a modeling effort that examined the impedance data for two misaligned electrodes considering only the secondary current distribution between them.

Figure 1 shows the impedance data of a full cell of Graphite/Ni-spinel. Through analysis of the 3-electrode impedance data, the 2-electrode data could be divided into 7 individual contributions, each with its own frequency. The analysis allowed for identification of three sources of impedance for each electrode plus a shared diffusion component attributed to salt transport in the electrolyte. These contributions were not obvious from the 3-electrode data since some of the signal from one electrode was found in the data of the other. Through the modeling, each contribution could be confidently assigned. In the end, one could show that even though the majority of the impedance appeared to be on the cathode side of the cell (the dominant electrode), it was the high frequency impedance in the anode that changed the most with cycling and this impedance was associated with the formation of a thin film due to the high frequency nature of the source.

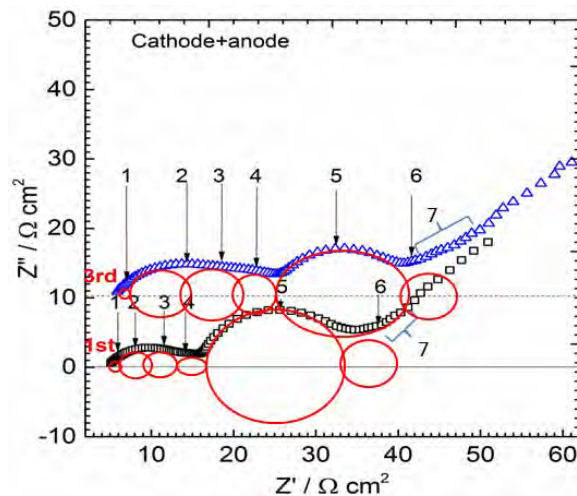


**Figure 1.** 2-electrode impedance data, divided into 7 contributions each of which be assigned to either the cathode or anode based on the reference electrode data and an understanding of the data acquired through a modeling effort.

### Assembly of Battery Materials and Electrodes

**PROJECT OBJECTIVE:** To develop high-capacity, low-cost electrodes with good cycle stability and rate capability to replace graphite in Li-ion batteries. The *in situ* analyses of Si based electrodes showed that the bigger particles (*ca.* 13  $\mu\text{m}$ ) start to crack at around 0.1 V. During the charging process, all of the major cracks remained, while some fissures collapsed and others expanded, but the smaller particles ( $< 2 \mu\text{m}$ ) did not crack. Furthermore, the *in situ* study revealed that delamination occurred at the interfaces of the particle/binder and the Cu current collector/electrode. These experiments provided a better understanding of the anode cycling mechanism and the failure mode associated with capacity fade. The results will be helpful to redesign the anode architecture. This study will also be beneficial to design the architecture of the high-voltage cathode (LMNO).

**PROJECT IMPACT:** This project will have a major impact on the wide spread adoption of EVs by (i) demonstrating scale-up production of nano-Si powders (to kilogram levels) for advanced EV batteries, and (ii) improving electrode performance by the understanding gained from *in situ* SEM and TEM studies. The success of the project will contribute to the advancement of EV battery technology by developing batteries with increased energy density and improved cycle life, leading to EVs with longer driving range.

**OUT-YEAR GOALS:** Complete the *in situ* SEM and TEM studies of the Si-anode material during electrochemical cycling and real-time monitoring of structure changes. These analyses will help to understand the failure mode and to guide further improvements in the electrode architecture. These studies will also help to investigate the high-voltage passivation layer to identify the appropriate electrolyte and electrode compositions. The results of this effort will help to identify an alternative supplier of Si powder material as a baseline for the BATT Program. As a final goal, the optimized Si-anode and LiMnNiO-doped Cr cathode will be evaluated in a laminate 20 Ah Li-ion cell.

**COLLABORATIONS:** Vince Battaglia and Gao Liu (LBNL) and John Goodenough (UT Austin).

#### Milestones

- 1) Identify Si-based anode materials that can achieve a capacity of 1200 mAh/g. (Dec. 13) **Complete**
- 2) Supply Si powder (1 Kg) from an alternative supplier as a baseline material for BATT PIs. (Mar. 14) **Complete**
- 3) Go/No-Go: Terminate production of Si powder in anode tests that show more than 20% capacity fade in the initial 100 cycles. Criteria: Supply laminated Si-based electrodes to BATT PIs. (Jun. 14) **Complete**
- 4) Supply a 20-Ah Li-ion flat cell based on Si and LiMNO materials to BATT PIs. (Sep. 14) **Ongoing.**

## Progress Report

This quarter, *in situ* measurements were conducted using impedance spectroscopy in order to improve the understanding of the failure mode of Si anodes. This technique is non-destructive and useful to study the electrochemical behaviour of electrode materials and their interfacial properties, such as resistance and capacitance as a result of SEI film formation. Electrodes made from an optimum composition (Si: Alginate: carbon; 50:25:25) by weight were characterized. The first discharge/charge cycle was conducted at a low rate (C/24) between cut off voltages of 10 mV on discharge and 1.0 V on charge with EC-DEC-1M LiPF<sub>6</sub>+2% VC as the electrolyte. The impedance measurement was monitored continuously on discharge and charge at C/24 based on the theoretical capacity (Fig. 1). The impedance was measured after each 10% state of discharge (SOD) and charge (SOC).

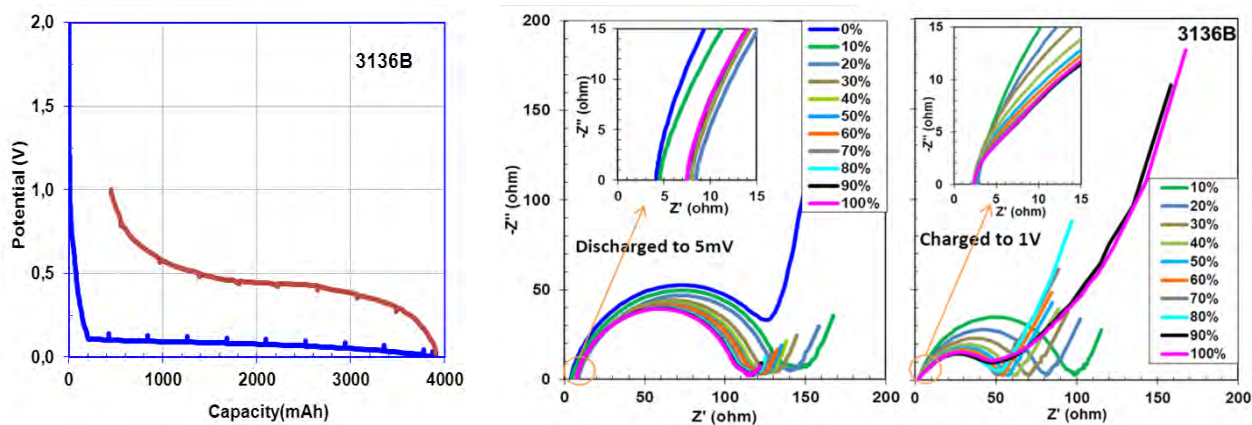


**Figure 1.** 1<sup>st</sup> discharge/charge curves at C/24 of Li/EC-DEC-LiPF<sub>6</sub>/Si cells with positions indicated where the impedance measurements were taken.

**Figure 2.** Impedance spectra of Li/EC-DEC-LiPF<sub>6</sub>/Si at different states of discharge and charge.

Figure 2 shows typical impedance spectra with semicircles and a tail from 0% to 100% SOD and 10 to 100% SOC, which implies a combination of charge transfer and diffusion processes. It was observed that the internal resistance ( $R_{int}$ ) on the discharge curve showed a small increase from 4.1  $\Omega$  before cycling to 4.5  $\Omega$  at 10% SOD, which is associated with SEI layer formation. However, this resistance doubled to 8.4  $\Omega$  at 20% SOD, then relaxed to 7.5  $\Omega$  at 100% SOD. This behavior is probably related to the volume expansion of the lithiated state. This result indicates that the major volume change occurred after 20% of lithiation, which corresponds to *ca.* 100 mV on the discharge plateaus. The charge transfer resistance ( $R_{tc}$ ) decreased with increased lithiation from 146  $\Omega$  to 103  $\Omega$ , a sign of surface changes on the Si particles, such as break down of the thin resistive Si-O layer and an enhanced surface area due to volume expansion of the Si particles. This process is associated with an increased ionic conductivity and lower charge transfer resistance. On the other hand, when the cell was charged (delithiated), the  $R_{int}$  was reduced continuously to 2.7  $\Omega$  and 2.6  $\Omega$  for 10 and 20% SOC, respectively, then to 2.2  $\Omega$  at 30% SOC and remained almost unchanged at SOC >30%. This decrease in  $R_{int}$  is probably related to the volume contraction of the delithiated Si particles after volume expansion during lithiation and thus particles are closer together. The biggest change occurs during the first 30% of SOC. The  $R_{tc}$  continues to decrease from 98  $\Omega$  to 48  $\Omega$  when the Si anode is delithiated at 10% and 80%, respectively. This study demonstrates that cycling at lower depth of discharge is less stressful to the electrode.

HQ supplied 10 m of Si laminated anode film, 1 kg of metallurgical Si particles, and LFP laminated film and LFP powder to LBNL (G. Liu); 900 g of Si nano powder to PNNL (C. Wang); and LFP laminated film and LFP powder to the University of Texas (J. Goodenough).

### Design and Scalable Assembly of High Density Low Tortuosity Electrodes

**PROJECT OBJECTIVE:** Develop a scalable high density binder-free low-tortuosity electrode design and fabrication process to enable increased cell-level energy density compared to conventional Li-ion technology. Characterize and optimize the electronic and ionic transport properties of controlled porosity and tortuosity electrodes as well as densely-sintered reference materials in Li(Ni,Co,Al)O<sub>2</sub>(NCA), high capacity Li<sub>2</sub>MnO<sub>3</sub>-LiMO<sub>2</sub> and high voltage LiM<sub>1-x</sub>Mn<sub>2-x</sub>O<sub>4</sub> and LiM<sub>1-x</sub>Mn<sub>2-x</sub>O<sub>4-y</sub>F<sub>y</sub> spinels in order to elucidate rate limiting steps.

**PROJECT IMPACT:** The high cost (\$/kWh) and low energy density of current automotive Li-ion technology is in part due to the need for thin electrodes and associated high inactive materials content. If successful this project will enable use of electrodes based on known families of cathode and anode actives but with at least 3 times the areal capacity (mAh/cm<sup>2</sup>) of current technology while satisfying the duty cycles of vehicle applications. This will be accomplished via new electrode architectures fabricated by scalable methods with higher active materials density and reduced inactive content, and will in turn enable higher energy density and lower-cost EV cells and packs.

**OUT-YEAR GOALS:** After downselection of cathodes, identify an anode approach that therefore allows full cells in which both electrodes have high area capacity under EV operating conditions. Anode approach will include identifying compounds amenable to same fabrication approach as cathode, or use of very high capacity anodes such as stabilized Li or Si-alloys that in conventional form can capacity-match the cathodes. Use data from best performing electrochemical couple in techno-economic modeling of EV cell and pack performance parameters.

**COLLABORATIONS:** Within BATT, this project collaborates with Antoni P. Tomsia (LBNL) in fabrication of low-tortuosity, high-density electrodes by directional freeze-casting and sintering, and with Gao Liu (LBNL) in the Si Anode Focus Group on acoustic emission-based characterization of electrochemically-induced microfracture of Si anodes. Outside of BATT, the project collaborates with Randall Erb (Northeastern U.) on magnetic-alignment based fabrication of low tortuosity electrodes.

#### Milestones

- 1) Measure electronic and ionic conductivities and diffusivity in sintered dense Li(Ni,Co,Al)O<sub>2</sub> (NCA) and Fe-doped high voltage spinel Li<sub>1-x</sub>Mn<sub>1.5</sub>Ni<sub>0.5</sub>O<sub>4</sub> spinel. Fabricate first freeze-cast samples of at least one cathode composition (Dec. 13) **Complete**
- 2) Go/No-Go: Downselect one cathode composition for follow-on work. Criteria: Based on transport measurements and cycling tests of freeze cast and sintered electrodes. (Mar. 14) **Go for downselecting one cathode composition for follow-on work**
- 3) Demonstrate at least 5 mAh/cm<sup>2</sup> capacity per unit area at 1C continuous cycling rate for a freeze-cast cathode (Jun. 14) **Complete**
- 4) Demonstrate at least 10 mAh/cm<sup>2</sup> capacity per unit area for a 2C 30 sec pulse for a freeze-cast cathode. (Sep. 14) **Ongoing**

## Progress Report

During the present reporting period, progress was made in understanding and controlling microstructures developed during freeze-casting of  $\text{LiNi}_{0.8}\text{Co}_{0.15}\text{Al}_{0.05}\text{O}_2$  (NCA) electrodes of aligned porosity and high area specific capacity ( $\text{mAh}/\text{cm}^2$ ), and measurement of electrochemical performance of the same. Figure 1 illustrates results showing the impact of one process parameter amongst several, the freeze-casting cooling rate, on the lamellae thickness of final sintered electrodes. As expected for a directional solidification process, the lamellae thickness (*i.e.*, the thickness of the dense electrode regions) increases as the cooling rate decreases. Furthermore, the microporosity of the lamellae is a function of sintering time and temperature. Thus the dual-scale porosity of the electrodes, defined by the separation between lamellae and the porosity within lamellae, respectively, can be independently adjusted.

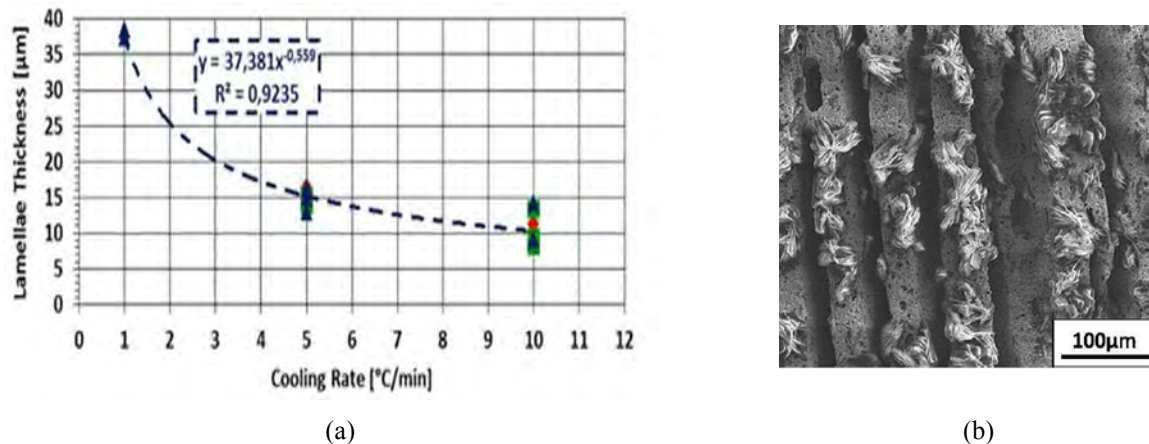


**Figure 1.** (a) Dependence of lamellae thickness on cooling rate in the freeze casting process, and (b) SEM micrograph of freeze-casted sintered NCA.

The resulting sintered electrodes were electrochemically tested in Li half-cells of the Swagelok type. The electrodes had the solidification direction oriented normal to the electrode plane, and were electrically connected to the stainless steel current collectors using a carbon paste. For continuous discharge at relatively low C-rates (C/5-C/10), the area capacity realized exceeded  $12 \text{ mAh}/\text{cm}^2$ , which is about four times higher than current Li-ion electrodes. At a 1C rate, over  $5 \text{ mAh}/\text{cm}^2$  is obtained, meeting the milestone for this quarter.

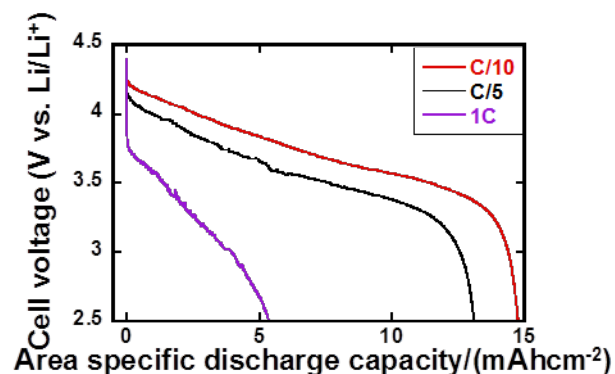


**Figure 2.** Voltage vs. capacity of directionally-solidified and sintered NCA electrode of  $330 \text{ μm}$  thickness, with capacity plotted as area capacity ( $\text{mAh}/\text{cm}^2$ ).

### Hierarchical Assembly of Inorganic/Organic Hybrid Si Negative Electrodes

**PROJECT OBJECTIVE:** This proposed work aims to enable Si as a high-capacity and long cycle-life material for negative electrode to address two of the barriers of Li-ion chemistry for EV/PHEV application: insufficient energy density and poor cycle life performance. The proposed work will combine material synthesis and composite particle formation with electrode design and engineering to develop high-capacity, long-life, and low cost hierarchical Si-based electrode. State of the art Li-ion negative electrodes employ graphitic active materials with theoretical capacities of 372 mAh/g. Silicon, a naturally abundant material, possesses the highest capacity of all Li-ion anode materials. It has a theoretical capacity of 4200 mAh/g for full lithiation to the  $\text{Li}_{12}\text{Si}_5$  phase. However, Si volume change disrupts the integrity of electrode and induces excessive side reactions, leading to fast capacity fade.

**PROJECT IMPACT:** This work addresses the adverse effects of Si volume change and minimizes the side reactions to significantly improve capacity and lifetime to develop negative electrode with Li-ion storage capacity over 2000 mAh/g (electrode level capacity) and significantly improve the coulombic efficiency to over 99.9%. The research and development activity will provide an in-depth understanding of the challenges associated with assembling large volume change materials into electrodes and will develop a practical hierarchical assembly approach to enable Si materials as negative electrodes in Li-ion batteries.

**OUT-YEAR GOALS:** There are three aspects of this proposed work - bulk assembly, surface stabilization and Li enrichment, which are formulated into 10 tasks in a four-year period. 1) Develop hierarchical electrode structure to maintain electrode mechanical stability and electrical conductivity. (Bulk assembly). 2) Form *in situ* compliant coating on Si and electrode surface to minimize Si surface reaction (surface stabilization). 3) Use prelithiation to compensate first cycle loss of the Si electrode. (Li enrichment) In the end of the 4th year, the goal is to achieve a Si based electrode at higher mass loading of Si, and can be extensively cycled cycles with minimum capacity loss at high coulombic efficiency to qualified for vehicle application.

**COLLABORATIONS:** Vince Battaglia and Venkat Srinivasan (LBNL), Xingcheng Xiao (GM), Jason Zhang (PNNL), Chongming Wang (PNNL), Yi Cui (Stanford), and the BATT Si-Anode Focus Group.

#### Milestones

- 1) Design and synthesize 3 more PEFM polymers with different EO content to study the adhesion and swelling properties of binder to the Si electrode performance. (Dec. 13) **Complete**
- 2) Go/No-Go: Down select Si vs. Si alloy particles and particle sizes (nano vs. micro.) Criteria: Down select based on cycling results. (Mar-14) **Complete**
- 3) Prepare one type of Si/conductive polymer composite particles and test its electrochemical performance. (Jun-14) **Complete**
- 4) Design and synthesize one type of vinylene carbonate (VC) derivative that is targeted to protect Si surface and test it with Si-based electrode. (Sep-14) **Ongoing**

## Progress Report

Mechanical failure at electrode interfaces (laminate/current collector and binder/particle) that leads to delamination and particle isolation has been regarded as one of the main reasons for the capacity decay and cell failure of Li-ion batteries (LIBs). The polymer binder is known to provide the key function for good interface properties and helps maintain the electrode integrity in LIBs. Incorporation of triethyleneoxide monomethylether (PTEGMA) moieties in the polymer is meant to increase both the interface adhesion and the ductility to better alleviate stress-induced fracture. To unveil the role of the polymer binders in the inhibition of electrode interface failure, a rigid binder, PMAA, was chemically modified to improve the flexibility of the binder and the resulting electrode laminate. Below, graphite electrodes assembled using the modified flexible binder inhibited the generation of cracking, leading to a higher specific capacity and higher cycling stability.

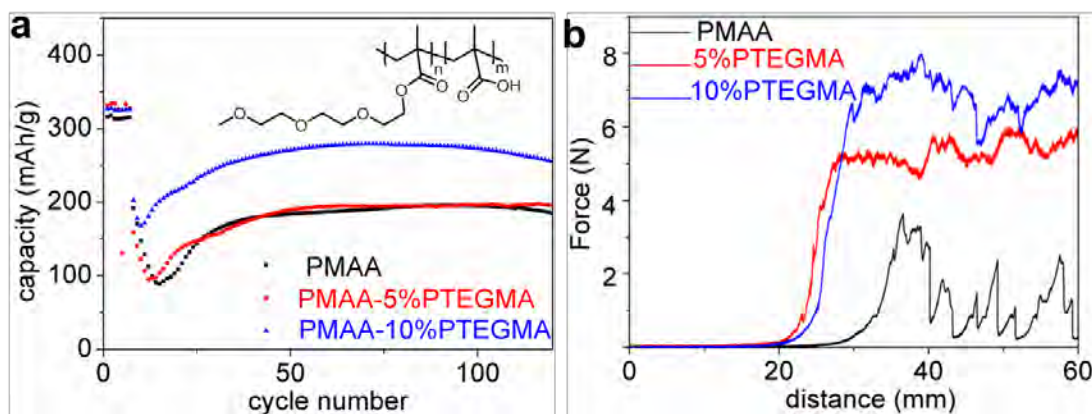


**Figure 1.** (a) Cycling performance of graphite half cells with different binders, C/25 for 2 cycles, C/10 for 5 cycles and then 1C, with the PMAA-based polymer structure embedded. (b) Peel test results of the graphite electrodes using PMAA-based binders.

The cycling performance of different PMAA-based binders is shown in Fig. 1a. A TEG structural moiety incorporated into the binder shows an advantage during slow cycling. Both 5% and 10% TEG content binders enable a higher specific capacity compared to the unmodified PMAA-binder based electrode. The cell acquires a reversible capacity of *ca.* 320 mAh/g in the formation cycles with PMAA; the addition of TEG resulted in an enhanced capacity to *ca.* 335 mAh/g. When the cycling rate was increased to 1C, 5% TEG content seems not to improve cell performance: both the PMAA and the PMAA-5%PTEGMA show similar cycling performance, with a reversible capacity of *ca.* 190 mAh/g. The PMAA-10%PTEGMA, on the other hand, enables a stable cycling of 270 mAh/g at 1C. The improved flexibility of the polymer and the enhanced adhesion strength is confirmed by the peel test, shown in Fig. 1b. A small maximum peel-off force (*ca.* 2 N) was shown initially for the PMAA-based electrodes, as the test proceeded this value fluctuated until electrode failure. A more compliant polymer binder should significantly strengthen the mechanical binding force and enhance the particle/particle cohesion strength. The peel-off force for the enhanced binders reached higher values (*ca.* 5 N for PMAA-5%PTEGMA and *ca.* 7 N for PMAA-10%PTEGMA), confirming the high cohesion strength. Introduction of the TEG structural moiety successfully enhanced the adhesion force, and this enhancement increased with the addition of TEG.

### Electrode Fabrication and Materials Benchmarking

**PROJECT OBJECTIVE:** The objective of this task is to bring together a large fraction of the BATT community together to work on a single chemistry. Thus, the best combination of materials we can find will be provided to multiple researchers in the BATT Program for the Focus Groups. The Liu Group will be supplying the Si anodes and our group will develop matching cathodes of  $\text{LiFePO}_4$  that will be used to benchmark the effect of side reactions at the anode on cell capacity fade. For the High Voltage Focus group, our Group will benchmark (i.e. measure reversible capacity, rate performance, cycle efficiency.) the latest NMO material from NEI and an NCM material for comparative testing. This project also serves as a hub for testing new materials developed in the BATT program.

**PROJECT IMPACT:** This project supports two focus groups. For the Si Focus Group, it is critical that the effect of the side reactions in a full cell are quantified as the side reaction on the Si is considered a major flaw of the material. For the High-Voltage Focus group, it is important to source good materials and to make good cells in order to compare the effects of side reactions on the performance of the active materials that address critical questions for the BATT Program. This project is the key to demonstrating progress within the program against industry standards.

**OUT-YEAR GOALS:** The long-term goal of this project is to support focus groups and identify and provide quality materials, electrodes, and cell performance data. This effort supplies a benchmark for the rest of the BATT Program to build upon. Advancing Li-ion chemistry through proper analysis of state-of-the-art materials.

**COLLABORATIONS:** Gao Liu (LBNL).

#### Milestones

- 1) Go/No-Go: Decide if the newest NMO material from NEI should be the baseline material or not.  
Criteria: Benchmark the newest NMO material from NEI. (Dec. 13) **Go to use NMO.**
- 2) Identify the NCM baseline material. (Jun. 14) **Ongoing – delayed to Sep. 14**
- 3) Demonstrate a cyclable  $\text{LiFePO}_4$  electrode. (Jun. 14) **Complete**
- 4) Measure the difference in side reactions of graphite and Si when cycled against  $\text{LiFePO}_4$ . (Sep. 14) **Ongoing**

## Progress Report

**Identify the NCM baseline material.** As indicated in the previous report, the possible NCM-baseline material arrived last quarter and was being developed into an electrode this quarter. As discussed below, under the present testing conditions, the electrode experienced some capacity fade. The testing of NCM will continue until a half-cell can be constructed with negligible capacity- and energy-fade.

Two laminates of NCM were fabricated with different levels of inactive material. One electrode consisted of the standard level of carbon and binder and the other with half of these inactive components. Since this effort is in relation with the BATT High-Voltage Focus Group and, specifically, the interactions of the electrolyte with the surface of the active material, it is important to be able to make electrodes that are easily studied. Electrodes from 1.2 to 2 mAh/cm<sup>2</sup> were constructed for each electrode composition and tested for rate capability in half-cells with charge rates equal to the discharge rate (symmetric) or set at C/10 (asymmetric cycling). The electrodes of both compositions displayed the same rate capability, indicating that the lower level of inactive materials was sufficient for discharging and charging the cells at rates equivalent to the standard inactive material loadings. This data also indicated that the top charge rate for this cathode material at loadings above 1 mAh/cm<sup>2</sup> is C/2 (from the symmetric data) and that the top discharge rate of this material is 2C (from the asymmetric data.)

The electrodes were also evaluated for cycling ability; Fig. 1 shows the results of this test. For a cell of 1.4 mAh/cm<sup>2</sup>, the capacity demonstrates a slight decline with cycling to *ca.* 60 cycles, where upon the cycling declines precipitously with erratic coulombic efficiency. Also, during the first 60 cycles, the efficiency steadily drops. It is believed that the baseline electrolyte used for these tests (1 M LiPF<sub>6</sub> in EC:DEC 1:2) may be responsible for some of this behavior (even though the electrolyte was colorless), so new electrolyte was recently ordered. Another source of the fade may be that the electrodes have a loading greater than 1 mAh/cm<sup>2</sup>.

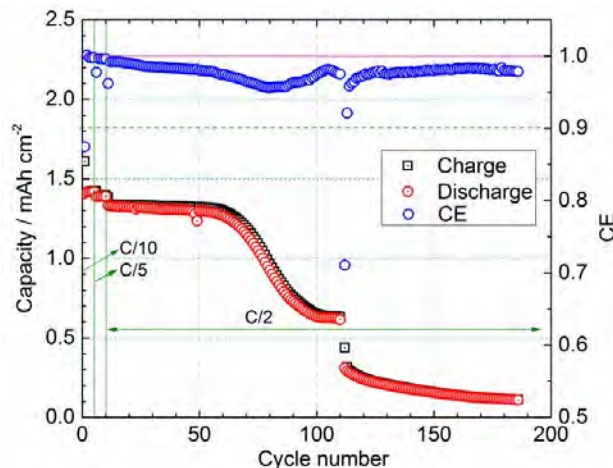


**Figure 1.** The capacity vs. cycle number of a Li/NCM cell cycled at different rates between 3.0 and 4.2 V.

In the next quarter, electrodes of loadings below 1 mAh/cm<sup>2</sup> will be tested with new electrolyte in Li half-cells to cutoff voltages below 4.2 V until an electrode composition, loading, and cutoff voltage can be identified that lead to negligible capacity fade over more than 100 cycles.

### Novel Anode Materials

**PROJECT OBJECTIVE:** The project seeks to understand how the cycling of elemental Si in a Li-ion cell configuration affects the local electrode structure and relate the information garnered to counter cell failure mechanisms. By using various types of electrode formulations and diagnostic spectroscopies, we can probe from the surface of the silicon to the final complex laminate electrode. Initial work included creation of an all-inorganic electrode that allowed the effects of cycling on the Si to be examined as the electrolyte was the only source of carbon in the cell. This work extended to developing thin film deposition techniques that allow tailoring of the surface chemistry of the Si that influence how the binder and silicon interact. In addition to normal cycling, imaging, and impedance spectroscopies we initiated tomography studies of conventional electrodes to examine how electrode porosity and particle size influenced the isolation of silicon particles on cycling, a major cause of capacity fade.

**PROJECT IMPACT:** The project utilizes a combination of synthesis and characterization to discern how the cycling of elemental Si in a Li-ion cell affects the surrounding electrode structure and how this can be modified to increase cycle life and stability. Results from these studies will be of interest to cell builders and end-users as degradation of the electrode structure can often be traced as the root cause of inconsistent results and premature cell failure. These goals are in line with EERE and OVT goals of furthering development of novel electrode materials and energy storage systems.

### **OUT-YEAR GOALS:**

- Using the new BATT standard Si source, design and formulate Si-based electrodes that allow for volume expansion in a less rigid environment than a porous copper substrate.
- Design and evaluate alternative structures that integrate the role of the current collector with the conductive additive requirement of the electrode to reduce materials requirements

**COLLABORATIONS:** Fikile Brushett (MIT), Lynn Trahey (ANL), Fulya Dogan (ANL)

### Milestones

- 1) Synthesize and evaluate a Si-based electrode that utilizes a multilayer structure to stabilize the active silicon. (Dec. 13) **Complete**
- 2) Synthesis and evaluation of at least three alternative electrode structures based on non-Cu porous substrates. (Mar. 14) **Complete**
- 3) Utilize surface sensitive techniques to develop a model of the Si - substrate interface in the alternative electrodes created. (Jun. 14) **Complete**
- 4) Evaluate optimized electrode structure against BATT standard Si electrode for rate capability and stability on cycling. Make recommendations to improve BATT standard electrode. (Sep. 14) **Ongoing**

## Progress Report

The stability of Si surfaces has significant effects on the cycling properties of Si anodes in Li-ion batteries. Previous studies have identified surface functional groups that interact with the electrolyte and these reactive groups have also been used by binder designers to make a stronger contact between the active particles and with the current collector. As part of the effort to examine surface stability on electrochemical properties, recent studies on Cu-Si multilayers and Si/SiO<sub>2</sub> passivation coatings are highlighted.

Building on Q2 studies, it was examined in more detail how the silica passivation coating on Si interacts with the environment. Several XPS studies have shown that this passivation layer is electrochemically active on first discharge, converting irreversibly to Li<sub>4</sub>[SiO<sub>4</sub>]. This compound has been found to form at around 800 mV (*vs* Li) and also to be the most thermodynamically stable product. However, this material is not in a static environment. Species such as Li<sub>4</sub>[SiO<sub>4</sub>] are, at the molecular level, isolated tetrahedral species, and as such can interact strongly with the polar electrolyte. During this quarter, the stability of this material to various electrolytes was investigated and its reactivity and chemical transformations were examined. The various materials were synthesized by a stoichiometric direct reaction of LiOH and hydrated silica as previously reported.

<sup>29</sup>Si MAS NMR studies were performed on the components to build a database of resonances to identify reaction products. The silicates were exposed to the BATT standard Si electrolyte, 1.2M LiPF<sub>6</sub> in EC/EMC (“Gen2”), and other simple solvents (battery grade). On exposure, all samples lost crystallinity and appeared to soften as the Li cations were solvated by the polar solvents. As an example, a mixed phase sample of Li<sub>x</sub>[SiO<sub>2</sub>] was exposed to the simple ether DME for a week. When iterated, the peak intensities (Fig. 1) confirm that the sample has lost Li<sub>4</sub>[SiO<sub>4</sub>] and its first condensation product Li<sub>6</sub>[Si<sub>2</sub>O<sub>7</sub>] gained the fully polymerized product Li<sub>2</sub>[SiO<sub>3</sub>]. This reaction can be envisioned to occur *via* simple condensation driven by the initial solvation of the Li by solvent as local charge on the silica anion is left uncompensated. The anion then reduces charge by a simple proton abstraction and polymerization happens gradually by loss of water.

Solution <sup>29</sup>Si NMR studies of the liquid phase above the solid, shown in Fig. 2, gave no indication of dissolved silica, eliminating this reaction as the source of the silicates or siloxanes previously identified in the literature. Overall, it has been shown that the silica surface plays a role in surface reactivity and can in fact lose oxygen in some fashion to the electrochemical cell environment. This is consistent with the Q2 EQCM results.

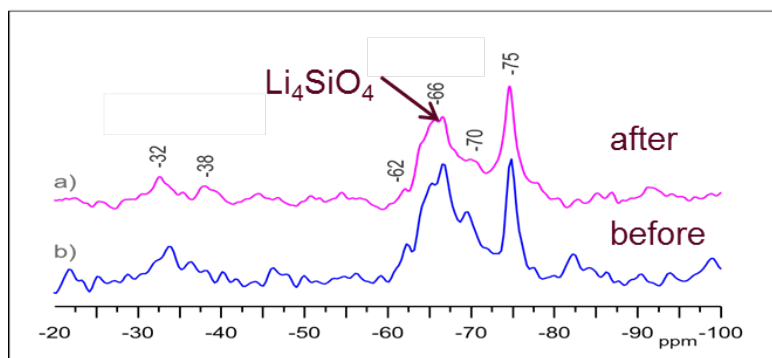


**Figure 1.** <sup>29</sup>Si MAS NMR of a) synthesized Li<sub>4</sub>SiO<sub>4</sub> stirred in DME, filtered, washed and dried, b) as synthesized Li<sub>4</sub>SiO<sub>4</sub>.

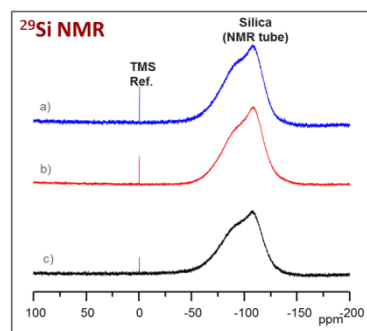


**Figure 2.** <sup>29</sup>Si solution NMR of synthesized Li<sub>4</sub>SiO<sub>4</sub> mixed in a) DME, b) PC and c) in Gen 2.

### Metal-Based High Capacity Li-Ion Anodes

**PROJECT OBJECTIVE:** To replace the presently used carbon anodes with safer materials that have double the volumetric energy density, and will be compatible with low cost layered oxide and phosphate cathodes and the associated electrolyte.

Specifically, the primary objectives are to:

- Increase the volumetric capacity of the anode by a factor of two over today's carbons
  - 1.6 Ah/cm<sup>3</sup>
- Increase the gravimetric capacity of the anode
  - $\geq 500$  Ah/kg
- Lower the cost of materials and approaches

**PROJECT IMPACT:** The volumetric energy density of today's Li-ion batteries is limited primarily by the low volumetric capacity of the carbon anode. If the volume of the anode could be cut in half, then the cell energy density can be increased by over 50% to approach 1 kWh/liter (actual cell). In addition, alloys with higher lithium diffusivity than carbon would minimize the possible formation of cell-shortening dendritic lithium under high charging rates or low temperature conditions. Moreover, smaller cells using lower cost manufacturing will lower the cost of tomorrow's batteries.

**OUT-YEAR GOALS:** The long-term goal of this project is to replace the present carbon used in Li-ion batteries with lower cost anodes that have double the volumetric energy density of carbon. This will be accomplished by using Sn- and/or Si-based materials. By the end of this project it is anticipated that a new Sn anode will be available that can exceed the charging and discharging rates of carbon thereby making it safer, that will have minimal excess capacity on the first cycle, and that can be cycled at greater than 99% efficiency over 200 cycles.

**COLLABORATIONS:** National Synchrotron Light Source (BNL) and Advanced Photon Source (ANL).

### Milestones

- 1) Identify the two most promising approaches for nano-silicon. (Dec. 13) **Complete**
- 2) Reduce the first cycle excess capacity to less than 20% for nano-tin. (Mar. 14) **Delayed to Sep. 14**
- 3) Go/No-Go: Decision on solvothermal approach for nano-tin. Criteria: Identify the optimum synthesis approach for nano-tin anode material. (Jun. 14) **Complete – No-Go on solvothermal**
- 4) Achieve more than 200 cycles on nano-tin at double the capacity of carbon at the 1C rate. (Sep. 14) **Ongoing**

## Progress Report

The goal of this project is to synthesize Sn- and Si-based anodes that have double the volumetric capacity of the present carbons, without diminishing the gravimetric capacity.

**Milestones (1) and (3):** Completed.

**Milestone (2):** A number of new approaches (such as voltage-assisted SEI control, binder modification, synthetic adjustment, *etc.*) are being investigated to decrease the first cycle excess capacity. The studies are underway and the results will be provided in the next quarter's report.

**Milestone (4):** The optimum synthesis approach for nano-tin anode is the mechanochemical method, with the initial ratio of SnO, Fe, and graphite of 1:0.25:10 (ball-milling for 8 h). Such an optimized nano Sn-Fe-C composite can deliver a capacity of *ca.* 550 mAh/g (*ca.* 1.8 Ah/cm<sup>3</sup>) along with good retention over 170 cycles (Fig. 1). Even on increasing the cycling to a 1C rate, the optimized Sn-Fe-C composite is close to doubling the volumetric capacity of standard graphite for at least 140 cycles, as indicated in Fig. 2.

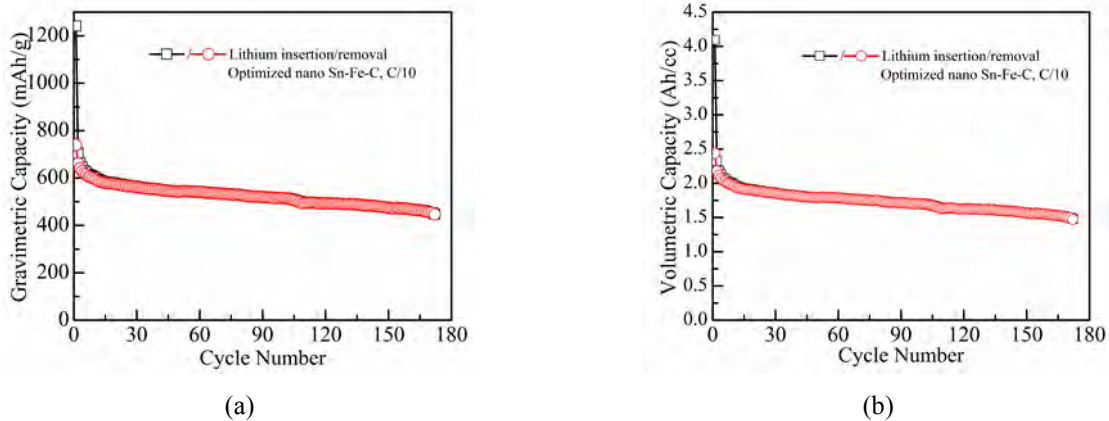


**Figure 1.** Electrochemical performance of the optimized Sn-Fe-C composite cycled under C/10 (1C corresponding to a current density of 600 mA/g) is shown by (a) gravimetric capacity and (b) volumetric capacity.

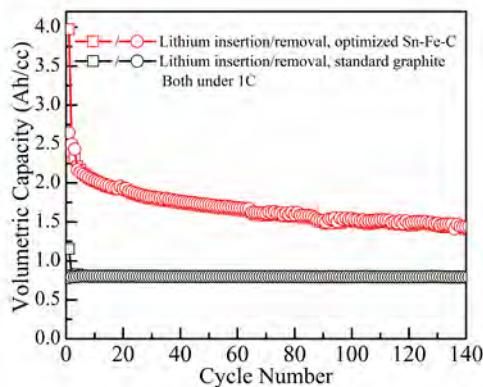


**Figure 2.** Volumetric capacity of the optimized Sn-Fe-C composite compared with standard graphite cycled at the 1C rate (1C corresponding to a current density of 600 mA/g for Sn-Fe-C, 372 mA/g for standard graphite).

### Nanoscale Composite Hetero-structures and Thermoplastic Resin Binders: Novel Li-ion Anode Systems

**PROJECT OBJECTIVE:** The objective is to identify novel materials and configurations, improved polymeric binders and cost effective scalable strategies to generate these systems to overcome the Si anode limitations. The goals of the present project are to identify an inexpensive nanoscale composites, new class of polymeric binders and electrode configurations displaying higher capacity ( $>1200$  mAh/g) than carbon while exhibiting similar first cycle irreversible loss ( $<15\%$ ), higher coulombic efficiency ( $>99.9\%$ ), and excellent cyclability to replace graphite.

**PROJECT IMPACT:** Identification of new Si based systems displaying higher gravimetric and volumetric energy densities than graphite will likely result in new commercial battery systems that are more robust, capable of delivering better energy and power densities and will be more lightweight than current Li-ion battery packs utilizing graphite anodes for identical performance specifications. New Si anode based strategies and configurations will also lead to more compact battery designs for the same energy and power density specifications as current Li-ion systems. Commercialization of these new Si anode based Li-ion battery packs will represent fundamentally, a major hallmark contribution of the BATT Program and the BATT community.

**OUT-YEAR GOALS:** This is a multi-year project comprising of four major phases to be successfully completed in four years. Phase 1: Development of cost effective high energy mechanical milling (HEMM) and direct mechano-chemical reduction (DMCR) approaches to generate nanocrystalline and amorphous Si, and  $\text{Li}_x\text{Si}(x>3.5)$  alloys exhibiting capacities in the  $\sim 1600$  mAh/g range and higher. This phase was completed in year 1. Phase 2: Use of chemical vapor deposition (CVD) to generate amorphous and nanocrystalline Si on vertically aligned carbon nanotubes (VACNT) based nano-scale heterostructures exhibiting specific capacity in the  $\sim 2000$ - $2500$  mAh/g range. This phase was completed in Year 2. Phase 3: Identify interface control agents (ICA) and surface electron conducting additives (SECA) to lower the first cycle irreversible (FIR) loss ( $<15\%$ ) and improve the coulombic efficiency (CE) ( $>99.9\%$ ). This phase was completed in Year 3. Phase 4: Develop elastic and high strength polymeric binders, to be completed in Year 4.

**COLLABORATIONS:** Ayyakkannu Manivannan (NETL), Spandan Maiti (University of Pittsburgh), Shawn Litster and Amit Acharya (Carnegie Mellon University)

#### Milestones

- 1) Go/No-Go: Stop microwave approach if it fails to generate nanoscale electrochemically-active architectures of Si and C resulting in capacities greater than or equal to 1200 mAh/g. (Dec. 13) **Discontinued**
- 2) Demonstrate generation of  $\alpha$ -Si hollow nanotubes using cost effective ( $< \$65/\text{kg}$ ) chemical approaches. (Dec. 13) **Complete**
- 3) Develop interface control agents (ICA) to reduce the first cycle irreversible loss to  $<15\%$ . (Mar. 14) **Complete**
- 4) Develop surface electron conducting additives (SECA) to improve the coulombic efficiency to  $>99.9\%$ . (Jul. 14) **Ongoing – delayed to Sep. 14**
- 5) Develop multilayered  $\alpha$ -Si/M (M = Matrix) composite films to lower the first-cycle irreversible loss ( $<15\%$ ) and improve the active mass loadings ( $2$ - $3\text{mg}/\text{cm}^2$ ). (Sep. 14) **Ongoing**

## Progress Report

Previously, it was demonstrated that hollow Si nanotubes (h-SiNTs) synthesized by a sacrificial template method demonstrated high stable specific capacity (1500 mAh/g at 2 A/g) and very good rate capability (Q3-2013). SEM analysis was conducted on h-SiNT electrodes after 1<sup>st</sup> cycle lithiation and delithiation (Fig. 1). The lithiated electrodes displayed large volume expansion corresponding to the formation of the intermetallic phases of Si with Li, as can be observed by the increase in the diameter of the h-SiNTs. The delithiated electrodes showed the expected volumetric shrinkage of the h-SiNTs corresponding to Si formation, albeit without any disintegration of the nanotube structure or of the mechanical integrity of the electrode. Subsequently, SEM analysis was conducted on the electrode consisting of h-SiNTs following 500 cycles of lithiation and delithiation (Fig. 2). The hollow nanotube architecture of the h-SiNTs was retained even after repeated cycling, thus withstanding the colossal volume expansion and contraction during the lithiation and delithiation cycles, respectively. This also directly correlates to the stable cycling of these electrodes over large numbers of cycles. The surface of the h-SiNTs appear roughened upon cycling due to the formation of a solid electrolyte interphase (SEI) during the first charge/discharge cycle.

In addition to the above, effects of improved mechanical properties of a “mechanical binder” on the structural stability and long term cyclability of a Si/C based system was studied. In this regard, PVDF, Na-CMC of elastic moduli *ca.* 1000 MPa, and *ca.* 2300 MPa, respectively, and a novel new polymer family named PGG of elastic modulus *ca.* 3200 MPa have been chosen as suitable binders for the Si/C system. The Si/C composite, derived by high energy mechanical milling, exhibiting a reversible specific capacity *ca.* 780mAh/g and *ca.* 620mAh/g at a charge/discharge rate of *ca.* 50mA/g and *ca.* 200mA/g, respectively, was selected as the model active electrode system. It has been identified that the long term cyclability of the Si/C system depends on the binder mechanical properties such as high elastic modulus. PGG and Na-CMC binder show better cyclability (*ca.* .04% loss per cycle up to 100 cycles) than the low elastic modulus PVDF binder (0.2% loss per cycle up to 100 cycles). To further confirm the degradation/disintegration of the matrix binder at a molecular level, the chemical structure of the polymer before and after electrochemical cycling was characterized by <sup>1</sup>H NMR. The <sup>1</sup>H-NMR data showed the structural degradation of the low elastic modulus PVDF following cycling (Fig. 3), whereas the high elastic modulus Na-CMC and PGG show no permanent deformation or structural damage. This result clearly suggests that the newly developed high elastic modulus PGG-based modified polymer is a promising binder family for Si/C based anodes.

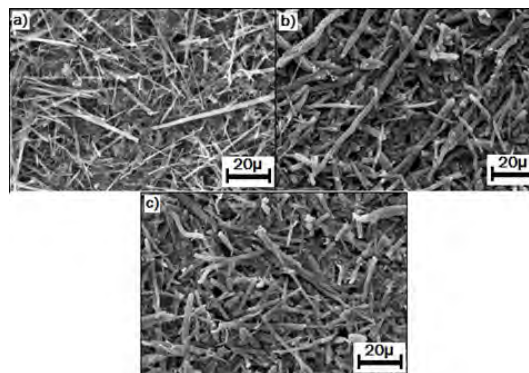


**Figure 1.** SEM images of h-SiNTs electrodes a) as prepared, b) after lithiation, and c) after delithiation.



**Figure 2.** SEM images of h-SiNTs electrodes a) before cycling, and b) after 500 cycles.

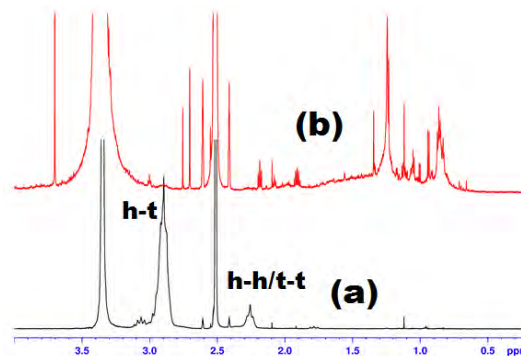


**Figure 3.** <sup>1</sup>H-NMR spectra of PVDF (a) before and (b) after cycling for 111 cycles in DMSO-d<sub>6</sub>.

## Development of Silicon-Based High Capacity Anodes

**PROJECT OBJECTIVE:** The objective of this project is to develop high-capacity, low-cost electrodes with good cycle stability and rate capability to replace graphite in Li-ion batteries. The porous Si and the rigid-skeleton supported Si/C composite anode (B<sub>4</sub>C/Si/C) will be further optimized. The optimized B<sub>4</sub>C/Si/C material will be used as the baseline material for both thick electrode fabrication and studies to advance our fundamental understanding of the degradation mechanism in Si based anode. New electrolyte additives, binders, and artificial SEI layers will be investigated to further improve the performance of anodes. New approaches will be developed to pre-lithiate Si-based and other Li-alloy anodes to minimize their first-cycle losses. Fundamental understanding on the formation and evolution of SEI layer, the effect of electrolyte additives and electrode thickness will be investigated by *in situ* microscopic analysis.

**PROJECT IMPACT:** Si-based anodes have much larger specific capacities compared with conventional graphite anodes. However, the cyclability of Si-based anodes is limited because of the large volume expansion that is characteristic of these anodes. This work will develop a low-cost approach to extend the cycle life of high-capacity, Si-based anodes. The success of this work will further increase the energy density of Li-ion batteries and accelerate market acceptance of electrical vehicles (EV), especially for plug-in hybrid electrical vehicles (PHEV) required by the EV Everywhere Grand Challenge proposed by DOE/EERE.

**OUT-YEAR GOALS:** The main goal of the proposed work is to enable Li-ion batteries with a specific energy of >96 Wh/kg (for PHEVs), 5000 deep-discharge cycles, 15-year calendar life, improved abuse tolerance, and less than 20% capacity fade over a 10-year period

### **COLLABORATIONS:**

Collaboration on anode development will continue with the following battery groups:

- Michael Sailor (UCSD): Preparation of porous Si.
- Gao Liu (LBNL): Binders.
- Yi Cui (Stanford): Failure mechanism study.
- Marina Yakovleva (FMC Corp): SLMP
- Chunmei Ben (NREL): Surface protection and failure mechanism study.
- David Ji (Oregon State University): Preparation of porous Si by thermite reactions.

### Milestones

- 1) Identify the fading mechanism in the thick Si electrode vs. thin electrode. (Dec. 13). **Complete**
- 2) Achieve Coulombic charge efficiency of the electrode >90% during the first cycle, through application of SLPMs and sacrificial Li electrode to PNNL's B<sub>4</sub>C/Si/C anode. (Mar. 14) **Complete**
- 3) Achieve high loading Si-based anode capacity retention of >1.2 mAh/cm<sup>2</sup> over 150 cycles using new binders/electrolyte additives. (Jun. 14) **Complete**
- 4) Achieve improved cycling stability of thick electrodes (> 3 mAh/cm<sup>2</sup>). (Sep. 14) **Complete**
- 5) Achieve a specific energy greater than 30 Wh/kg and the specific power greater than 5 kW/kg, and cycle life greater than 30,000 cycles for Li ion capacitors. (Sep. 14) **Ongoing**

## Progress Report

Porous Si electrodes show good cycling stability at high mass-loading. Figure 1a shows the long term cycling of a porous Si electrode with the loading of *ca.* 2.9 mg/cm<sup>2</sup>. It was cycled at a low current density of 0.06 mA/cm<sup>2</sup> for 10 cycles and then charged at 0.75 mA/cm<sup>2</sup> and discharged at 0.5 mA/cm<sup>2</sup>. It exhibits a capacity of *ca.* 2.9 mAh/cm<sup>2</sup> at low current density and a capacity of *ca.* 2.2 mAh/cm<sup>2</sup> at the higher rate. Its capacity retention is *ca.* 86% over 300 cycles. An electrode with a high loading of *ca.* 3.5 to 4 mg/cm<sup>2</sup> also demonstrated good cycling stability. Figure 1b shows that porous Si electrodes can have a capacity of *ca.* 3 mAh/cm<sup>2</sup> with *ca.* 90% capacity retention over 100 cycles. Further improvement of the cycling stability at higher loading is ongoing.

In another effort, rigid skeleton-supported Si nanocomposite is further optimized to improve the cycling stability at high loading. The composition and structure of the composite is tuned to achieve good cycling stability while maintaining high capacity. Leveraging the knowledge gained from the porous Si, well-controlled void space is introduced to the composite to further accommodate the volume change and hence improve the cycling stability of the thick electrodes. New combinations of binders as well as electrolyte additives will also be further developed.

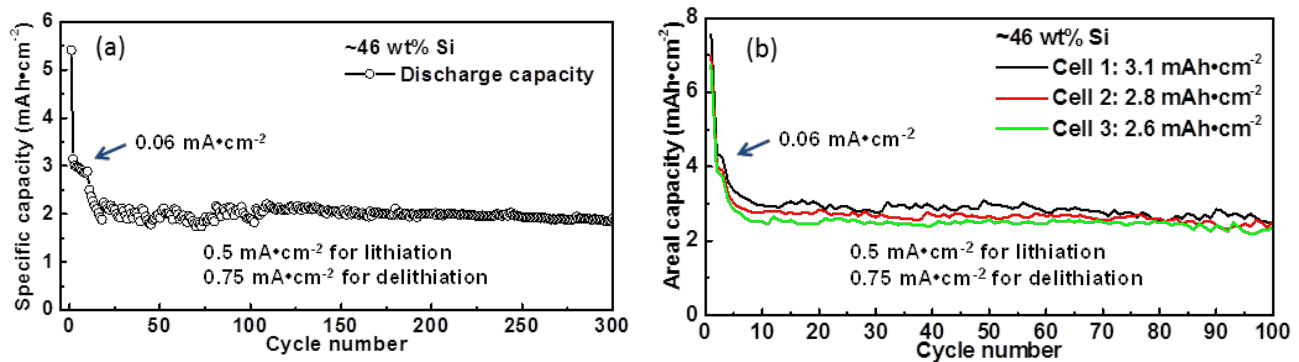


**Figure 1.** (a) Cycling stability of the porous Si electrode of *ca.* 2.2 mAh/cm<sup>2</sup>, (b) Cycling stability of the porous Si electrode of *ca.* 3 mAh/cm<sup>2</sup>.

## Atomic Layer Deposition for Stabilization of Amorphous Silicon Anodes

**PROJECT OBJECTIVE:** The objective of the project is to develop a low-cost, thick, high-capacity silicon anode with sustainable cycling performance. Our specific objectives are to develop a novel conductive and elastic scaffold by using Atomic Layer Deposition (ALD) and Molecular Layer Deposition (MLD), demonstrate durable cycling by using the new coating and electrode design, and investigate the effect of atomic surface modification on irreversible capacity loss and cycling performance.

**PROJECT IMPACT:** Due to its high theoretical capacity and natural abundance, Si has attracted much attention as a promising Li-ion anode material. However, progress towards a commercially-viable Si anode has been impeded by the rapid capacity fade of silicon caused by large volumetric expansion. In this project, new ALD/MLD conformal nanoscale coatings with desirable elastic properties and good conductivity are developed to accommodate the volumetric expansion and to protect the surface from reactive electrolytes, as well as to ensure the electronic paths through the composite electrodes. Successful completion of this project will enable the coated Si anodes to have high Coulombic efficiency, as well as durable high-rate capability. This project supports the goals of the DOE EV Everywhere Grand Challenge and EERE's Vehicle Technologies Office to develop high-energy batteries for wider adoption of electric vehicles to reduce consumption of imported oil and generation of gaseous pollutants.

### **OUT-YEAR GOALS:**

- Demonstrate durable cycling performance of thick Si anodes (>15 $\mu$ m) by using new ALD/MLD coatings and electrode designs
- Explore the importance and mechanism of various coatings *via* the BATT coating group
- Collaborate within the BATT program with the aim of developing high-rate plug-in hybrid electric (PHEV)-compatible electrodes (both anodes and cathodes)

**COLLABORATIONS:** Phil Ross, Gao Liu and Robert Kostecki (LBNL), Jason Zhang (PNNL), Yue Qi (MSU), Xingcheng Xiao (GM), Perla Balbuena (Texas A&M) and Kevin Leung (SNL).

### Milestones

- 1) Identify the impact of Alucone MLD coating on the structure and morphology of Si anodes during cycling. (Dec. 13) **Complete**
- 2) Develop Al<sub>2</sub>O<sub>3</sub>/carbon composite coatings by pyrolysis of Alucone MLD film. (Mar. 14) **Complete**
- 3) Go/No-Go: Test coated electrodes in coin cells. Criteria: Stop the development of Al<sub>2</sub>O<sub>3</sub>/carbon composite coatings if the coating cannot help the performance of Si anodes. (Jun. 14) **Complete**
- 4) Synthesize and characterize novel AlF<sub>3</sub>/Alucone hybrid coating by using ALD and MLD. (Sep. 14) **Ongoing**

## Progress Report

Previous work reported the development of ultrathin aluminum oxide-hydroquinone coatings (ALHQ) applied by using molecular layer deposition (MLD) on Si:carbon black:PVDF electrodes (60:20:20 wt%). The new ALHQ coating is composed of an aromatic ring interconnected with  $\text{Al}_2\text{O}_3$ , which is expected to possess better conductivity and mechanical flexibility.

This quarter, our investigation focused on the electrochemical behavior and if there were correlations with the mechanical properties. The new ALHQ coating has a lower Young's modulus, *ca.* 29 GPa, compared with the previous aluminum oxide-glycerol (ALGL) coating with a Young's modulus of *ca.* 39 GPa. Both MLD organic-inorganic hybrid coatings have much lower Young's moduli than the atomic layer deposition  $\text{Al}_2\text{O}_3$  coating with a Young's modulus of *ca.* 195 GPa. The flexible coatings are expected to provide both a suitable protection layer on and accommodate the massive volume changes in Si anodes.

The ALHQ-coated Si anodes showed greatly improved performance as indicated in Fig. 1a. The Si anode coated with this new ALHQ coating has even higher reversible capacity than the ALGL-coated Si anode. Both coatings have improved the 1<sup>st</sup> cycle coulombic efficiency from 65% in bare Si anodes to 85% for the coated anodes. Interestingly, both MLD-coated anodes show different 1<sup>st</sup> discharge voltage profiles than that of bare Si, as illustrated in Fig. 1b. The voltage plateau at *ca.* 0.7 V, attributed to the SEI formation on the bare Si anode, has diminished in the coated anodes. This behavior implies that the coatings modify the interfacial chemistry, as well the SEI formation. Since the hybrid coatings chemically grow on the surface of the electrode, the conformal coatings act as an artificial SEI to prevent direct contact between the Si and electrolyte.

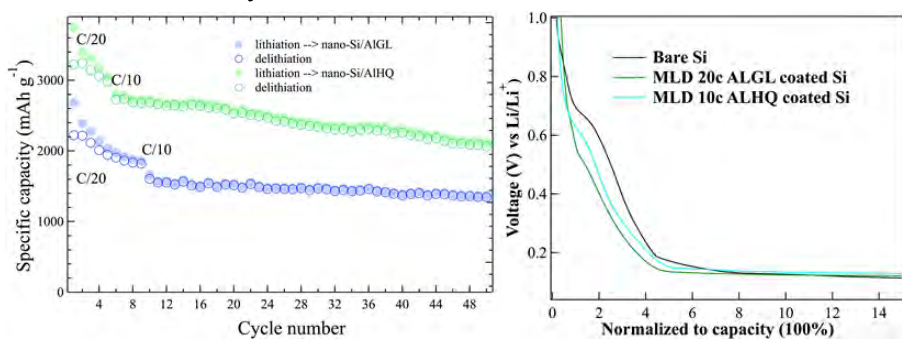


**Figure 1.** (a) Stable cycling performance of MLD ALGL- and ALHQ-coated electrodes; (b) Voltage profile of bare Si anode, MLD ALGL- and ALHQ-coated Si anodes during the initial lithiation.

Further, enhanced rate performance was achieved after post-annealing, which resulted in the cross-linked polymerization of the aromatic rings in the ALHQ coating. These results are displayed in Fig. 2. After air-annealing, the ALHQ-coated Si anode exhibits a higher rate capability than the as-prepared ALHQ coating. This behavior suggests that enhanced conductivity results from the cross-linking in the ALHQ coating. The cross-linked coating also has a higher critical tensile strain than that exhibited by ALGL – 1.8% *versus* 1%. This robust coating ensures the mechanical stability of the electrode and stabilizes thick electrodes (thickness  $\geq 12 \mu\text{m}$ , mass loading  $\geq 1.2 \text{ mg/cm}^2$ ).

The MLD ALHQ-coated Si anode also exhibits stable cycling behavior: 2,000 mAh/g for 50 cycles. The robust mechanical support and good conductivity of this ALHQ coating is a promising avenue for Si anodes.

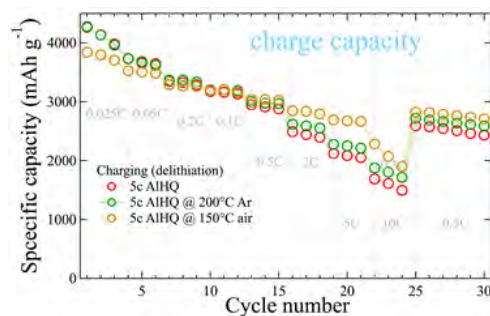


**Figure 2.** Rate capability of MLD ALHQ-coated electrodes under different annealing conditions.

## New Layered Nanolaminates for Use in Lithium Battery Anodes

**PROJECT OBJECTIVE:** Replace graphite with a new material selected from a group of layered (two-dimensional) binary carbides and nitrides known as MXenes, which may offer combined advantages of graphite and Si anodes with a higher capacity than graphite, less expansion, longer cycle life and a lower cost than Si nanoparticles.

**PROJECT IMPACT:** As a result of this project, a new family of 2D materials (MXenes) was discovered. Using MXenes as anode materials in LIB could lead to higher capacities than graphite with the ability to handle higher cycling rates than graphite anodes. Since each MXene has its own voltage window, considering their rich chemistry and the possibility of solid solutions, MXene compositions can be selected and tuned for certain voltages to produce high-performance batteries with improved safety.

**OUT-YEAR-GOALS:** The project's long term goal is to produce new anode materials (MXenes) that may replace graphite in anodes of Li-ion batteries.

**FY2014** - Improvement of the cycle-life of the anodes. Optimization and modification of the material manufacturing processes to enable large-volume, low-cost production.

### **COLLABORATIONS:**

- Xiao-Qing Yang and Kyung-Wan Nam, BNL
- Yu Xie and Paul Kent, ORNL
- Jun Lu, Lars Hultman and Per Eklund, Linkoping University, Sweden.
- Jérémy Come, Yohan Dall'Agnese and Patrice Simon, Université Paul Sabatier, Toulouse, France

### Milestones

- 1) (a) Produce MXene anodes with capability of delivering a stable performance at 10 C cycling rates (Dec. 13). **Complete**  
(b) Complete *in situ* and *ex situ* studies of the lithiation and delithiation of MXenes and determine the most promising materials (Jun. 14). **Complete**
- 2) Maximize capacity of MXenes and test newly discovered MXenes that have shown the highest capacity so far (Mo<sub>2</sub>C) (Jun. 14). **Complete**
- 3) Predict the theoretical capacity and Li insertion potential of MXenes, and synthesize and test MXenes that are expected to have the largest Li uptake (>600 mAh/g theoretical capacity) and a lithiation/delithiation potential below 1 V (Jun. 14). **Partially completed, delayed to Sep. 14**
- 4) Demonstrate improved charge/discharge behavior by controlling particle size and surface chemistry of MXenes (Sep. 14). **Ongoing**

## Progress Report

Following the previous report on maximizing the areal capacity of multilayered MXene using carbon black (CB), the effect of other C additives (C-onions and C-nanotubes) was tested. The additives were mixed with multilayered  $\text{Ti}_3\text{C}_2$ , pressed into free-standing discs with loadings of *ca.* 50  $\text{mg}/\text{cm}^2$  and tested as anodes. The areal capacities vs. cycle number are shown in Fig. 1 for cells with additive loadings of 10 wt.% (this loading value was justified in the last report). Among those, the  $\text{Ti}_3\text{C}_2/\text{CB}$  mixture showed the highest reversible areal capacity, 5.9  $\text{mAh}/\text{cm}^2$  after 50 cycles, at a rate of  $\approx C/3$  (Fig. 1).

The performance of other multilayered MXenes was also improved by using CB.  $\text{Nb}_2\text{C}$  anodes pressed with 10 wt.% of CB showed higher performance than  $\text{Ti}_3\text{C}_2$  with a capacity of 7  $\text{mAh}/\text{cm}^2$  after 50 cycles at a current of 1.5  $\text{mA}/\text{cm}^2$  (Fig. 2A). The values achieved for both  $\text{Ti}_3\text{C}_2$  and  $\text{Nb}_2\text{C}$  are well above those currently reported for other anode systems (Fig. 2B). To enhance volumetric capacity while retaining high areal capacity, thinner  $\text{Ti}_3\text{C}_2$  electrodes were produced with mass loading of *ca.* 15  $\text{mg}/\text{cm}^2$  compared to an initial of *ca.* 50  $\text{mg}/\text{cm}^2$ . While this decreased the areal capacity to 2  $\text{mAh}/\text{cm}^2$  due to the lower mass loading, it is still comparable to literature values. The volumetric capacity was doubled compared to the original high mass-loading films and reached *ca.* 260  $\text{mAh}/\text{cm}^3$ .

Using density functional theory, the theoretical capacities of different MXene monolayers with bare, O- and OH-terminated surfaces were calculated (Table 1). Bare MXenes were found to have higher capacities than surface terminated ones. Among those,  $\text{V}_2\text{C}$  and  $\text{Ti}_2\text{C}$  showed the highest values. Experimentally,  $\text{V}_2\text{C}$  gives a specific capacity of 260  $\text{mAh}/\text{g}$  at 1 C and 125  $\text{mAh}/\text{g}$  at 10 C after 150 cycles, being the most promising among the multilayered MXenes listed in Table 1.  $\text{Nb}_2\text{C}$  yields 170  $\text{mAh}/\text{g}$  at 1 C, and 110  $\text{mAh}/\text{g}$  at 10 C after 100 cycles. Both  $\text{Ti}_3\text{C}_2$  and  $\text{Ti}_2\text{C}$  yield *ca.* 110  $\text{mAh}/\text{g}$  at 1 C after 50 cycles. However, when  $\text{Ti}_3\text{C}_2$  is delaminated, the capacity increases dramatically to 410  $\text{mAh}/\text{g}$  at 1 C after 50 cycles, which significantly exceeds the maximum predicted theoretical value. This somewhat surprising result is possibly due to the increased surface area and the formation of Li multilayers. The work on delaminating other MXenes is ongoing.

The theoretical calculations yielded another important insight. It was found that surface terminated MXenes could in principle decompose into bare MXenes and metal oxides when in contact with multivalent metals, such as Mg, Ca, and Al. This is especially important considering that bare MXenes are expected to have the highest capacities (Table 1). The values shown in Table 1 are for single Li layers, while a double-layer formation predicted by DFT doubles those values. The single-layer values for  $\text{Ti}_3\text{C}_2$  has already been exceeded, as mentioned above. These results suggest that, in addition to maximizing active surface area by delamination, further efforts to enhance Li-ion uptake for MXenes should also be focused on modifying the MXene surface chemistries.

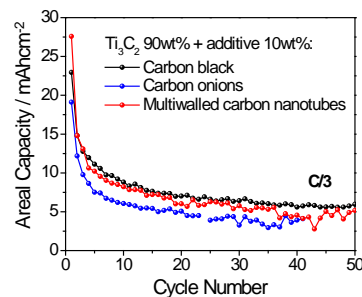


**Figure 1.** Areal capacity vs. cycle number for pressed  $\text{Ti}_3\text{C}_2$  discs with 10 wt.% of different carbon additives at  $C/3$ .

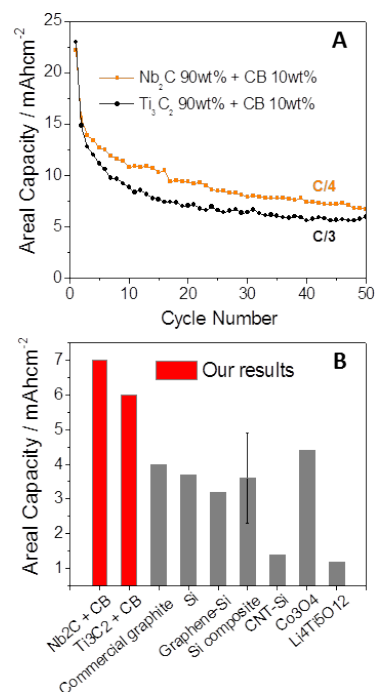


**Figure 2.** (A) Areal capacity vs. cycle number for pressed  $\text{Ti}_3\text{C}_2$  and  $\text{Nb}_2\text{C}$  discs with 10 wt.% of CB content at  $C/3$  and  $C/4$ , respectively. (B) Comparison of our results with other systems.

**Table 1.** Capacities ( $\text{mAhg}^{-1}$ ) corresponding to one metal layer on bare, O- and OH-terminated MXene monolayers.

	$\text{M}_{n+1}\text{X}_n$	$\text{M}_{n+1}\text{X}_n\text{O}_2$	$\text{M}_{n+1}\text{X}_n(\text{OH})_2$
$\text{Ti}_2\text{C}$	439	348	95
$\text{V}_2\text{C}$	418	335	91
$\text{Nb}_2\text{C}$	252	219	58
$\text{Ti}_3\text{C}_2$	294	250	67

## Synthesis and Characterization of Si/SiO<sub>x</sub>-Graphene Nanocomposite Anodes and Polymer Binders

**PROJECT OBJECTIVE:** Novel structured Si/SiO<sub>x</sub>-carbon nanocomposites and polymer binders will be designed and synthesized to improve Si-based anode electrode kinetics and cycling life, and decrease initial irreversible capacity loss in high capacity Li-ion batteries. By combining the new Si-based anode materials and new polymer binders and investigating their structure-performance relationships, a high performance Si anode can be achieved.

1. Synthesis and characterization of Si/SiO<sub>x</sub>-based nanocomposite Li-ion battery anodes.
2. Identify and evaluate the electrochemical performance of the Si/SiO<sub>x</sub>-based nanocomposite and the polymer binder.
3. Develop understanding of long-lifetime Si anodes for Li-ion batteries by considering both the Si active phase and the polymer binder and surface interactions between the electrode components.

**PROJECT IMPACT:** The proposed collaborative effort closely integrates synthesis of Si-based composite anodes with controlled structure and composition, development of novel functional polymer binders, and materials characterization and electrochemical evaluation. The resulting optimized Si anode electrode will provide electrochemical performances which are essential to achieving higher energy densities in PHEV and EV applications.

**OUT-YEAR GOALS:** According to the accomplishments of the project, several types of Si-based composite with promising electrochemical performance will be developed and demonstrated. New functional polymer binders will be developed. The mechanical and chemical influences of the structure, chemical composition and surface modification on electrochemical performance of those materials will be identified and demonstrated, thus to provide systematic fundamental understanding to guide the Si-based anode material design. The Si-based electrode design, including the selection of materials and polymer binders, will be demonstrated in cell testing at Penn State and with BATT project partners.

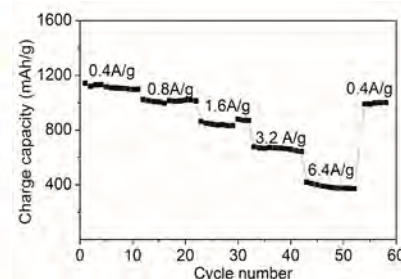
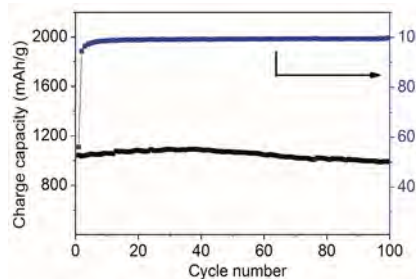
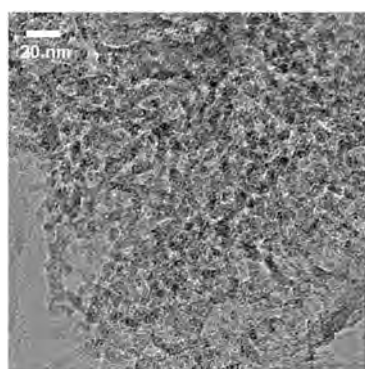
**COLLABORATIONS:** Gao Liu (LBNL), Chunmei Ban (NREL), Nissan R&D center.

### Milestones

- 1) Go/No-Go: Stop the metal composites coating approach and focus on carbon coating approach if the capacities are less than 1500 mAh/g. Criteria: Synthesize, characterize and evaluate Si-based composite with novel coating (e.g. non-oxidic metal composites). (Dec. 13) **Go for carbon coating**
- 2) Identify and demonstrate the optimized composition, structure and surface modification of micro-sized Si/C and porous Si/C composites. (Mar. 14) **Complete**
- 3) Synthesize acidic/semiconducting polymer binders using grafting approach. (Jun. 14) **Complete and go for binder testing.**
- 4) Go/No-Go: Determine if semiconducting polymer approach can generally be applied to Si anodes. Criteria: Synthesis and electrochemical evaluation of Si/Si alloy composites. Fully characterize acidic/semiconducting polymer binders. Supply laminates of the optimized Si/Si alloy electrodes with electrode capacity of 800 mAh/g that cycle 100 cycles to BATT PIs. (Sep. 14) **Ongoing evaluation of new binders is continuing.**

## Progress Report

**Si-based anode materials:** A micro-sized, porous Si-C composite (PSi/C) has been developed by reduction of  $\text{SiCl}_4$  with alkaline alloy followed by a thin layer of carbon coating by thermal deposition of acetylene. Both the pore size and Si building blocks size are about 10 nm. The initial discharge and charge capacity of PSi/C are  $1862 \text{ mAhg}^{-1}$  and  $1044 \text{ mAhg}^{-1}$  ( $2482 \text{ mAhg}^{-1}$  and  $1392 \text{ mAhg}^{-1}$  based on Si, at a current density of  $0.4 \text{ Ag}^{-1}$ ), giving a first cycle coulombic efficiency of 56%. After 100 cycles, the material shows a reversible capacity of  $990 \text{ mAhg}^{-1}$  ( $1320 \text{ mAhg}^{-1}$  based on Si) with capacity retention of 94.8%. The coulombic efficiencies reach 99% after 10 cycles and remain at  $> 99\%$ . The rate performance of the PSi/C anode was also tested at current densities of 0.4, 0.8, 1.6, 3.2, and  $6.4 \text{ Ag}^{-1}$ . The capacity at current density of  $6.4 \text{ Ag}^{-1}$  is  $395 \text{ mAhg}^{-1}$ , which is superior to the theoretical capacity of graphite. A capacity of  $1032 \text{ mAhg}^{-1}$  recovers when the current density is reset to  $0.4 \text{ mAhg}^{-1}$  after 55 cycles, showing the good reversibility of the PSi/C anode material.



**Semiconducting binders:** Progress has been made in the synthesis of high molecular weight semiconducting binder polymers. Poly(9,9-dihexyl fluorene) was synthesized from dibromo and diboronic ester monomers under the conditions reported in the table below in single-phase Suzuki polymerizations with no aqueous secondary phase. Consistent degrees of polymerization ( $X_n$ ) of over 300 were obtained for the conditions attempted. This single phase Suzuki polymerization scheme will be used in the remaining part of the project to obtain high molecular weight binders.

“Base” (equiv)	Solvent	Catalyst (1 mol%)	Rxn time (days)	$M_n$ (kg/mol)	$M_w$ (kg/mol)	PDI	$X_n$
TBAF (4)	THF	$\text{PdCl}_2(\text{dppf})$	2	100	133	1.3	300
TBAF (4)	THF	$\text{Pd}(\text{PPh}_3)_4$	6	105	131	1.3	312
TBAF (4)	THF	$\text{PdCl}_2(\text{dppf})$	6	110	140	1.3	313
TBAF (4)	toluene	$\text{PdCl}_2(\text{dppf})$	2	108	140	1.2	322
$\text{CsOH}\cdot\text{H}_2\text{O}$ (4)	THF	$\text{PdCl}_2(\text{dppf})$	2	132	160	1.2	394

Ionic functionalization of these high molecular weight polymers is progressing to meet the binder testing milestones of September. Work is also continuing on A-B chain-growth, non-aqueous, Suzuki polymerizations using bromo-boronic ester A-B functional monomers. So far the degrees of polymerization for the A-B chain growth scheme are low, so refinement of the catalyst coordination step continues in order to improve the molecular weights of these polymers.

### Wiring up Silicon Nanoparticles for High Performance Lithium Ion Battery Anodes

**PROJECT OBJECTIVE:** The charge capacity limitations of conventional carbon anodes are overcome by designing optimized nano-architected Si electrodes.

This study pursues two main directions:

- 1) fabricating novel nanostructures that show improved cycle life, and
- 2) developing methods to study the lithiation/delithiation process to understand volume expansion for higher efficiency.

**PROJECT IMPACT:** The Li-ion storage capacity, as well as the cycling stability of Si anodes, will be dramatically increased. This project's success will make Si the high performance Li-ion battery anode material toward high energy batteries to power vehicles.

**OUT-YEAR GOALS:** Mass loading, cycling life and first cycle coulombic efficiency (1st CE) will be improved and optimized (over 1 mg/cm<sup>2</sup> and >85%) by varying material synthesis and electrode assembly. Fundamentals of volume expansion as well as SEI formation in Si nanostructures will be identified. A detailed study of inter-particle interactions during electrochemical reaction will be performed by *in situ* and *ex situ* microscopy.

#### **COLLABORATIONS:**

- BATT Program PIs
- SLAC: *In situ* X-ray
- Stanford: Prof. Nix, mechanics; Prof. Bao, materials.

#### Milestones

- 1) Utilize Si particles as an anode with capacity > 1000 mAh/g, mass loading of 1mAh/cm<sup>2</sup> and cycle life >100 cycles (Dec. 13) **Complete**
- 2) Go/No-Go: Try other conducting coating materials. Criteria: If the first cycle coulombic efficiency cannot go >80%. (Mar. 14) **Go for trying different conducting coating materials.**
- 3) Complete *in situ* TEM and *ex situ* SEM studies of two or multiple Si nanostructures during lithiation/delithiation to understand how neighboring particles affect each other and volume changes. (Jun. 14) **Ongoing – delayed to Sep. 14**
- 4) Increase mass loading of Si material to achieve 2 mAh/cm<sup>2</sup> and first cycle coulombic efficiency (>85%) and cycle life >300 cycles (Sep. 14) **Complete**

## Progress Report

A bottom-up, microemulsion approach was developed to synthesize spherical Si pomegranate microbeads ranging from 500 nm to 10  $\mu\text{m}$  in diameter (Fig. 1a). Si nanoparticles are individually encapsulated by a carbon framework, with well-defined void spaces between the Si and carbon (Figs. 1c-f). The synthesis approach is highly controllable. As a result, the parameters of pomegranate structure, including the size of the pomegranate ( $D$ ), the ratio of Si nanoparticles size to void space ( $d/a$ ), and the thickness of the C shell ( $t$ ) can be well tuned to optimize for battery performance (Fig. 1b).

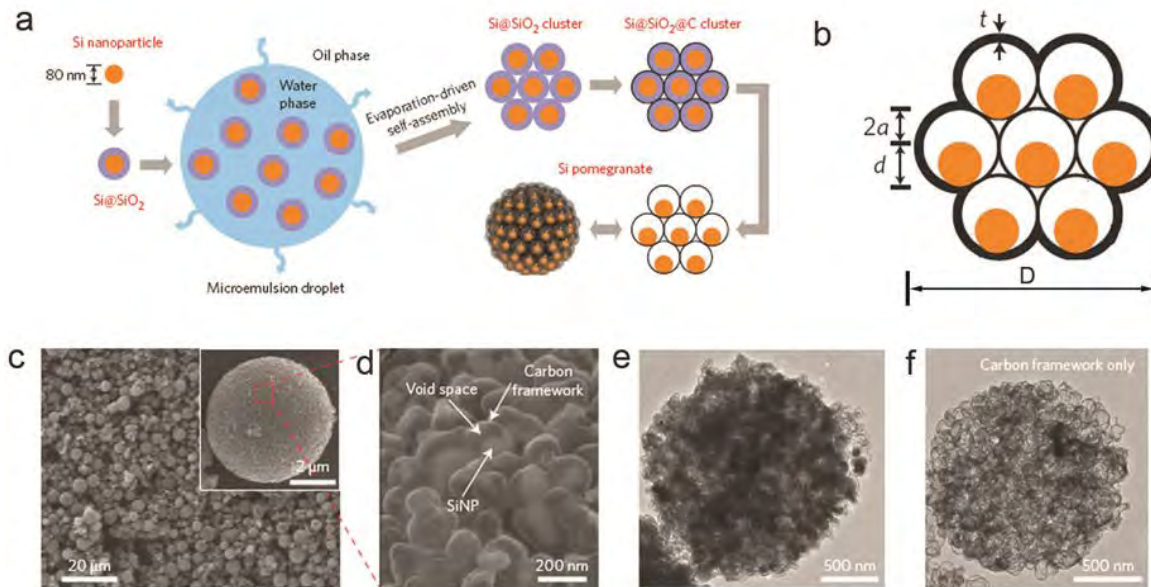


**Figure 1.** (a, b) Schematic of the fabrication process for Si pomegranates. (c) SEM images of Si pomegranates showing the micrometer-sized and spherical morphology. (d) Magnified SEM image showing the local structure of Si nanoparticles and the conductive carbon framework with well-defined void space between. (e, f) TEM image of one Si pomegranate particle and carbon framework after etching away Si

In the pomegranate structure, the conformally-coated carbon shell not only limits the continuous SEI formation on the Si nanoparticles, but also functions as an electrical highway and a mechanical backbone so that all of the nanoparticles are electrochemically active. The Si pomegranate/CNT (mass ratio: 7/3) electrodes with active material mass-loading over  $3 \text{ mg/cm}^2$  could result in an areal capacity of more than  $3 \text{ mAh/cm}^2$  after 100 deep cycles. The specific capacity of a high mass-loading cell reaches  $950 \text{ mAh/g}$ , indicating almost all of the Si nanoparticles are active in the thick electrode. Even with less (5%) or no CNT additive, high mass-loading cells (over  $1 \text{ mAh/cm}^2$ ) also demonstrated stable cycling, as shown in Fig. 2. This excellent battery performance at high mass-loading indicates successful design of the pomegranate structures.

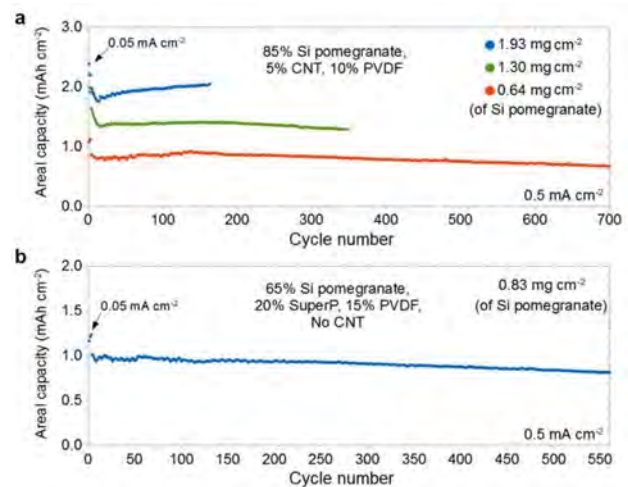


**Figure 2.** Cycle performance of slurry-coated, calendared, Si pomegranate anodes, with (a) 5% CNT or (b) no CNT.

### Fluorinated Electrolyte for 5-V Li-ion Chemistry

**PROJECT OBJECTIVE:** The objective of this project is to develop a new advanced electrolyte system with outstanding stability at high voltage and high temperature and improved safety characteristic for an electrochemical couple consisting of the high voltage  $\text{LiNi}_{0.5}\text{Mn}_{1.5}\text{O}_4$  (LNMO) cathode and graphite anode. The specific objectives of this proposal are the design, synthesis and evaluation of (1) non-flammable high voltage solvents to render intrinsic voltage and thermal stability in the entire electrochemical window of the high-voltage cathode materials, and (2) electrolyte additives to enhance the formation of a compact and robust solid electrolyte interphase (SEI) on the surface of the high-voltage cathode. A third objective is to gain fundamental understanding of the interaction between electrolyte and high voltage electrode materials, the dependence of SEI functionality on electrolyte composition, and the effect of high temperature on the full Li-ion cells using the advanced electrolyte system.

**PROJECT IMPACT:** This innovative fluorinated electrolyte is intrinsically more stable in electrochemical oxidation due to the fluorine substitution; therefore it would be also applicable to cathode chemistries based on TM oxides other than LNMO. The results of this project can be further applied to a wide spectrum of high-energy battery systems oriented for PHEVs that operate at high potentials, such as  $\text{LiMPO}_4$  (M=Co, Ni, Mn), or battery systems that require a high-voltage activation process, such as the high-capacity Li-Mn-rich  $x\text{Li}_2\text{MnO}_3 \cdot (1-x)\text{Li}[\text{Ni}_x\text{Mn}_y\text{Co}_z]\text{O}_2$ . This electrolyte innovation will push the U.S. supply base of batteries and battery materials past the technological and cost advantages of foreign competitors, thereby increasing economic value to the USA. ANL's new fluorinated electrolyte material will enable the demand for more PHEVs and EVs, which directly transforms to much less gasoline consumption and less pollutant emissions.

**OUT-YEAR-GOALS:** The goal of this project is to deliver a new fluorinated electrolyte system with outstanding stability at high voltage and high temperature with improved safety characteristic for an electrochemical couple consisting of 5-V Ni-Mn spinel  $\text{LiNi}_{0.5}\text{Mn}_{1.5}\text{O}_4$  (LNMO) cathode and graphite anode. The specific objectives of this proposal are the design, synthesis, and evaluation of (1) non-flammable high voltage fluorinated solvents to attain intrinsic voltage stability in the entire electrochemical window of the high-voltage cathode material and (2) effective electrolyte additives that form a compact and robust solid-electrolyte interphase (SEI) on the surfaces of the high-voltage cathode and graphitic anode.

**COLLABORATIONS:** Kang Xu, U.S. Army Research Laboratory; Xiao-Qing Yang, BNL; Brett Lucht, University of Rhode Island; Andrew Jansen and Gregory Krumbick, ANL.

#### Milestones

- 1) Complete theoretical calculation of electrolyte solvents (fluorinated carbonate, fluorinated ether) and additives (fluorinated phosphate, fluorinated phosphazene); Validate the electrochemical properties of the available fluorinated solvents by CV and leakage current experiment. (Dec. 13) **Complete**.
- 2) Synthesize and characterize the Gen-1 electrolyte (3 linear/cyclic F-carbonate solvents + 1 additive) by NMR, FT-IR, GC-MS, DSC. (Mar. 14) **Complete**.
- 3) Evaluate the LNMO/graphite cell performance of Gen-1 electrolyte [Solvent(s) + Additive(s)]. (Jun. 14) **Ongoing – delayed to Sep. 14**
- 4) Optimize the Gen-1 high voltage F-electrolyte; Deliver 10 baseline pouch cells. (Sep. 14) **Ongoing**

## Progress Report

The anodic stability of the new fluorinated carbonate solvents synthesized in Q2 was investigated by a series of floating tests. LNMO/Li cells were assembled with formulations of fluorinated cyclic and linear carbonates (1:1 ratio, 0.5M LiPF<sub>6</sub>) as electrolytes and then fully charged and maintained at 4.9V, 5.0V, 5.1V, and 5.2V to determine the leakage currents. The data in Fig. 1 indicates the electrolytes with cyclic carbonates show similar leakage current at RT; however, tremendous differences were observed when the temperature was raised to 55°C, with FEC being the most stable and TFE-PC-E being the least stable (Fig. 1b). For the linear carbonates, the mildly fluorinated F-EMC shows a similar level of stability with that of the non-fluorinated DMC and EMC, but all the other highly fluorinated carbonates and ethers are more stable than DMC and EMC (Fig. 1c, 1d). This result provides guidance for the formulation of the 2<sup>nd</sup> generation of high-voltage electrolytes (HVE2).

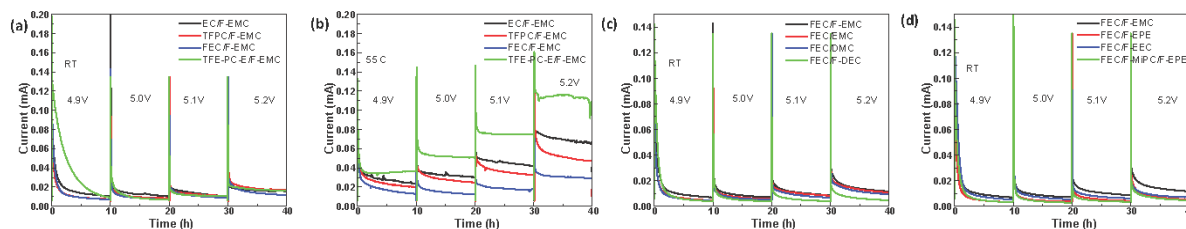


**Figure 1.** Electrochemical floating test of EC, TFPC, FEC and TFE-PC-E with F-EMC at (a) RT and (b) 55°C; Electrochemical floating test of (c) EMC, DMC, F-DEC and (d) F-EPE, F-EEC, F-MiPC with FEC compared with F-EMC/FEC at RT.

Post-test analysis of the 1<sup>st</sup> generation high-voltage F-electrolyte (HVE1) (1.0 M LiPF<sub>6</sub> in FEC/F-EMC/F-EPE=3/5/2 with 1% LiDFOB) was performed to understand the improvement and capacity fading mechanism under high voltage cycling. The transition metal dissolution of the LNMO cathode into Gen 2 and HVE1 electrolyte was examined by ICP-MS using the harvested electrolyte and harvested graphite anodes from cycled cells. Data in Table 1 strongly indicate that the HVE1 shows much less transition metal (Mn and Ni) dissolution than the conventional Gen 2 electrolyte, especially at 55°C.

**Table 1.** ICP-MS data of Mn and Ni dissolution in Gen 2 and HVE1 with and without LiDFOB additive and the harvested graphite anodes cycled at RT and 55°C (after 20 cycles).

Cycling Temp. (°C)	Electrolyte	Total Mass of Element in Harvested Electrolyte (ug)		Concentration of Element in Harvested Anode (ug/g)	
		Mn	Ni	Mn	Ni
RT	Gen 2	0.009	0.010	702	232
	HVE1 without LiDFOB	0.008	0.023	283	221
	HVE1 with LiDFOB	0.006	0.005	473	227
55°C	Gen 2	18.1	19.0	1100	370
	HVE1 without LiDFOB	3.00	1.77	1501	530
	HVE1 with LiDFOB	0.022	0.017	953	480

The morphology of the SEI on graphite anodes and CEI on LNMO cathodes was examined by TEM. Figure 2 shows a comparison between the pristine LNMO cathode (Fig. 2a-b) and a harvested LNMO cathode (Fig. 2c-d) from cycled LNMO/A12 cells with Gen 2 electrolyte. TEM study with fluorinated electrolyte is ongoing and the results will be shown in the 4<sup>th</sup> quarter report.

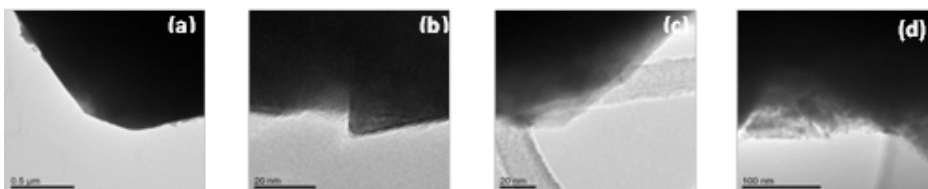


**Figure 2.** TEM image of (a,b) pristine LNMO cathode and (c,d) LNMO cathode harvested from LNMO/A12 cells with Gen 2 electrolyte cycled at 55°C for 20 cycles.

## Daikin America High Voltage Electrolyte

**PROJECT OBJECTIVE:** Development of a stable (300 – 1000 cycles), high-voltage (at 4.6 volts), and safe (self-extinguishing) formulated electrolyte.

Exploratory Development (Budget Period #1 – October 1, 2013 to January 31, 2015)

- Identify promising electrolyte compositions for high-voltage (4.6 v) electrolytes via the initial experimental screening and testing of selected compositions

Advanced Development (Budget Period #2 – February 1, 2015 to September 31, 2015)

- Detailed studies and testing of the selected high-voltage electrolyte formulations and the fabrication of final demonstration cells

**PROJECT IMPACT:** Fluorinated small molecules offer the advantage of low viscosity along with high chemical stability due to the strength of the C-F bond. Due to this bond strength, Daikin fluorochemical materials are among the most electrochemical stable materials that still have the needed performance attributes for a practical electrolyte. Such an electrolyte will allow routine operating voltages to be increased to 4.6 volts. This technological advance would allow significant cost reduction by reducing the number of cells needed in a particular application and/or allow for greater driving range in PHEV applications.

**OUT-YEAR-GOALS:** This project has a clearly defined goals for both temperature and voltage performance which are consistent with the deliverables of this proposal. Those goals are to deliver an electrolyte capable of 300 - 1000 cycles at 3.2 - 4.6 V at nominal rate with stable performance. An additional goal is to have improved high temperature (> 60°C) performance. An additional safety goal is to have this electrolyte be self-extinguishing.

**COLLABORATIONS:** At present, the team is collaborating with and receiving great advice from Vince Battaglia's group at LBNL. In addition, there are plans to collaborate with another group (TBD) for electrode surface analysis.

### Milestones

Budget Period #1 – Oct. 1, 2013 to Jan. 31, 2015

- 1) Complete identification of promising electrolyte formulations. Experimental design completed with consistent data sufficient to build models. Promising electrolyte formulations are identified which are suitable for high-voltage battery testing. **Ongoing**
- 2) Successful fabrication of 10 interim cells and delivery of cells to DOE laboratory to be specified. **Ongoing**
- 3) Electrochemical and battery cycle tests are completed and promising results are obtained which demonstrate stable performance at 4.6 volts. **Ongoing**

## Progress Report

The first PDCA cycle is complete with the exception of gassing data. First series of property data is now being compiled. The properties under consideration are: conductivity, voltage stability, gassing, and battery properties (cell impedance, first capacity, OCV). The creation of composition-property maps like the one to the right for conductivity in a FEC/EMC/fluoroether mixture is now in progress. The intention is to overlay the maps to optimize compositions for cycle testing.

Preliminary work for PDCA cycle 3 which will involve optimizing additives was completed. It is believed that FEC works well for two reasons: it improves the voltage stability of the solvent mixture and it works like an SEI layer-making additive. The comparison of FEC to Daikin fluoro-additives (fluorocyclic carbonate, HFEEC) as well as hydrocarbon (VC, EC) SEI forming additives is being examined. First charge cycle data is being used as the screening tool. The first charge data is measured for an electrolyte with and without the additive. The difference in energy between the two samples is considered to be proportional to the film formation energy, as shown in the graph on the right, a comparison of FEC/fluorocyclic carbonate/VC.

Additional data show that FEC has a bigger parasitic energy (film formation). It is unclear that all the parasitic energy is due to surface films which would be proportional to the concentration of additive as well as surface area of the carbon. Measurements were made to vary the FEC concentration and watch the parasitic energy to determine an upper limit for forming the film (*i.e.*, if the parasitic energy keeps increasing with increasing FEC content than there is another process). At present, the upper limit of the parasitic energy as a function of FEC concentration is still not known and additional experiments are being run.

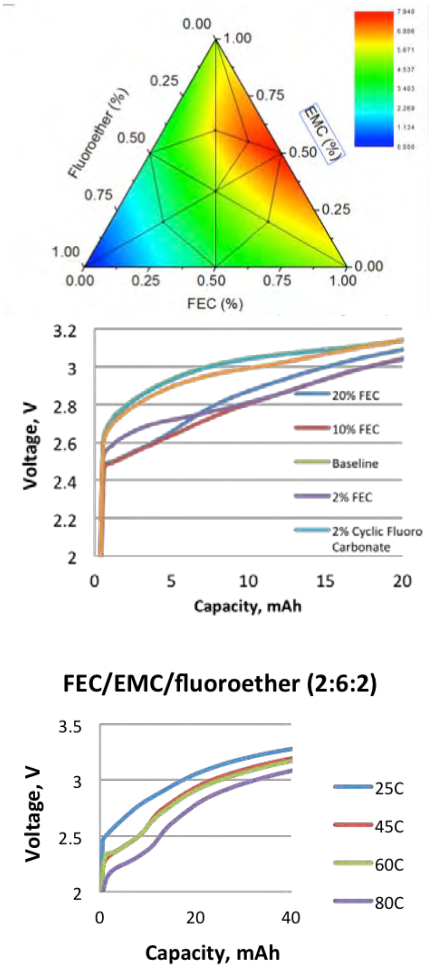
An additional round of first charge experiments were done on the same electrolyte at various temperatures. The hypothesis was that due to wetting and mobility of fluorochemicals more efficient film formation would be seen if the batteries were formed at higher temperatures. Some example data is shown here.

In general, the parasitic energy decreased with higher temperature which would be a product of more efficient film formation. However, when the batteries formed at 80°C were cycled, the cycle behavior became poorer for the batteries containing FEC. This is attributed to the poor thermal stability of the FEC shown in the last progress report. It is being investigated by DSC now.

High voltage (3.0-4.6 V) cycling is still in progress for the baseline electrolytes (1.0 M LiPF<sub>6</sub> EMC/EC 7:3, 1.2 LiPF<sub>6</sub> FEC/EMC/ Fluoroether 2:6:2). This data is being run at constant temperature now.

The agreement has been negotiated for cell fabrication at Coulometrics (Chattanooga, TN). The proposed start date will be Aug. 1, 2014. Coulometrics will do electrode fabrication and cell assembly for Daikin as well as provide use of cycling ovens.

All actives and materials of construction have been delivered for fabrication of high voltage LMNO cells. A NDA negotiation is in progress with Umicore so that Daikin can also obtain a high-voltage cathode being used at LBNL.



### Novel Non-Carbonate Based Electrolytes for Silicon Anodes

**PROJECT OBJECTIVE:** The objective of this project is to develop non-carbonate electrolytes that form a stable solid electrolyte interphase (SEI) on silicon alloy anodes, enabling substantial improvements in energy density and cost relative to current lithium ion batteries (LIBs). These improvements are vital for mass market adoption of electric vehicles. At present, commercial vehicle batteries employ cells based on  $\text{LiMO}_2$  (M = Mn, Ni, Co),  $\text{LiMn}_2\text{O}_4$ , and/or  $\text{LiFePO}_4$  coupled with graphite anodes. Next generation cathode candidates include materials with higher specific capacity or higher operating voltage, with a goal of improving overall cell energy density. However, to achieve substantial increases in cell energy density, a higher energy density anode material is also required. Silicon anodes demonstrate very high specific capacities, with a theoretical limit of 4200 mAh/g and state-of-the-art electrodes exhibiting capacities greater than 1000 mAh/g. While these types of anodes can help achieve target energy densities, their current cycle life is inadequate for automotive applications. In graphite anodes, carbonate electrolyte formulations reductively decompose during the first cycle lithiation, forming a passivation layer that allows lithium transport, yet is electrically insulating to prevent further reduction of bulk electrolyte. However, the volumetric changes in silicon upon cycling are substantially larger than graphite, requiring a much more mechanically robust SEI film.

**PROJECT IMPACT:** Silicon alloy anodes enable substantial improvements in energy density and cost relative to current Li-ion batteries. These improvements are vital for mass market adoption of EVs, which would significantly reduce  $\text{CO}_2$  emissions as well as eliminate the US dependence on energy imports.

#### **OUT-YEAR-GOALS:**

Development of non-carbonate electrolyte formulations that

- form stable SEIs on 3M silicon alloy anode, enabling coulombic efficiency > 99.9% and cycle life > 500 cycles (80% capacity) with NMC cathodes;
- have comparable ionic conductivity to carbonate formulations, enabling high power at room temperature and low temperature;
- are oxidatively stable to 4.6V, enabling the use of high energy NMC cathodes in the future; and
- do not increase cell costs over today's carbonate formulations.

#### **COLLABORATIONS:**

Wildcat is working with 3M on this project. To date, 3M is supplying the silicon alloy anode films and NMC cathode films for use in Wildcat cells.

#### Milestones

- 1) Assemble materials, establish baseline performance with 3M materials (Dec. 13) **Complete**
- 2) Develop initial additive package using non-SEI forming solvent. (Mar. 14) **Complete**
- 6) Screen initial solvents with initial additive package. (Jun. 14) **Ongoing – delayed to Sep. 14**
- 3) Design/build interim cells for DOE (Sep. 14) **Ongoing**

## Progress Report

The third quarter of this project focused on two main efforts. First, we continued to screen new additives based on hypotheses described in the original Wildcat proposal for effectiveness in PC/EMC based electrolytes. As promising additives are identified, these will be incorporated into formulations of new solvents. Second, we began to screen non-carbonate solvents and formulations.

In the continuation of screening from 2Q, an additional 99 additives were tested at two concentrations in NMC//Si alloy full cells in both EC:EMC (1:2), 1M LiPF<sub>6</sub> and PC:EMC (1:4), 1M LiPF<sub>6</sub> baseline electrolytes. Initial requirements for additives in each electrolyte were that they did not decrease either the capacity or the first cycle coulombic efficiency relative to the control (no additive). For those additives that meet these first criteria, cycle life studies were performed. As previously shown in the last report, all additives are sorted in categories based on functionalities contained within the chemical structure.

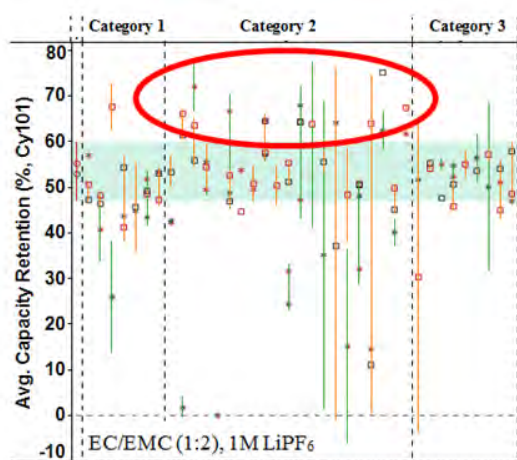


**Figure 1.** Category 2 additives show cycle life improvements (Cycle 101) in EC/EMC baseline electrolyte.

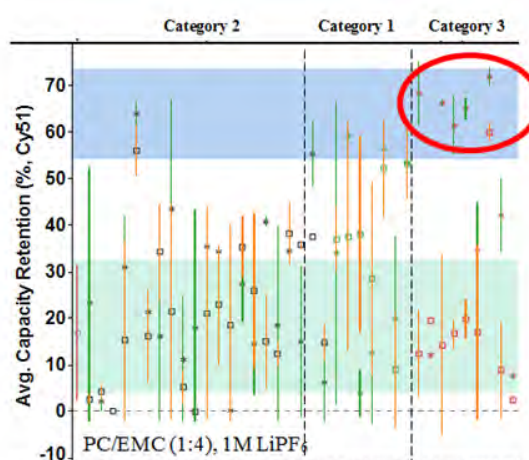


**Figure 2.** Category 3 additives show cycle life improvements (Cycle 51) in PC/EMC baseline electrolyte.

Figure 1 summarizes results for three additive categories, showing that many of the category 2 additives improve capacity retention at Cycle 101 relative to the EC/EMC control electrolyte (green band represents +/- 1 standard deviation about the mean of the control). Figure 2 shows the same additives tested in the PC/EMC control electrolyte. Standard deviations of the PC/EMC controls (green band) are large as the performance of the non-EC containing electrolyte with no additive is very poor on silicon. The blue band represents the performance of the EC/EMC electrolyte with no additives. For the PC-based electrolyte, several of the Category 3 additives give performance similar to an EC-based electrolyte. Interestingly, the Category 2 additives which performed well in an EC-based formulation do not provide the same benefit when EC is absent, and show a special synergy when combined with EC. Further mechanistic studies are in progress to elucidate different performances within categories that showed clear trends with structures.

The second major effort this quarter was initial screening of non-carbonate solvent candidates. High dielectric constant solvents (27) and low viscosity solvents (22) were screened in combination to determine 1) LiPF<sub>6</sub> solubility and 2) mechanical integrity of the electrodes during soaking. Electrochemical screening is being performed for all high permittivity solvents formulated with EMC and all low viscosity solvents formulated with EC, which passed the solubility and electrode screen. Once baseline electrochemical performance is established for these formulations, the effects of the best additive packages will be determined. The next quarter of work will be to complete the evaluation of the best formulations with the initial additive hits.

### Novel Cathode Materials and Processing Methods.

**PROJECT OBJECTIVE:** The end-goal of this project is the development of low-cost, high-energy and high-power, Mn-oxide-based cathodes for PHEV and EV vehicles. Improvement of design, composition and performance of advanced electrodes with stable architectures, facilitated by an atomic-scale understanding of electrochemical and degradation processes, is a key objective of this work. New processing routes as well as Argonne National Laboratory's comprehensive characterization facilities will be used to explore novel, surface and bulk structures both in-situ and ex-situ in the pursuit of advancing lithium-ion battery cathode materials.

**PROJECT IMPACT:** Standard Li-ion technologies are currently unable to meet the demands of next-generation PHEV and EV vehicles. Battery developers and scientists alike will take advantage of the knowledge, both applied and fundamental, generated from this project to further advance the field. In particular, it is expected that this knowledge will significantly enable progress towards meeting the DOE goals for 40-mile, all-electric range, PHEVs.

#### **OUT-YEAR-GOALS:**

- Identify composite electrode structures that mitigate or eliminate voltage fade.
- Identify and characterize surface chemistries and architectures that allow fast Li-ion transport, are stable to ~5 V, and mitigate or eliminate transition-metal dissolution.
- Scale-up, evaluate and verify promising cathode materials using Argonne National Laboratory's Scale-up and Cell Fabrication facilities.
- Take advantage of Argonne National Laboratory's user facilities (e.g., the Advanced Photon Source (APS), the Center for Nanoscale Materials (CNM), the Electron Microscopy Center (EMC) and the Argonne Leadership Computing Facility (ALCF) to build on the fundamental knowledge gained to promote and implement the rational design of new electrode materials.
- Use complementary theoretical approaches to further the understanding of electrode structures and electrochemical processes to accelerate the progress of materials development.

**COLLABORATIONS:** Joong Sun Park, Anil Mane, Jeff Elam.

#### Milestones

- 1) Evaluate the stabilization and performance of near end-member,  $\text{Li}_2\text{MnO}_3$ -containing composite electrodes. Specifically, high and low  $\text{Li}_2\text{MnO}_3$ -content electrodes. (Dec. 13) **Ongoing – see progress report**
- 2) Evaluate new synthetic routes using layered  $\text{LiMO}_2$  (M = Mn, Ni, Co) precursors to prepare composite electrode materials. (Mar. 14) **Complete**
- 3) Synthesize and characterize unique surface architectures that enable  $>200$  mAh/g at a  $>1\text{C}$  rate with complementary theoretical studies of surface structures. (Jun. 14) **Ongoing – see progress report**
- 4) Identify structures and compositions, including surface and bulk, that can deliver *ca.* 230 mAh/g at an average discharge voltage of ~3.5 V on extended cycling. (Sep. 14) **Ongoing – see progress report**

## Progress Report

It has been shown through recent results that lowering the  $\text{Li}_2\text{MnO}_3$  content,  $x$ , in  $x\text{Li}_2\text{MnO}_3 \cdot (1-x)\text{LiMO}_2$  ( $M = \text{Mn, Ni, Co}$ ) electrodes below  $x \sim 0.3$  can yield exceptional capacities ( $>200$  mAh/g) while improving low voltage characteristics. However, activation of the  $\text{Li}_2\text{MnO}_3$  component is still necessary to achieve these high capacities and, as a result, the surface of the activated electrode particles is damaged, which impairs their electrochemical behavior. As such, modifying and stabilizing the surface of cathode particles is of particular interest to improve the performance of these materials.

Atomic layer deposition (ALD) of various oxides has been shown to enhance electrochemical properties of cathode materials, particularly their rate, capacity retention, and thermal stability.  $\text{Al}_2\text{O}_3$  is known to improve these properties as a supposed HF scavenger. Unfortunately, these coatings eventually degrade as the oxide coating is slowly etched away. In this respect,  $\text{AlF}_3$  has been used to bypass the etching of  $\text{Al}_2\text{O}_3$  and create a more stable surface from the outset. Wet chemical methods do not always lead to complete and uniform fluorinated surfaces; controlled coating of particle surfaces can, therefore, be difficult. The ALD technique promises to circumvent these problems by producing uniform and controllable (e.g., thickness) surface films, although deposition of fluorides by ALD can be complex. In collaboration with the Energy Systems Division at ANL, the use of a unique ALD coating process has been developed to control the deposition of  $\text{AlW}_x\text{F}_y$  thin films on electrode particles and/or laminates. Figure 1a shows a standard  $\text{LiCoO}_2$  (Sigma Aldrich) electrode cycled between 4.4 and 2.5 V at 20 mA/g in a Li half-cell at room temperature. Because  $\text{LiCoO}_2$  shows predictably poor performance with respect to rate and capacity retention when cycled above *ca.* 4.3 V, it was selected as a baseline cathode material for these initial studies. As expected, the voltage profiles of cells with the baseline  $\text{LiCoO}_2$  cathode show a significant capacity loss and voltage decay within 25 cycles. Figure 1(b) shows the performance of the same  $\text{LiCoO}_2$  electrode after the laminate had been protected by ALD with a newly developed  $\text{AlW}_x\text{F}_y$  thin film. Remarkable stability, with capacities  $>160$  mAh/g, is observed for 50 cycles. In addition, the phase transition at *ca.* 135 mAh/g, which is well known for  $\text{LiCoO}_2$ , is reversible throughout the 50 cycles. This finding reveals that the coating has indeed modified the surface properties and not the bulk of the  $\text{LiCoO}_2$  electrode particles. Figure 1(c), which compares the performance of untreated and coated electrodes, reiterates this result. The coated electrodes demonstrate exceptional performance, showing  $>90\%$  retention of the C/8 discharge capacity at 2.5 C, and a full capacity recovery on returning to C/8 cycling. The data in Fig. 1 highlight the promise of these newly developed surface materials as well as the ALD process itself.  $\text{AlW}_x\text{F}_y$  and other F-containing compounds are being explored for improving the surface properties of other Li-metal-oxide electrode materials, including high-capacity “layered-layered” and “layered-layered-spinel” materials. The status of Tasks 1, 3 and 4 is therefore reflected as “ongoing.”

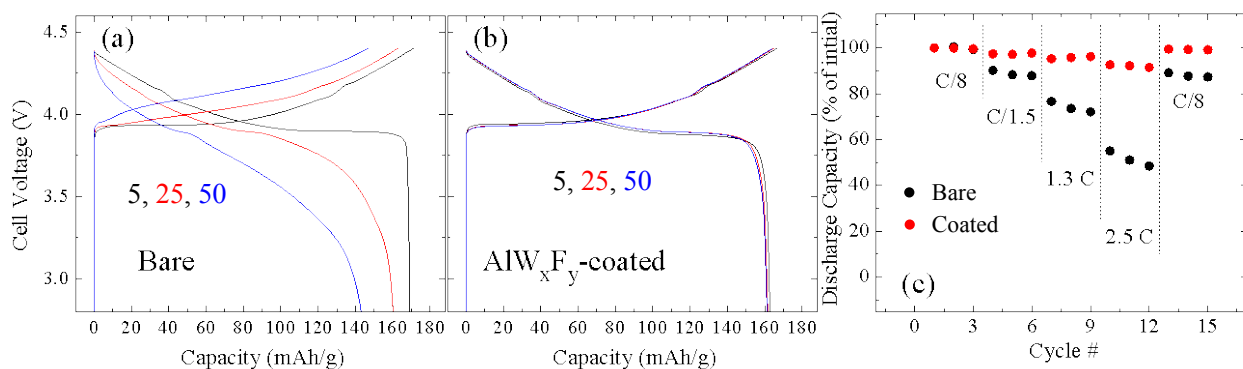


**Figure 1.** Charge and discharge profiles of cycles 5, 25, and 50 (4.4 – 2.5 V, 20 mA/g, half-cells at RT) for (a) bare and (b) ALD  $\text{AlW}_x\text{F}_y$ -coated  $\text{LiCoO}_2$ . (c) Comparison of rate capability for bare (black) and  $\text{AlW}_x\text{F}_y$ -coated (red)  $\text{LiCoO}_2$ .

### Design of High Performance, High Energy Cathode Materials

**PROJECT OBJECTIVE:** To develop high energy, high performance cathode materials including composites and coated powders, using spray pyrolysis and other synthesis techniques. The emphasis is on two systems; modified NMC materials and the high voltage spinel,  $\text{LiNi}_{0.5}\text{Mn}_{1.5}\text{O}_4$  (LNMO). Partial substitution of Ti for Co in NMCs results in higher discharge capacities (up to 225 mAh/g) without the need for a formation reaction and without risk of structural change during cycling. Experiments are directed towards optimizing the synthesis, improving cycle life, and understanding the effect of Ti substitution. For LNMO, particle size and morphology are controlled during spray pyrolysis synthesis by varying residence time, temperature, precursors and other synthetic parameters. By exploiting differences in precursor reactivity, coated materials can be produced, and composites can be prepared by post-processing techniques such as infiltration. These approaches are expected to improve cycling due to reduced side reactions with electrolytes.

**PROJECT IMPACT:** To increase the energy density of Li ion batteries, cathode materials with higher voltages and/or higher capacities are required, but safety and cycle life cannot be compromised. In the short term, the most promising materials are based on high voltage spinels or modified NMCs that do not require formation cycles or undergo structural transformations during cycling. Ti-substituted NMCs exhibit increased discharge capacity, due to improved first cycle efficiencies and are not expected to undergo structural changes or voltage decay during cycling. Optimizing LNMO particle morphologies, utilizing coatings and composites are expected to improve coulombic efficiencies and safety as well as cycle life.

**OUT-YEAR GOALS:** Two high-energy cathode systems will have been optimized for this work; LNMO and high capacity Ti-substituted NMC cathodes, which do not require activation via charge to high potentials. Materials will be synthesized by a simple, low cost spray pyrolysis method, which has potential for commercialization. This technique produces phase-pure, unagglomerated powders and allows for excellent control over particle morphologies, sizes and distributions. Coated materials will also be produced in either one or two simple steps by exploiting differing precursor reactivities during the spray pyrolysis procedure, or by first preparing hollow spheres of an electroactive material, infiltrating the spheres with precursors of the high voltage cathodes, and subsequent thermal treatment. The final result is expected to be a high energy density cathode material with good safety and cycling characteristics suitable for use in vehicular applications, which can be made by a low-cost process that is easily scalable.

**COLLABORATIONS:** Huolin Xin (BNL), Dennis Norlund, Tsu-Chien Weng and Dimosthenis Sokaras (SLAC), Mark Asta (U.C. Berkeley) and Shirley Meng (UCSD)

#### Milestones

- 1) Complete optimization of Ti-NMC synthesis with  $\text{TiOSO}_4$  precursor (Dec. 13) **Discontinued. This effort has been transferred to the ABR program**
- 2) Go/No-Go: Decision on infiltration of  $\text{LiFePO}_4$  into LNMO. Criteria: A “no go” decision will be made if attempts to prevent reaction of  $\text{LiFePO}_4$  with LNMO during processing fail (Mar. 14) **No go. Effort will be redirected towards composites with spray pyrolyzed NMCs.**
- 3) Complete soft XAS experiments on Ti-NMCs (Jun. 14) **Complete**
- 4) Go/No-Go: Decision on spray pyrolysis of NMCs. Criteria: A “no go” decision will be made if the electrochemical performance of the spray-pyrolyzed material does not equal that of the material made by co-precipitation. (Sep. 14). **Ongoing**

## Progress Report

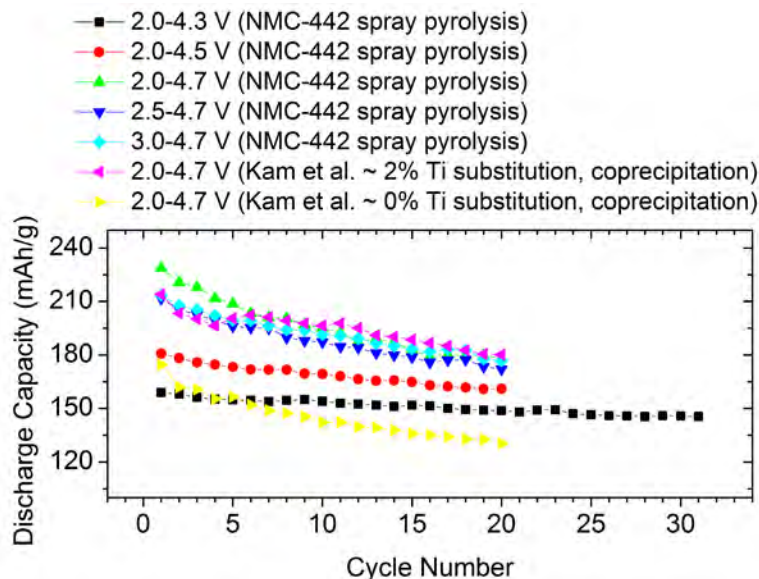


**Figure 1.** Discharge capacity retention profiles for NMC-442 materials prepared by spray pyrolysis and cycled between different voltage cutoffs. Data from Kam *et al.* JES 159 A1383 (2012) are provided for comparison.

Spray pyrolysis synthesis of cathode materials was continued this quarter with more syntheses and electrochemical measurements. One of the high-quality NMC-442 materials was electrochemically tested using a variety of voltage cutoffs and the cell impedance was analyzed before and after 20 GCPL cycles. Here only the discharge capacity retention profiles are provided, as shown in Fig. 1. Overall, the material produced by spray pyrolysis shows quite promising discharge capacities. As the upper cutoff voltage limit increases from 4.3 V to 4.7 V vs.  $\text{Li}^+/\text{Li}$  in half cells, an obvious improvement in the discharge capacity was observed and the improvement is still maintained after 20 cycles (compare black, red, and green data points). When the upper voltage limit was set at 4.7 V, tuning the lower voltage limit seemed to only change the discharge capacity insignificantly (compare green, blue and cyan data points). The discharge capacity retention profiles of the materials reported in the previous study (Kam *et al.* JES 2012) are shown here for comparison. The current materials prepared without Ti substitution showed equivalent discharge capacities compared to the 2% Ti-substituted NMC-442 material prepared by coprecipitation (compare green and magenta data points) and were superior to the NMC-442 material prepared by coprecipitation (compare green and yellow data points). Further improvements for these materials are possible with suitable aliovalent substitution and surface protection, and efforts in these respects are being implemented. Last but not least, the size of primary NMC particles has been controlled by a polymer templated method in the spray pyrolysis.

Synchrotron X-ray spectroscopy and S/TEM have also been used this quarter to characterize NMC materials undergoing numerous treatments, including electrode-electrolyte interactions. Work done in collaboration with Mark Asta (UCB), Huolin Xin (BNL), Dennis Nordlund (SSRL), Tsu-Chien Weng (SSRL), and Dimosthenis Sokaras (SSRL). A collaboration with Shirley Meng (UCSD) has been initiated to compare the behavior of stoichiometric NMCs with that of LMR-NMCs.

### High-capacity, High-voltage Cathode Materials for Lithium-ion Batteries

**PROJECT OBJECTIVE:** A significant increase in capacity and/or operating voltage is needed to make the lithium-ion technology viable for vehicle applications. This project addresses this issue by focusing on the design and development of cathode materials based on polyanions that have the possibility for reversibly inserting/extracting more than one Li-ion per transition-metal ion and/or operating above 4.3 V. Specifically, high-capacity and/or high-voltage Li transition-metal phosphate, silicate, and carbonophosphate cathodes are investigated. The major issue with the phosphate and silicate cathodes is the poor electronic and ionic transport, which limits the practical capacity, energy density, and power density. To overcome these difficulties, novel microwave-assisted solvothermal, microwave-assisted hydrothermal, and template-assisted synthesis approaches are pursued to realize controlled morphology with smaller particle size and to integrate conductive additives like graphene in a single synthesis step.

**PROJECT IMPACT:** The critical requirements for the widespread adoption of Li-ion batteries for vehicle applications are high energy, high power, long cycle life, low cost, and acceptable safety. The currently available cathode materials do not adequately fulfill these requirements. The polyanion cathodes with the novel synthesis approaches pursued in this project have the potential to significantly increase the energy and power. More importantly, the covalently bonded polyanion groups can offer excellent thermal stability and enhanced safety. The microwave-assisted synthesis approaches pursued also lower the manufacturing cost of the cathodes through a significant reduction in reaction time and temperature.

**OUT-YEAR GOALS:** The overall goal is to enhance the electrochemical performances of high-capacity, high-voltage polyanion cathode systems and to develop a fundamental understanding of their structure-composition-performance relationships. Specifically, the project is focused on enhancing the electrochemical performance of systems such as  $\text{LiMPO}_4$ ,  $\text{Li}_2\text{MP}_2\text{O}_7$ ,  $\text{Li}_2\text{MSiO}_4$ ,  $\text{Li}_3\text{V}_2(\text{PO}_4)_3$ ,  $\text{Li}_9\text{V}_3(\text{P}_2\text{O}_7)_3(\text{PO}_4)_2$ ,  $\text{Li}_3\text{M}(\text{CO}_3)(\text{PO}_4)$ , and their solid solutions with  $\text{M} = \text{Mn, Fe, Co, Ni, and VO}$ . Advanced structural, chemical, surface, and electrochemical characterizations of the materials synthesized by novel approaches are anticipated to provide in-depth understanding of the factors that control the electrochemical properties of the polyanion cathodes. For example, the possible segregation of certain cations to the surface in solid solution cathodes consisting of multiple transition-metal ions and the role of conductive graphene integrated into the polyanion cathodes can help design better-performing cathodes.

**COLLABORATIONS:** None this quarter.

#### Milestones

- 1) Establish whether or not  $\text{LiMnPO}_4$  can be aliovalently doped with  $\text{V}^{3+}$  and determine its effect on electrochemical performance. (Dec. 13) **Complete**
- 2) Demonstrate  $> 200$  mAh/g capacity with  $\text{LiVOPO}_4$  prepared by novel synthesis approaches. (Mar. 14) **Complete**
- 3) Establish whether or not  $\text{LiCoPO}_4$  can be aliovalently doped with  $\text{V}^{3+}$  and determine its effect on electrochemical performance. (Jun. 14) **Complete**
- 4) Go/No-Go: Stop the microwave-assisted synthesis if capacities are  $< 150$  mAh/g. Criteria: demonstrate  $> 150$  mAh/g capacity with  $\text{Li}_3\text{M}(\text{CO}_3)(\text{PO}_4)$  prepared by microwave-assisted synthesis. (Sep. 14) **Ongoing**

## Progress Report

This quarter's focus was the aliovalent doping of olivine  $\text{LiCoPO}_4$ . Specifically, the substitution of  $\text{V}^{3+}$  for  $\text{Co}^{2+}$  in  $\text{LiCo}_{1-3x/2}\text{V}_x\text{PO}_4$  (LCVP) with  $0 \leq x \leq 0.2$  was explored analogous to what was previously investigated with  $\text{LiFePO}_4$  and  $\text{LiMnPO}_4$ . A phase-pure tetragonal form (space group:  $\text{Pn}2_1$ ) of LCVP was first synthesized by a low-temperature microwave-assisted solvothermal (MW-ST) method at  $260^\circ\text{C}$  as the olivine form of LCVP could not be accessed. The tetragonal polymorphs were then converted to the olivine phase by heating in argon at  $525^\circ\text{C}$  (Fig. 1). The temperature dependence of the conversion of  $\text{LiCo}_{0.85}\text{V}_{0.1}\text{PO}_4$  from the tetragonal to olivine phase is shown by X-ray diffraction (XRD) in Figs. 1d-f. The compositions of the samples with varying V substitutions were verified before and after heating at  $525^\circ\text{C}$  by inductively coupled plasma analysis. The XRD data indicate the formation of single-phase olivine LCVP for  $x \leq 0.1$  and the formation of impurity phases for  $x \geq 0.125$ . However, no shifts in lattice parameters with  $x$  could be observed due to the similar ionic radii values of  $\text{V}^{3+}$  (78 pm) and  $\text{Co}^{2+}$  (79 pm). Additionally, the single-phase LCVPs disproportionate on heating to  $725^\circ\text{C}$  to give  $\text{LiCoPO}_4$  and  $\text{Li}_3\text{V}_2(\text{PO}_4)_3$ .

The Fourier transform-infrared spectroscopy (FT-IR) data shown in Fig. 2 indicate that the band corresponding to the antisymmetric stretching ( $\nu_3$ ) of  $\text{PO}_4^{3-}$  at  $1070\text{ cm}^{-1}$  in the  $x = 0$  sample shifts to lower wavenumbers while the peak corresponding to the symmetric stretching mode ( $\nu_1$ ) of  $\text{PO}_4^{3-}$  shifts to higher wavenumbers with increasing V content. The particle size of the as-synthesized samples decreases with increasing V doping as shown in Fig. 3. The morphology of the particles is maintained before and after heating at  $525^\circ\text{C}$ . Electrochemical data shown in Fig. 4 indicate that the discharge capacity increases from  $52\text{ mAh g}^{-1}$  for  $x = 0$  to  $109\text{ mAh g}^{-1}$  for  $x = 0.025$  and then decreases.

The above characterization data establishes that  $\text{LiCoPO}_4$  can be aliovalently doped, and future work will focus on further detailed characterization and on the electrochemical properties of tetragonal LCVP.

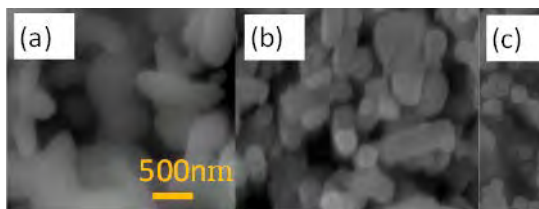


**Figure 3.** SEM images of  $\text{LiCo}_{1-3x/2}\text{V}_x\text{PO}_4$ : (a)  $x = 0.025$ , (b)  $x = 0.075$ , and (c)  $x = 0.125$ .

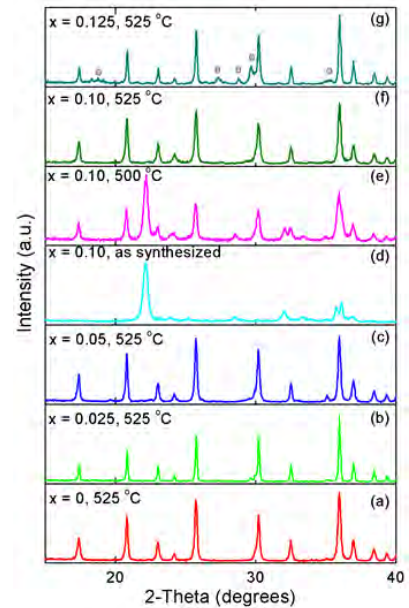


**Figure 1.** XRD patterns of  $\text{LiCo}_{1-3x/2}\text{V}_x\text{PO}_4$  before and after heating.

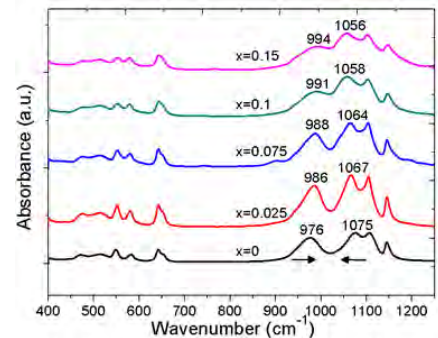


**Figure 2.** FT-IR spectra of  $\text{LiCo}_{1-3x/2}\text{V}_x\text{PO}_4$  after heating at  $525^\circ\text{C}$

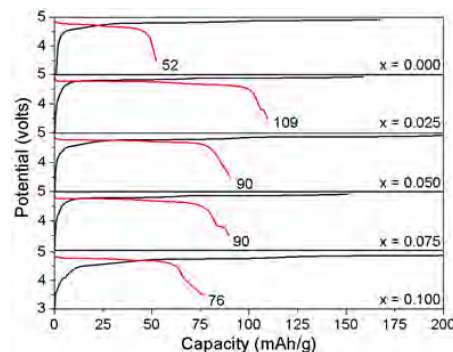


**Figure 4.** First charge/discharge profiles of  $\text{LiCo}_{1-3x/2}\text{V}_x\text{PO}_4$  after heating at  $525^\circ\text{C}$ .

### Development of High Energy Cathode Materials

**PROJECT OBJECTIVE:** The objective of this project is to develop high-energy, low-cost, and long-life cathode materials. Synthesis of Li-Mn-rich (LMR) layered composite cathodes will be further optimized by using the novel approaches we developed for high-voltage spinel in FY 2013. The working mechanism of the identified electrolyte additive will be systematically explored to reveal key factors that enable stable cycling of the LMR cathode. Advanced characterization techniques will be combined with electrochemical measurements to understand and mitigate the challenges in the LMR cathode.

**PROJECT IMPACT:** Although state-of-the-art cathode materials such as LMR layered composites have very high energy densities, their voltage fade and long-term cycling stability still need to be further improved. In this work, we will investigate the fundamental fading mechanism of LMR cathodes and develop new approaches to reduce the energy loss of these high-energy cathode materials. The success of this work will increase the energy density of Li-ion batteries and accelerate market acceptance of electrical vehicles (EV), especially for plug-in hybrid electrical vehicles (PHEV) required by the EV Everywhere Grand Challenge proposed by DOE/EERE.

**OUT-YEAR GOALS:** The long-term goal of the proposed work is to enable Li-ion batteries with a specific energy of >96 Wh/kg (for PHEVs), 5000 deep-discharge cycles, 15-year calendar life, improved abuse tolerance, and less than 20% capacity fade over a 10-year period.

#### **COLLABORATIONS:**

- Bryant Polzin (ANL): LMR electrode supply
- X.Q. Yang (LBNL): *in situ* XRD characterization during cycling
- Karim Zaghib (Hydro-Québec): material synthesis
- Kang Xu (ARL): new electrolyte

#### Milestones

- 1) Preparatory work on stable cycling of 80% capacity retention after 150 cycles high energy cathode based on  $x\text{Li}_2\text{MnO}_3 \cdot (1-x)\text{LiMO}_2$  ( $M = \text{Mn, Ni, Co}; 0 \leq x \leq 1$ ) (Dec. 13). **Complete**
- 2) Obtain stable cycling of 80% capacity retention after 150 cycles from high energy cathode based on  $x\text{Li}_2\text{MnO}_3 \cdot (1-x)\text{LiMO}_2$  ( $M = \text{Mn, Ni, Co}; 0 \leq x \leq 1$ ). (Mar. 14) **Complete**
- 3) Identify the fundamental mechanism responsible for electrolyte-additive-induced performance improvement of LMR cathode. (Jun. 14) **Complete**
- 4) Demonstrate the effects of elemental doping to improve the cycling stability of >200 cycles. (Sep. 14) **Ongoing**

## Progress Report

The working mechanism of tris (pentafluorophenyl) borane ( $(C_6F_5)_3B$ , TFPFB) as an electrolyte additive was proposed earlier this year. A thick LMR electrode (Toda HE5050 LMR-NMC) provided by ANL was used to evaluate its effectiveness. Specifically, for this quarter, the passivation film on the  $Li[Li_{0.2}Ni_{0.2}Mn_{0.6}]O_2$  (LMR) particles cycled with and without TFPFB as the additive was investigated. The results support the proposed mechanism: that TFPFB coordinates with oxygen anions/radicals thus mitigating the parasitic reactions between the cathode and the electrolyte. The milestone of identifying the working mechanism of electrolyte-additive-induced performance improvement was met for this quarter.

Figure 1 compares the TEM images of fresh LMR cathode and cycled LMR with and without TFPFB additive. Before cycling, a relatively smooth particle surface was observed (Fig. 1a). After 300 cycles, clear differences in particle surfaces was identified for electrodes (recovered from duplicate cells) cycled in electrolyte with and without TFPFB. In baseline electrolyte (Fig. 1b) without TFPFB, the image revealed a distinguishable passivation layer on the surface of a cycled  $Li[Li_{0.2}Ni_{0.2}Mn_{0.6}]O_2$  particle, with a thickness of 10 to 15 nm. In comparison, an electrode cycled in the presence of TFPFB (Figs. 1c and 1d) displayed well-maintained particle morphologies with smooth particle surfaces covered by a much thinner passivation layer. These findings substantiate the proposed hypothesis earlier in Q1 on the capability of TFPFB in modifying the interfacial reactions through the stabilization of anions/radicals as well as dissolution of oxygen species and insulating byproducts. Therefore, the underlying working mechanism of TFPFB additive was experimentally explained along with the previously reported enhanced electrochemical properties of LMR cathodes. Future work will continue to refine the synthesis approaches to further improve the electrochemical performance of LMR to accelerate its practical application.

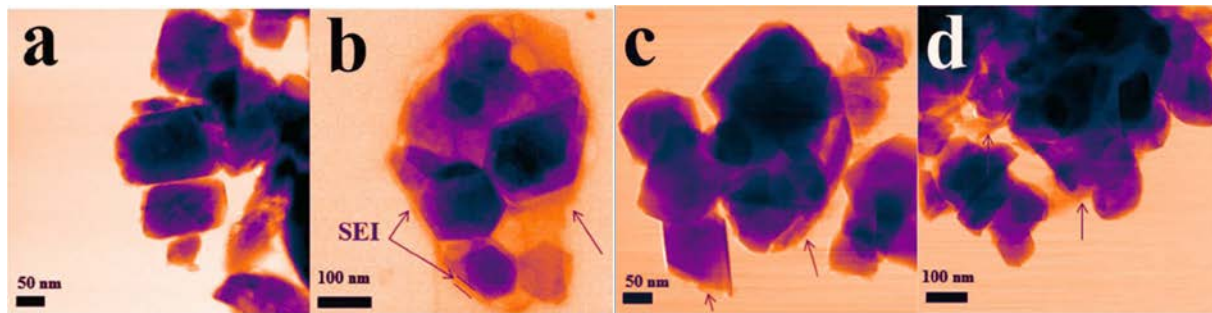


**Figure 1.** TEM images of a fresh  $Li[Li_{0.2}Ni_{0.2}Mn_{0.6}]O_2$  electrode and electrodes cycled in electrolytes without and with TFPFB additive after 300 cycles at  $C/3$ . (a) Fresh, (b) baseline, (c) 0.1 M TFPFB, (d) 0.2 M TFPFB.

### In-situ Solvothermal Synthesis of Novel High Capacity Cathodes

**PROJECT OBJECTIVE:** Develop low-cost cathode materials that offer high energy density ( $\geq 660$  Wh/kg) and electrochemical properties (cycle life, power density, safety) consistent with USABC goals.

**PROJECT IMPACT:** Present-day Li-ion batteries are incapable of meeting the 40-mile all-electric-range within the weight and volume constraints established for PHEVs by DOE and the USABC. Higher energy density cathodes are needed for Li-ion batteries to be widely commercialized for PHEV applications. This effort will focus on increasing energy density (while maintaining the other performance characteristics of current cathodes) using synthesis methods that have the potential to lower cost. The primary deliverable for this project is a reversible cathode with an energy density of about 660 Wh/kg or higher.

**OUT-YEAR GOALS:** In FY14, work on Cu-V-O cathodes will be concluded, and efforts will be directed to the synthesis and electrochemical characterization of V-based (fluoro)phosphates. Hydrothermal-based synthesis techniques for preparing ternary and/or quaternary Li-V-PO<sub>4</sub>(-X) type cathodes will be explored, either *via* direct chemical reaction or through ion exchange. By the end of FY14, structural and electrochemical characterization of two different types of Cu-V-O compounds will be completed, as well as the preparation of multiple Li-V-PO<sub>4</sub>(-X) cathodes. *In situ* x-ray analysis will be used to determine the precursors and reaction conditions for optimal synthesis procedures. Electrochemical testing, along with material characterization (*in situ* and *ex situ*), will be used to identify lithium reaction mechanisms and limitations to cycling stability of synthesized cathodes.

**COLLABORATIONS:** Jianming Bai, Lijun Wu, and Yimei Zhu (BNL), Arumugam Manthiram (U. Texas at Austin), Brett Lucht (U. Rhode Island), Zaghbir Karim (Hydro-Quebec), Jason Graetz (HRL), Peter Khalifha (StonyBrook U.), Kirsuk Kang (Seoul Nat. U., Korea), Nitash Balsara (LBNL).

#### Milestones

- 1) Complete the structural and electrochemical characterization of  $\epsilon$ -Cu<sub>x</sub>V<sub>2</sub>O<sub>5</sub> cathodes. (Dec. 13) **Complete**
- 2) Develop synthesis procedures to prepare Li-V-PO<sub>4</sub> cathodes. (Mar. 14) **Complete**
- 3) Optimize the synthesis and characterize the structural and electrochemical properties of 2<sup>nd</sup> class of Cu-V-O cathode. (Jun. 14) **Complete**
- 4) Develop synthesis procedures to prepare Li-V-PO<sub>4</sub>-X cathodes, and electrochemically characterize at least one Li-V-PO<sub>4</sub>-X compound. (Sep. 14) **Ongoing**

## Progress Report

In previous quarters, significant progress has been made in developing Cu-based vanadium oxides for use as high-capacity cathodes, among which  $\alpha$ -phase ( $\alpha$ -CuVO<sub>3</sub>) is particularly interesting for its unique 3D framework. Following the success of preparing pure  $\alpha$ -CuVO<sub>3</sub>, efforts in this quarter sought to optimize the synthesis and to make relevant structural and electrochemical characterizations, aiming to further improve its electrochemical performance. A capacity as high as 350 mAh/g (twice of commercial cathodes), along with reasonable cycling reversibility in  $\alpha$ -CuVO<sub>3</sub> electrodes is reported.

Although synthesis procedures for preparing  $\alpha$ -CuVO<sub>3</sub> have been reported previously, a new solid-state reaction procedure was developed for making the material with much higher yield and lower cost. In this study, extensive evaluation was made on the impact of key process parameters (precursors, atmosphere, pressure, and temperature of reaction) by combining *ex situ* and *in situ* synthesis techniques to develop procedures for making phase-pure  $\alpha$ -CuVO<sub>3</sub> at the lowest possible temperature (450°C, or lower). The structure of as-synthesized materials was determined by synchrotron XRD and refinement (Fig. 1).  $\alpha$ -CuVO<sub>3</sub> has a rhombohedral structure (space group: R-3 (148)), with lattice parameters of  $a = 12.855 \text{ \AA}$  and  $c = 7.194 \text{ \AA}$  and stoichiometry of about Cu<sub>6.89</sub>V<sub>6</sub>O<sub>19</sub>. Mixed valence states of Cu (+1/+2) and V (+4/+5) were identified by XAS.

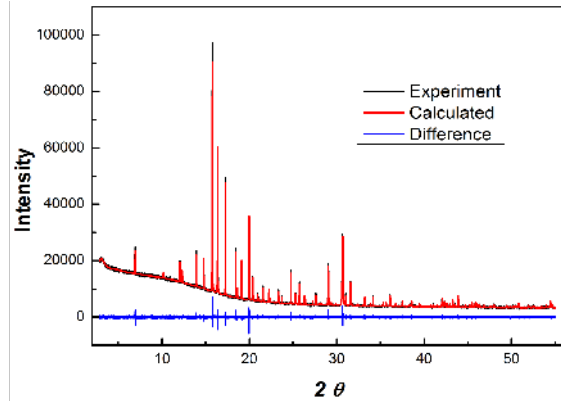


**Figure 1.** Synchrotron XRD pattern and refinement for structural analysis of synthesized  $\alpha$ -CuVO<sub>3</sub>.

The as-synthesized  $\alpha$ -CuVO<sub>3</sub> materials are generally composed of  $\mu\text{m}$ -sized particles that can only deliver very low capacity. With post-processing (using a patent-protected procedure), a capacity as high as 350 mAh/g along with reasonable cycling reversibility is obtained in  $\alpha$ -CuVO<sub>3</sub> electrodes under moderate cycling conditions (with the window 2.0 to 3.6 V and rate C/20; Fig. 2a, b). Such high reversible capacity, which has only been found in  $\alpha$ -CuVO<sub>3</sub> (not in other Cu vanadates), is attributed to its robust 3D framework that can accommodate multiple electron redox reactions. Cu dissolution in liquid electrolyte is one common issue for all Cu-containing electrodes (including  $\alpha$ -CuVO<sub>3</sub>) during cycling in batteries. Given the extremely high capacity,  $\alpha$ -CuVO<sub>3</sub> is a potentially appealing cathode for use in solid-state batteries.

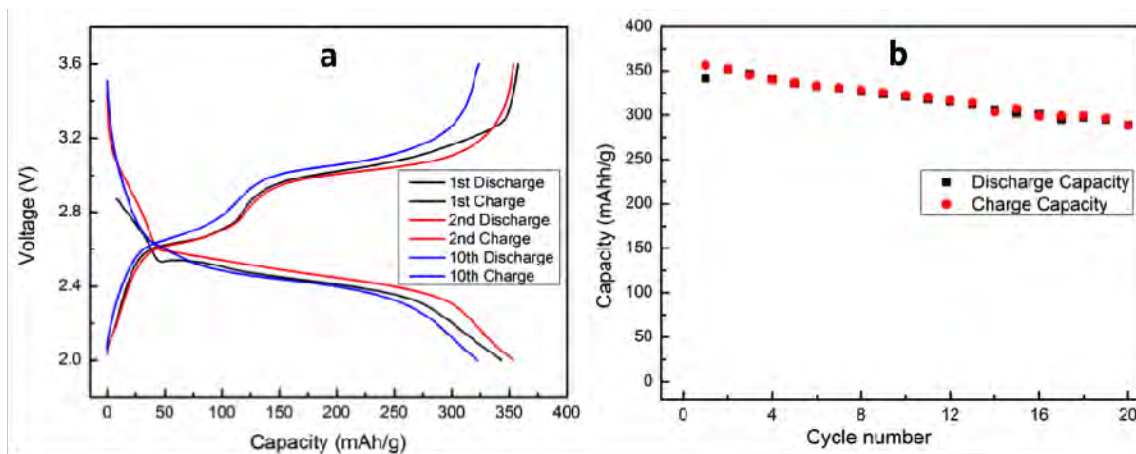


**Figure 2.** Electrochemical properties of  $\alpha$ -CuVO<sub>3</sub> electrodes, (a) voltage profiles, and (b) cycling performance under galvanostatic cycling at a moderate rate (C/20) between 2.0-3.6 V.

## Lithium-bearing Mixed Polyanion (LBMP) Glasses as Cathode Materials

**PROJECT OBJECTIVE:** Develop mixed polyanion glasses as potential cathode materials for Li-ion batteries with superior performance to lithium iron phosphate for use in electric vehicle applications. Modify compositions of mixed polyanion glasses to provide higher electrical conductivities, specific capacities, and specific energies than similar crystalline polyanionic materials. Test mixed polyanion glasses in coin cells for electrochemical performance and cycleability. The final goal is to develop mixed polyanion glass compositions for cathodes with specific energies up to near 1,000 Wh/kg.

**PROJECT IMPACT:** The projected performance of glass cathode materials addresses the Vehicle Technology Multi-Year Plan goals of higher energy densities, excellent cycle life, and low cost. Mixed polyanion glasses offer the potential of exceptional cathode energy density up to 1,000 Wh/kg, excellent cycle life from a rigid polyanionic framework, and low cost conventional glass processing.

**OUT-YEAR GOALS:** The composition of successful mixed polyanion glasses with multivalent transitions will be used as the basis to model, produce, and electrochemically test glasses from multiple polyanion systems (*e.g.*, phosphates, borates, silicates), polyanion substitutions (*e.g.*, vanadate, molybdate), and transition metal contents. The electrochemical performance of these compositionally varied glasses will be used to develop optimized glass compositions to obtain maximum specific energy within a desirable voltage window. Cathode processing of the most promising mixed polyanion glasses will be refined to obtain desired cycling and rate performance. Complex mixed polyanion glasses will be modeled, and those glasses with excellent predicted properties will be produced and tested. In-depth electrochemical testing will be performed on the most successful mixed polyanion glasses. The predicted and experimentally verified electrochemical performances from computational thermodynamic models for different glass systems will be used to develop a summary perspective on the design of mixed polyanion glasses for use as cathodes.

**COLLABORATIONS:** Worked with Kyler Carroll (MIT) to perform XAS at the National Synchrotron Light Source at BNL in order to measure the valence states of transition metal cations in *ex situ* glass cathodes.

### Milestones

- 1) Synthesize, characterize, and perform electrochemically testing on a mixed polyanion glass that is theoretically capable of a multi-valent transition. (Dec. 13) **Complete**
- 2) Demonstrate the effect of submicron particle size on the electrochemical performance of mixed polyanion glass cathodes. (Mar. 14) **Complete**
- 3) Measure the electrical conductivities of a series of mixed polyanion glasses as a function of polyanionic substitution. (Jun. 14) **Complete**
- 4) Synthesize, characterize, and perform electrical testing on at least four different glass cathode compositions with theoretical specific energies exceeding lithium iron phosphate. (Sep. 14) **Ongoing; completed 3 out of 4 glass cathode materials.**

## Progress Report

Mixed cation content (usually Fe) has been shown in the literature to improve the electrochemical performance of crystalline, polyanion, cathode materials, although solubility of the second cation into the crystal structure can often be limited. Glass structures typically permit wide variation in the cation content without phase separation, so the effect of mixed cation content on glass cathodes is being explored. Two mixed cation/mixed polyanion (MC/MP) glasses have been produced: manganese iron metaphosphate/vanadate and copper iron metaphosphate/vanadate. A series of iron metaphosphate/vanadate glasses have also been produced as a baseline to highlight the effect of mixed cation content. Electrical conductivity has been measured on this series of glasses by impedance spectroscopy of glass splats using sputtered gold electrodes (Fig. 1). Electrical conductivity and electrochemical performance of the MC/MP glasses will soon be compared to the iron metaphosphate/vanadate glasses to determine the mixed cation effect.

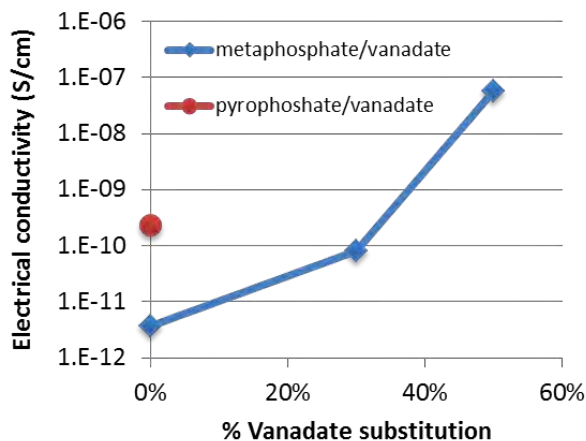


**Figure 1.** Electrical conductivity measurements on iron phosphate/vanadate glasses

Nickel (II) metaphosphate/vanadate and ruthenium (IV) metaphosphate/vanadate glasses were produced and electrochemically tested in order to further validate model predictions of glass-state conversion reaction voltages. According to modeling predictions by Northwestern University based on crystalline polyanionic material data from the Open Quantum Materials Database, nickel (II) metaphosphate and nickel (II) metavanadate theoretically would have conversion reaction voltages of 2.65 V and 2.49 V, respectively. Nickel (II) metaphosphate/vanadate glass had a maximum voltage for the glass-state conversion reaction at *ca.* 2.1 V in standard battery testing and *ca.* 2.25 V from GITT testing, which showed reasonable agreement with the modeling predictions. Ruthenium (III) metaphosphate had a model predicted voltage of 3.71 V. A higher valence state of ruthenium would be expected to result in an even higher voltage. The ruthenium (IV) metaphosphate/vanadate glass exhibited a low-capacity (*ca.* 30 mAh/g) reaction at *ca.* 4.1V. It is currently unknown if this reaction is a partial intercalation reaction or a partial glass-state conversion reaction.

## Lithium Batteries of Higher Capacity and Voltage

**PROJECT OBJECTIVE:** To develop a solid  $\text{Li}^+$  electrolyte that (1) can block dendrites from a  $\text{Li}^0$  anode, (2) has a  $\text{Li}^+$  conductivity  $\sigma_{\text{Li}} > 10^{-4} \text{ S cm}^{-1}$ , (3) is stable in different liquid electrolytes at anode and cathode, (4) has a low impedance for  $\text{Li}^+$  transfer across a solid/liquid electrolyte interface, (5) is capable of low-cost fabrication as a thin, mechanically robust film.

**PROJECT IMPACT:** A solid  $\text{Li}^+$ -electrolyte separator would permit use of a  $\text{Li}^0$  anode, thus maximizing energy density for a given cathode, and liquid flow-through and air cathodes of high capacity as well as high-voltage solid cathodes given two liquid electrolytes having different windows.

**OUT-YEAR-GOALS:** Prepare an oxide/polymer composite  $\text{Li}^+$  electrolyte having a  $\sigma_{\text{Li}} > 10^{-4} \text{ S cm}^{-1}$  that can be fabricated at low cost as a mechanically robust membrane and can demonstrate a viable performance of a test cell with a  $\text{Li}^0$  anode and a variety of solid, liquid, and air cathodes. Prepare dense garnet membranes with  $\sigma_{\text{Li}} \approx 5 \times 10^{-4} \text{ S cm}^{-1}$  that have a reduced impedance for  $\text{Li}^+$  transfer across the oxide interface with a liquid electrolyte.

**COLLABORATIONS:** Li/S cell with Arumugam Manthiram (UT Austin), and membrane characterization with Karim Zaghib (Hydro-Québec).

### Milestones

- 1) **Go-No/Go:** Polymer composite membrane project will stop if demonstration of a liquid cathode without crossover of the redox molecule and blocking of Li dendrites with a PEO/ $\text{Al}_2\text{O}_3$  membrane fails. **Criteria:** Suppression of drying of anolyte with an  $\text{Al}_2\text{O}_3$ /PEO membrane. Elimination of redox-molecule crossover to anolyte. Demonstration that Li dendrites are blocked. (Dec. 13) **Go for polymer composite membrane project**
- 2) Determine TEM garnet surface structure in contact with a liquid electrolyte. Design of a surface coat of a garnet membrane to minimize impedance of  $\text{Li}^+$  transfer across garnet surface. (Sep. 14) **Discontinued - Stopped garnet work as the garnet is unstable in water**
- 3) Prepare dense  $\text{Li}^+$ -electrolyte alternative to garnet and test impedance of  $\text{Li}^+$  transfer across it. (Jun. 14) **Delayed to Sep. 14 - searching for alternative  $\text{Li}^+$  electrolyte**
- 4) Construct and test a Li/S cell with a solid  $\text{Li}^+$ -electrolyte separator. (Sep. 14) **Ongoing**

## Progress Report

With regard to milestones (2) and (3), in the last report, it was confirmed that the garnet electrolytes  $\text{Li}_{7-x}\text{La}_3\text{Zr}_{2-x}\text{Ta}_x\text{O}_{12}$  were attacked by water. A solid  $\text{Li}^+$  electrolyte was needed in order to develop a dual electrolyte cell to enable the air cathode, which requires an aqueous catholyte. Thus, exploration has begun for alternative  $\text{Li}^+$  electrolytes stable in water.

A PEO/ $\text{Al}_2\text{O}_3$  composite electrolyte membrane (Fig. 1) was modified to have better  $\text{Li}^+$  transport properties since the single bond oxygen of the PEO component allows fast  $\text{Na}^+$  transport, but not  $\text{Li}^+$  transport. The new strategy is to replace the C-O unit with F<sup>-</sup> ions to reduce the interaction between  $\text{Li}^+$  and the polymer backbone.

Thiol-ene chemistry was adopted to fabricate the new membrane presented in Fig. 1. Unlike the PEO/ $\text{Al}_2\text{O}_3$  membrane, an additional solvent (e.g. THF) was necessary to mix the reactants because the tetrathiol cross-linker has hydrophilic ester groups and the fluorinated hexyl monomer is hydrophobic. The monomer solution was polymerized under UV radiation.

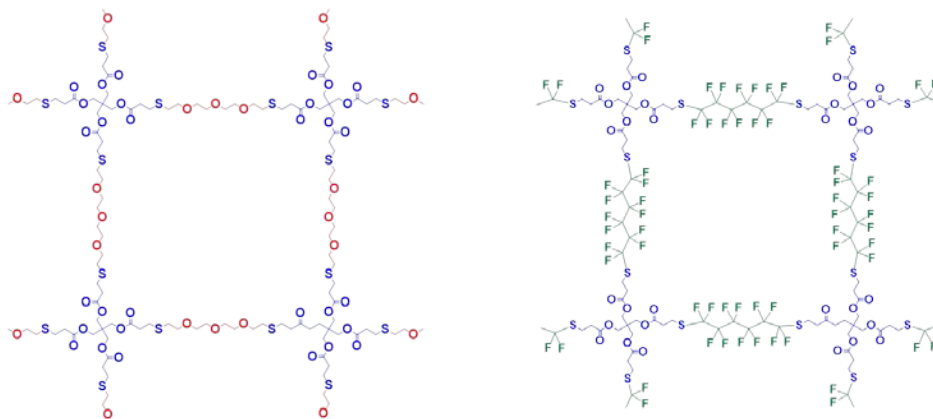


**Figure 1.** Cross-linked polymer electrolyte membrane structures. Tetrathiol cross-linkers are connected to polyethylene oxide units (left) or fluorinated alkyl units (right).

A transparent, cross-linked, polymer membrane was successfully obtained by the thiol-ene method described above, and it has been tested as a Li-ion battery membrane. The  $\text{LiFePO}_4$  cathode based cell shows better performance than cells with the PEO/ $\text{Al}_2\text{O}_3$  membrane in preliminary results with Hydro-Québec, which suggests this approach is acceptable. Process optimization is underway to control membrane thickness and to enhance dimensional stability of the membrane. Incorporation of ceramic particles and  $\text{Li}^+$  salt will also be pursued to block Li dendrites and to increase  $\text{Li}^+$  conductivity, respectively.

### Interfacial Processes - Diagnostics

**PROJECT OBJECTIVE:** The main objective of this task is to obtain detailed insight into the dynamic behavior of molecules, atoms, and electrons at electrode/electrolyte interfaces of intermetallic anodes (Si) and high voltage Ni/Mn-based materials at a spatial resolution that corresponds to the size of basic chemical or structural building blocks. The aim of these studies is to unveil the structure and reactivity at hidden or buried interfaces and interphases that determine battery performance and failure modes. To accomplish these goals novel far- and near-field optical multifunctional probes must be developed and deployed *in situ*. The proposed work constitutes an integral part of the concerted effort within the BATT Program and it attempts to establish clear connections between diagnostics, theory/modeling, materials synthesis, and cell development efforts.

**PROJECT IMPACT:** This project provides a better understanding of the underlying principles that govern the function and operation of battery materials, interfaces and interphases, which is inextricably linked with successful implementation of high energy density materials such as Si and high voltage cathodes in Li-ion cells for PHEVs and EVs. This task also involves the development and application of novel innovative experimental methodologies to study and understand the basic function and mechanism of operation of materials, composite electrodes, and Li-ion battery systems for PHEV and EV applications.

**OUT-YEAR GOALS:** Design and employ novel and sophisticated *in situ* analytical methods to address the key problems of the BATT baseline chemistries. The proposed experimental strategies combine imaging with spectroscopy aimed at probing electrodes at an atom, molecular, or nanoparticulate level to unveil structure and reactivity at hidden or buried interfaces and determine electrode performance and failure modes in baseline  $\text{Li}_x\text{Si}$ -anodes and high-voltage LMNO cathodes. The main goal is to gain insight into the mechanism of surface phenomena on thin-film and monocrystal Sn and Si intermetallic anodes and evaluate their impact on the electrode long-term electrochemical behavior. Comprehensive fundamental study of the early stages of SEI layer formation on polycrystalline and single crystal face Sn and Si electrodes will be carried out. *In situ* and *ex situ* far- and near-field scanning probe spectroscopy will be employed to detect and monitor surface phenomena at the intermetallic anodes high-voltage (>4.3V) model and composite cathodes.

**COLLABORATIONS:** Vince Battaglia (LBNL), Chunmei Ban (NREL)

#### Milestones

- 1) Determine the origin of fluorescent species that are produced at high-energy Li-ion cathodes. (Dec. 13) **Complete**
- 2) Resolve SEI layer chemistry of Si model single crystal anodes (collaboration with the BATT Anode Group. (Mar. 14) **Complete**
- 3) Characterize interfacial phenomena in high-voltage composite cathodes (collaboration with the BATT Cathode Group. (Jun. 14) **Complete**
- 4) Go/No-Go: Stop development of *in situ* near-field techniques, if the preliminary experiments fail to deliver adequate surface-bulk selectivity. Criteria: Demonstrate feasibility of *in situ* near-field techniques to study interfacial phenomena at Li-battery electrodes. (Sep. 14) **Ongoing**

## Progress Report

In the third quarter of FY2014, the focus was on the investigation of surface phenomena in a high-voltage Ni/Mn-based system in organic carbonate electrolytes. Previous studies (Q1 FY2014) revealed formation of Ni and Mn fluorescent species at the  $\text{LiNi}_{0.5}\text{Mn}_{1.5}\text{O}_4$ /electrolyte interface as the result of reactions between the cathode  $\text{LiNi}_{0.5}\text{Mn}_{1.5}\text{O}_4$  atoms and products of oxidation of organic carbonate solvents. Although the oxidation state of manganese deposited on the anode surface was identified as Mn(II) and there is a correlation between deposited Mn concentration and observed impedance rise, the true nature of the Mn species role in the poisoning mechanism remains unclear.

Figure 1a displays *ex situ* average Raman spectra of aged graphite from a cell that was cycled 625 times against a  $\text{LiNi}_{0.5}\text{Mn}_{1.5}\text{O}_4$  composite electrode and reference spectra of trimeric Mn(II) bisacetylacetonate, Mn(II) oxalate, and Mn(II) carbonate. The fluorescent background of the Raman spectrum of the cycled graphite electrode is very similar to that of Mn(II)acetylacetonate and confirms the presence of Mn metal complexes with  $\beta$ -diketone ligands. This is supported by the Mn K-edge transmission X-ray absorption near edge spectra (XANES) of the graphite negative electrode shown in Fig. 1b, which exhibit spectral features similar to that of Mn(II) bisacetylacetonate and Mn(II) oxalate. A linear combination analysis revealed that the Mn species present within the SEI is mainly Mn(II)(acac)<sub>2</sub>.

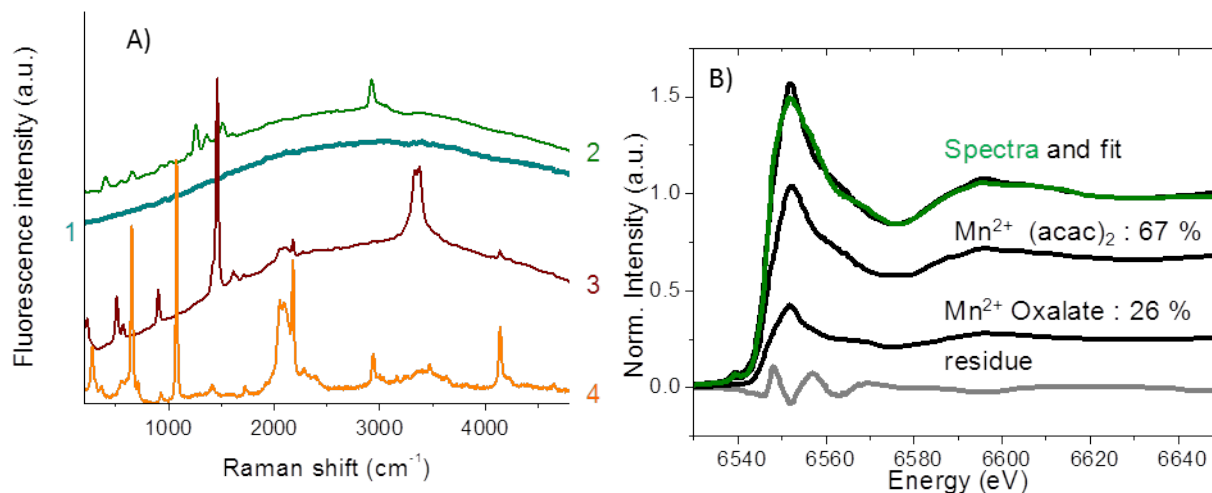


**Figure 1.** a) Normalized *ex situ* Raman spectra of the aged graphite (1) compared with Mn(II) bisacetylacetonate (2), Mn(II) oxalate (3) and Mn(II) carbonate (4), b) Linear combination analysis results for the normalized Mn K-edge transmission XANES spectra of the cycled graphite electrode, using reference spectra of Mn(II) bisacetylacetonate, and Mn(II) oxalate.

These new results are consistent with recent literature reports of Ni(II) and Mn(II) species in the SEI layer. However, the exact nature of these species revealed in this work clearly points at Ni(II) and Mn(II) complexes. A non-uniform distribution of these compounds accumulating in the SEI layer may indicate different chemical affinity of those species to the SEI basic building blocks. *In situ* and *ex situ* LIB and near-field IR measurements are underway to further study the mechanism of metal complex formation and its detrimental effect on Li-ion transport in the SEI layer and the electrode impedance (Milestone 4.)

## Advanced *In situ* Diagnostic Techniques for Battery Materials

**PROJECT OBJECTIVE:** The primary objective of this proposed project is to develop new advanced *in situ* material characterization techniques and to apply these techniques to support the development of new cathode and anode materials for the next generation of Li-ion batteries (LIBs) for PHEVs. In order to meet the challenges of powering the PHEV, LIBs with high energy and power density, low cost, good abuse tolerance, and long calendar and cycle life must be developed.

**PROJECT IMPACT:** In the Multi Year Program Plan (MYPP) of Vehicle Technology Program (VTP), the goals for battery were described as: “Specifically, lower-cost, abuse-tolerant batteries with higher energy density, higher power, better low-temperature operation, and longer lifetimes are needed for the development of the next-generation of HEVs, PHEVs, and EVs.” If this project is successfully carried out, the knowledge learned from diagnostic studies and collaborations with US industries and international research institutions through this project will help US industries to develop new materials and processes for new generation of Li-ion batteries in their efforts to reach these VTP goals.

**OUT-YEAR GOALS:** For the Si-based anode materials, the capacity fading needs to be resolved, which is caused by the pulverization of the Si particles during cycling. In order to overcome these barriers, fundamental understanding of the physical and chemical changes of the cathode and anode materials in the bulk and at the surface are critical. This project will focus on applying integrated advanced *in situ* diagnostic characterization techniques to investigate these issues, through collaborative efforts with synthesis groups and industrial end users.

**COLLABORATIONS:** The BNL team will work closely with material synthesis groups at ANL (Mike Thackeray and Khalil Amine) for the high energy composite; at UT Austin (Ram Manthiram) for the high voltage spinel; and at PNNL (Jun Liu and Jason Zhang) for the Si-based anode materials. Such interaction between the diagnostic team at BNL and synthesis groups of these other BATT members will catalyze innovative design and synthesis of advanced cathode and anode materials. The team will also collaborate with industrial partners at General Motors (Yan Wu), Duracell (In Tae Bae), and Johnson Controls (Sung-Jin Cho and Frederic Bonhomme) to obtain feedback information as battery end users.

### Milestones

- 1) Complete the studies of the kinetic properties of  $\text{Li}_{1.2}\text{Ni}_{0.15}\text{Co}_{0.1}\text{Mn}_{0.55}\text{O}_2$  [ $0.5\text{Li}(\text{Ni}_{0.375}\text{Co}_{0.25}\text{Mn}_{0.375})\text{O}_2 \cdot 0.5\text{Li}_2\text{MnO}_3$ ] high energy density cathode materials during constant current charge using x-ray absorption spectroscopy. (Dec. 13) **Complete**
- 2) Complete the development of using quick x-ray absorption spectroscopy technique to study the kinetic properties of  $\text{Li}_{1.2}\text{Ni}_{0.15}\text{Co}_{0.1}\text{Mn}_{0.55}\text{O}_2$  [ $0.5\text{Li}(\text{Ni}_{0.375}\text{Co}_{0.25}\text{Mn}_{0.375})\text{O}_2 \cdot 0.5\text{Li}_2\text{MnO}_3$ ] high energy density cathode materials during constant voltage charge. (Mar. 14) **Complete**
- 3) Complete the *in situ* x-ray diffraction studies of Fe-substituted high-voltage spinel during charge-discharge cycling. (Jun. 14) **Complete**
- 4) Complete the *in situ* x-ray absorption studies of Fe-substituted high-voltage spinel during charge-discharge cycling. (Sep. 14) **Ongoing**

## Progress Report

In the 3rd quarter of FY 2014, BNL has been focused on studying the *in situ* XRD spectrographs of Fe-substituted, high-voltage spinel during charge-discharge cycling, for Milestone 3. This milestone was successfully completed.

The *in situ* XRD spectra for an Fe-substituted  $\text{LiNi}_{1/3}\text{Fe}_{1/3}\text{Mn}_{4/3}\text{O}_4$  sample were collected at 11-BM, at the Advanced Photon Source (APS) at ANL. The wavelength of the x-ray sources was  $0.414 \text{ \AA}$ . The cells were composed of a Li-metal anode, a porous separator, and an Al foil pasted with 4 mg of active cathode material mixed with carbon black powders and PVdF binder. These cell components were assembled in an Al pouch cell (coated with nylon and polypropylene) with an electrolyte solution (1 M  $\text{LiPF}_6$  in a 1:1 volume ratio mixture of ethylene carbonate and dimethyl carbonate) in a glove box with an Ar atmosphere. XRD patterns were collected continuously during the charging/discharging process with about 30 minutes for each scan. A cycling current of  $46 \mu\text{A}$  corresponding to a C/10 rate was applied to the cell.

The *in situ* XRD spectra for the Fe-substituted  $\text{LiNi}_{1/3}\text{Fe}_{1/3}\text{Mn}_{4/3}\text{O}_4$  sample are shown in Fig. 1 together with the charge-discharge voltage curve. During charge, it is clearly seen that the reaction proceeds in a solid-solution fashion until 0.4Li was extracted from the material. After that, phase separation occurs and each phase reacts in a solid-solution fashion, leading to two solid-solution reactions taking place simultaneously. This also happened in the following discharge process until around 0.6Li was inserted back into the material. Afterwards, the two phases merge into one and reacts in a single solid-solution fashion until the end of discharge. This behavior is quite different from the non-substituted, high-voltage spinel  $\text{Li}_x\text{Ni}_{0.5}\text{Mn}_{1.5}\text{O}_4$ . In both charge and discharge,  $\text{Li}_x\text{Ni}_{0.5}\text{Mn}_{1.5}\text{O}_4$  exhibits a two-phase reaction for  $0 < x < 0.5$  and another two phase reaction for  $0.5 < x < 1$  absent a solid solution region. These results are being analyzed further for integration into future publications.

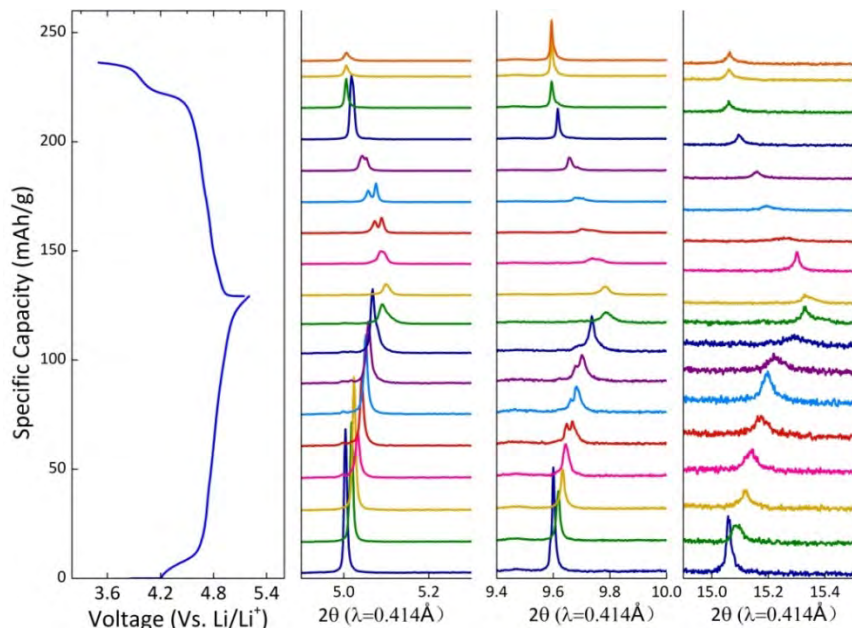


**Figure 1.** *In situ* XRD spectra for Fe-substituted  $\text{LiNi}_{1/3}\text{Fe}_{1/3}\text{Mn}_{4/3}\text{O}_4$  high-voltage spinel sample during charge-discharge cycle between 3.6 to 5.0V.

### NMR and Pulse Field Gradient Studies of SEI and Electrode Structure

**PROJECT OBJECTIVE:** The formation of a stable surface electrode interphase (SEI) is critical to the long-term performance of a battery, since the continued growth of the SEI on cycling/aging results in capacity fade (due to Li consumption) and reduced rate performance due to increased interfacial resistance. Although arguably a (largely) solved problem with graphitic anodes/lower voltage cathodes, this is not the case for newer, much higher capacity anodes such as silicon, which suffer from large volume expansions on lithiation, and for cathodes operating above 4.3 V. Thus it is essential to identify how to design a stable SEI. The objectives are to identify major SEI components, and their spatial proximity, and how they change with cycling. SEI formation on Si vs. graphite and high voltage cathodes will be contrasted. Li<sup>+</sup> diffusivity in particles and composite electrodes will be correlated with rate. The SEI study will be complemented by investigations of local structural changes of high voltage/high capacity electrodes on cycling.

**PROJECT IMPACT:** The first impact of this project will be an improved, molecular based understanding of the surface passivation (SEI) layers that form on electrode materials, which are critical to the operation of the battery. Second, we will provide direct evidence for how additives to the electrolyte modify the SEI. Third, we will provide insight to guide and optimize the design of more stable SEIs on electrodes beyond LiCoO<sub>2</sub>/graphite.

**OUT-YEAR GOALS:** The goals of this project are to identify the major components of the SEI as a function of state of charge and cycle number different forms of silicon. We will determine how the surface oxide coating affects the SEI structure and establish how the SEI on Si differs from that on graphite and high voltage cathodes. We will determine how the additives that have been shown to improve SEI stability affect the SEI structure and explore the effect of different additives that react directly with exposed fresh silicon surfaces on SEI structure. Via this program, we will develop new NMR based methods for identifying different components in the SEI and their spatial proximities within the SEI, which will be broadly applicable to the study SEI formation on a much wider range of electrodes. These studies will be complemented by studies of electrode bulk and surface structure to develop a fuller model with which to describe how these electrodes function.

**COLLABORATIONS:** Brett Lucht (Rhode Island), Kristin Persson (LBNL), Jordi Cabana (UICC), Stan Whittingham (SUNY Binghamton), Shirley Meng (UCSD) and Stephan. Hoffman (Cambridge.)

#### Milestones

- 1) Identify major components (LiF, phosphates, carbonates and organics) in Si SEI by NMR methods. (Dec. 13). **Complete**
- 2) Correlate presence of SEI components with cycle number and depth of discharge of Si. Complete preliminary TOF-SIMS measurements to establish viability of approach. (Sep. 14) **Ongoing – a much bigger task than initially anticipated (NMR). Difficulties encountered with sample reproducibility and Si cracking (TOF-SIMS)**
- 3) Identify SEI components in the presence of FEC and VC in Si and determine how they differ from those present in the absence of additives. (Jun. 14) **Ongoing – delayed to Sep. 14. Studies on reduced VC and FEC model compounds complete.**
- 4) Go/No-Go: Stop Li<sup>+</sup> PFG diffusivity measurements of electrodes. Criteria: If experiments do not yield correlation with electrochemical performance. (Sep. 14) **PFG studies initiated.**

## Progress Report

The decomposition (SEI) products that form on Si have been investigated by using NMR methods. Initial experiments focused on a Si-carbon electrode with no binder, to maximize the amount of SEI formed (Fig. 1). Electrodes were investigated at the top of charge (fully delithiated) so as to avoid complications due to air- and moisture-sensitive  $\text{Li}_x\text{Si}$  phases. A range of NMR probes have been used, including  $^1\text{H}$ ,  $^7\text{Li}$ ,  $^{19}\text{F}$  and  $^{13}\text{C}$  NMR single and double resonance experiments to probe spatial proximity between species. The first challenge to be addressed was how to work up the electrodes for further NMR analysis. In initial experiments, the electrodes were soaked in DMC to remove excess electrolyte. However, this resulted in considerable removal of the SEI, leading to very few observable signals in the NMR measurements. Therefore, it was decided not to rinse any of the samples before performing the experiments, realizing that this would result in considerable electrolyte being trapped in the SEI. However, the goal was to identify all the products of the SEI. Shorter washing treatments in future experiments will be explored, once a baseline of all the species present is established.

Initial experiments used  $^1\text{H}$ ,  $^{19}\text{F}$  and  $^7\text{Li}$  NMR to characterize the SEI. The  $^{19}\text{F}$  NMR spectra were dominated by the  $\text{LiPF}_6$  signals from dried electrolyte (Fig. 2).  $\text{LiF}$  was also observed, but this phase was only observed in significant concentrations when samples were exposed to moisture (*e.g.*, by washing with reagents that had not been dried carefully, leaving samples in nominally air-tight NMR rotors, *etc.*). Thus, the  $\text{LiF}$  that forms in the system (at least) reflects moisture introduced by the subsequent handling of the electrode and is not inherent to the SEI formation mechanism *per se*. This may be very different when, *e.g.*, CMC binders are used, which are more difficult to fully dry.  $^7\text{Li}$  1D NMR spectra, while being less useful diagnostically, were combined with 2D NMR experiments to determine which phases contained Li. The  $^1\text{H}$  spectra were also dominated by EC but, when combined with  $^1\text{H}$ - $^{13}\text{C}$ , correlation experiments provided signatures for a series of decomposition products. Experiments are now in progress to analyze the 1 and 2D  $^{13}\text{C}$  spectra in more detail.

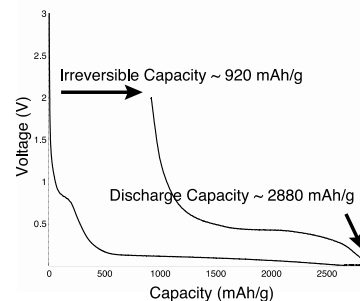


**Figure 1.** The first lithiation cycle of a Si:superP carbon electrode (1:1 Si:C ratio by mass). Electrolyte = EC/DMC. Galvanostatic cycling was performed at a rate of  $C/75$  based on a theoretical capacity of  $3579 \text{ mAhg}^{-1}$ .

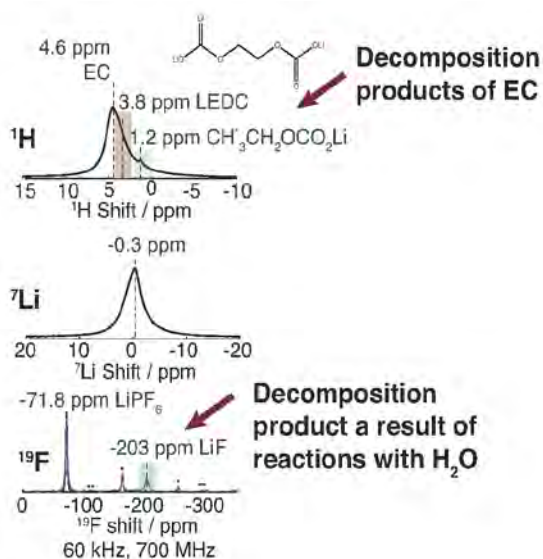


**Figure 2.** NMR spectra obtained after 1 charge/discharge cycle (see Fig. 1) of the Si:C electrode.

### Simulations and X-ray Spectroscopy of Li-S Chemistry

**PROJECT OBJECTIVE:** Li-S cells are attractive targets for energy storage applications as their theoretical specific energy of 2600 Wh/kg is much greater than the theoretical specific energy of current lithium-ion batteries. Unfortunately, the cycle-life of Li-S cells is limited due to migration of species generated at the sulfur cathode. These species, collectively known as polysulfides, can transform spontaneously, depending on the environment, and it has thus proven difficult to determine the nature of redox reactions that occur at the sulfur electrode. The objective of this project is to use X-ray spectroscopy to track species formation and consumption during charge-discharge reactions in a Li-S cell. Molecular simulations will be used to obtain X-ray spectroscopy signatures of different polysulfide species, and to determine reaction pathways and diffusion in the sulfur cathode. The long-term objective of this project is to use the mechanistic information to build high specific energy Li-S cells.

**PROJECT IMPACT:** Enabling rechargeable Li-S cells has the potential to change the landscape of rechargeable batteries for large-scale applications beyond personal electronics due to: (1) high specific energy, (2) simplicity and low cost of cathode (the most expensive component of current lithium-ion batteries), and (3) earth abundance of sulfur. The proposed diagnostic approach also has significant potential impact as it represents a new path for determining the species that form during charge-discharge reactions in a battery electrode

**OUT-YEAR GOALS:** Year 1 Goals: Simulations of sulfur and polysulfides (PSL) in oligomeric polyethylene oxide (PEO) solvent. Prediction of X-ray spectroscopy signatures of PSL/PEO mixtures. Measurement of X-ray spectroscopy signatures PSL/PEO mixtures. Year 2 Goals: Use comparisons between theory and experiment to refine simulation parameters. Determine speciation in PSL/PEO mixtures without resorting to adhoc assumptions. Year 3 Goals: Build an all-solid lithium-sulfur cell that enables measurement of X-ray spectra *in situ*. Conduct simulations of reduction of sulfur cathode. Year 4 Goals: Use comparisons between theory and experiment to determine the mechanism of sulfur reduction and Li<sub>2</sub>S oxidation in all-solid lithium-sulfur cell. Use this information to build lithium-sulfur cells with improved life-time.

**COLLABORATIONS:** Tsu-Chien Weng, Dimosthenis Sokaras, and Dennis Nordlund (SLAC).

#### Milestones

- 1) Complete simulations of PSL/PEO mixtures including calculation of solvation free energy and X-ray spectra; compare spectra with experimental measurements. (Dec. 13) **Complete**
- 2) Go/No-Go: Viability of the use of X-ray spectroscopy to study speciation of lithium sulfides in lithium-sulfur cells. Criteria: Determine speciation using X-ray spectra. (Mar. 14) **Complete**
- 3) Build *in situ* cell for generating polysulfides by electrochemically driven redox reactions and measuring X-ray spectra. (Jun. 14) **Ongoing – delayed to Sep. 14**
- 4) Synthesize an electron- and ion-conducting polymer binder for the sulfur cathode. (Sep. 14) **Original target binder did not work. Working on synthesizing new binder.**

## Progress Report

**Milestone 1.** The first ever theoretical calculation of the sulfur K-edge XAS of isolated  $\text{Li}_2\text{S}_x$  species solvated in tetraglyme were determined.

**Milestone 2.** Using principal component analysis, it was determined and demonstrated that XAS is capable of speciating Li polysulfide molecules. Calculations indicate that the ratio of the main-/pre-edge peak area, and not the peak intensities, can be used to differentiate dissolved Li polysulfides.

**Milestone 3.** An *in situ* battery cell that allows X-rays to probe the cathode requires an X-ray transparent window that may also serve as the cathode current collector. The extent to which battery cathodes can be measured when set behind these windows is particular to each beamline (*e.g.*, beamlines use different fluorescence detectors). For that reason, recent XAS experiments were used to ascertain that the following windows can be used for experiments on beamlines 9.3.1 of the Advanced Light Source and 4-3 of Stanford Synchrotron Radiation Light source:

1. 8  $\mu\text{m}$  thick Kapton film with 50 nm Au deposited on the surface.
2. 3  $\mu\text{m}$  thick Mylar film with 50 nm Au deposited on the surface.

Results of these experiments showed that X-ray fluorescence data can be gathered for sulfur cathodes set behind the above windows. Furthermore, an ultrathin cathode (<500 nm in thickness) that was spin-cast on to these windows still provided satisfactory results. Now that these experiments have been performed and heating stages have been built and tested for the two beamlines, *in situ* XAS battery cycling tests can proceed.

### Design and Synthesis of Advanced High-Energy Cathode Materials

**PROJECT OBJECTIVE:** The successful development of next-generation electrode materials requires particle-level knowledge of the relationships between materials' specific physical properties and reaction mechanisms to their performance and stability. This single-crystal-based project was developed specifically for this purpose and it has the following objectives: 1) obtain new insights into electrode materials by utilizing state-of-the-art analytical techniques that are mostly inapplicable on conventional, aggregated secondary particles, 2) gain fundamental understanding on structural, chemical and morphological instabilities during Li extraction/insertion and prolonged cycling, 3) establish and control the interfacial chemistry between the cathode and electrolyte at high operating voltages, 4) determine transport limitations at both particle and electrode levels, and 5) develop next-generation electrode materials based on rational design as opposed to more conventional empirical approaches.

**PROJECT IMPACT:** This project will reveal performance-limiting physical properties, phase-transition mechanisms, parasitic reactions, and transport processes based on the advanced diagnostic studies on well-formed single crystals. The findings will establish rational, non-empirical design methods that will improve the commercial viability of next-generation  $\text{Li}_{1+x}\text{M}_{1-x}\text{O}_2$  (M=Mn, Ni and Co) and spinel  $\text{LiNi}_x\text{Mn}_{2-x}\text{O}_4$  cathode materials.

#### **OUT-YEAR GOALS:**

- Synthesize single-crystal samples of lithium transition-metal oxide cathode materials.
- Characterize structural and morphological changes and establish their correlation to rate performance and cycling stability.
- Determine crystal-plane specific reactivity between cathode particles and the electrolyte.
- Measure lithium-concentration dependent transport and kinetic properties.
- Define performance-limiting fundamental properties and mechanisms and outline mitigating approaches. Design, synthesize, and evaluate the improved electrode materials.

**COLLABORATIONS:** Robert Kostecki, Marca Doeff, Kristin Persson, Vassilia Zorba, Tolek Tyliczszak, and Zhi Liu (LBNL), Clare Grey (Cambridge), Brett Lucht (URI), and Yet-Ming Chiang (MIT).

#### Milestones

- 1) Synthesize at least five new cathode crystal samples with at least two new morphologies. (Dec. 13) **Complete**
- 2) Characterize the interface between the high-voltage cathode and the electrolyte. Identify the role of particle surface planes in interfacial reactivity (Mar. 14) **Complete**
- 3) Complete the studies on structural evolution during initial Li extraction/insertion and extended cycling. Illustrate the impact of structural changes and phase transformation on rate capability and stability. (Jun. 14) **Complete**
- 4) Go/No-Go: Continue low-temperature based solvothermal synthesis. Criteria: If the crystal samples show similar quality and performance to those made at high temperatures. (Sep. 14) **Ongoing**

## Progress Report

**Thermal-driven structural transformation in Ni/Mn spinels:** Understanding the kinetic implication of solid solution vs. biphasic reaction pathways is critical for the development of advanced electrode materials. This quarter, temperature-controlled *in situ* XRD (TXRD) studies were performed to investigate the thermal behavior of the  $\text{Li}_x\text{Mn}_{1.5}\text{Ni}_{0.5}\text{O}_4$  ( $\text{Li}_x\text{MNO}$ ,  $0 \leq x \leq 1$ ) system and the synthesis of room-temperature solid solution intermediates that may lead to an understanding of their role in battery electrode performance. A series of delithiated  $\text{Li}_x\text{MNO}$ , with  $x=0.90, 0.82, 0.71, 0.51, 0.40, 0.25, 0.11, 0.06,$  and  $0$ , were prepared by chemical oxidation with varying amounts of a  $0.1 \text{ M}$  solution of nitronium tetrafluoroborate ( $\text{NO}_2\text{BF}_4$ ) in acetonitrile. The reactions resulted in a variety of mixtures among three cubic phases:  $\text{LiMn}_{1.5}\text{Ni}_{0.5}\text{O}_4$  (Phase I),  $\text{Li}_{0.5}\text{Ni}_{0.5}\text{Mn}_{1.5}\text{O}_4$  (Phase II) and  $\text{Ni}_{0.5}\text{Mn}_{1.5}\text{O}_4$  (Phase III), with refined lattices parameters of  $8.1687(2), 8.0910(6)$  and  $8.0005(3) \text{ \AA}$ , respectively. The samples were subjected to heating and cooling in air at a rate of  $5^\circ\text{C}/\text{min}$  while collecting TXRD patterns at a step size of  $25^\circ\text{C}$ . The selected patterns from  $x=0.82, 0.25,$  and  $0$  are shown in Fig. 1. In all cases, no significant changes were detected below  $150^\circ\text{C}$ . Between  $150$  and  $225^\circ\text{C}$ , the peaks from Phase I and II broadened and started to merge in  $x=0.82$  (Fig. 1a), with complete transformation into a single cubic phase observed at  $225^\circ\text{C}$ . In the fully delithiated sample composed of Phase III only ( $x=0$ , Fig. 1c), a new spinel-type phase with expanded lattice dimensions appeared above  $200^\circ\text{C}$ , suggesting that Phase III is susceptible to thermal-induced phase conversion. It is possible that the new phase is a mixture of several structurally similar phases and/or compounds. For  $x=0.25$  consisting of Phase II and III in the as-prepared sample, three components, Phase II, a new spinel-type phase, and Phase III, were observed above  $175^\circ\text{C}$  (Fig. 1b). At  $225^\circ\text{C}$ , the mixture was composed mostly of the spinel-type phase along with a small amount of remaining Phase III. The relationship between the lattice parameters of the phases present, established from the full-pattern Rietveld refinements of the TXRD patterns and the heating temperature, is shown in Fig. 2. For samples with  $0.51 \leq x < 1$  that have minimal presence of Phase III, the cubic lattice parameters grew closer to each other when the temperature is raised above  $150^\circ\text{C}$  which eventually became a single lattice parameter in the range of  $200$  to  $250^\circ\text{C}$  (Fig. 2a), confirming the formation of a single-phase solid solution in these samples. The formed single phases remained phase pure after cooling to room temperature. For samples with  $0 < x \leq 0.40$  that have a predominant presence of Phase III, the merging of three lattice parameters was not observed during heating (Fig. 2b). Phase III remained in all samples even at  $250^\circ\text{C}$ , although its content was significantly reduced. The results suggest that heating reduces the miscibility gap and promotes the formation of solid solutions between Phase I and II. Phase III, however, is thermally unstable and it decomposes before its dissolution in Phase I or II.

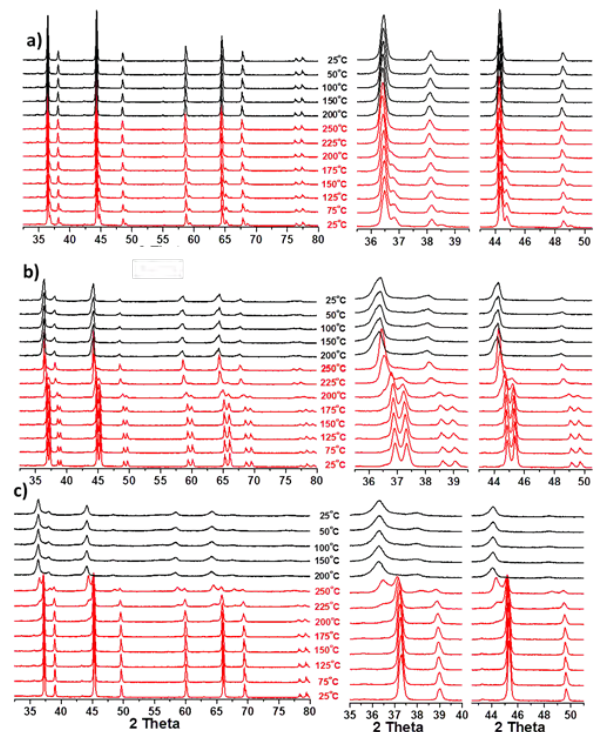


**Figure 1.** TXRD patterns of selected  $\text{Li}_x\text{Mn}_{1.5}\text{Ni}_{0.5}\text{O}_4$  crystal samples: a)  $x=0.82$ , b)  $x=0.25$ , and c)  $x=0$ .

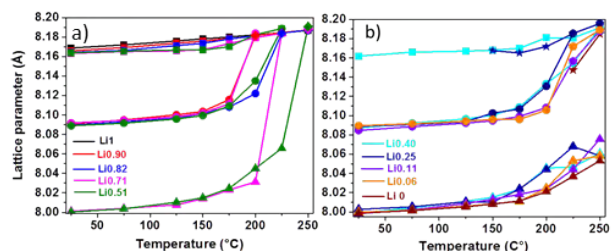


**Figure 2.** Changes in the lattice parameters upon heating the  $\text{Li}_x\text{Mn}_{1.5}\text{Ni}_{0.5}\text{O}_4$  crystal samples: a)  $0.51 \leq x < 1$  and b)  $0 \leq x < 0.40$ . Phase I: square; Phase II: circle; Phase III: triangle; solid solution: diamond; spinel-type phase: star.

### Optimization of Ion Transport in High-Energy Composite Cathodes

**PROJECT OBJECTIVE:** This project aims to probe and control the atomic-level kinetic processes that govern the performance limitations (rate capability and voltage stability) in a class of high energy composite electrodes. A systematic study with powerful suite of analytical tools (including atomic resolution scanning transmission electron microscopy (a-STEM) & Electron energy loss spectroscopy (EELS), X-ray photoelectron spectroscopy (XPS) and first principles (FP) computation) will be used to pin down the mechanism and determine the optimum bulk compositions and surface characteristics for high rate and long life, and to help the synthesis efforts to produce the materials at large scale with consistently good performance. It is also aimed to extend the suite of surface-sensitive tools to diagnose the silicon type of anodes.

**PROJECT IMPACT:** If successful, this research will provide a major breakthrough in commercial applications of the class of high energy density cathode material for lithium ion batteries. Additionally, it will provide in-depth understanding of the role of surface modifications and bulk substitution in the high voltage composite materials. The diagnostic tools developed here can also be leveraged to study a wide variety of cathode and anode materials for rechargeable batteries.

**OUT-YEAR GOALS:** Careful engineering of the surface (coating) and bulk compositions (substitution) of the high energy composite cathode materials can lead to significant improvement on ion transport and voltage stability. The goals are to establish the STEM/EELS and XPS as quantities diagnostic tools for surface and interface characterization and to enable quick identification of causes of surface instability (or stability) in various types of cathode materials. It is also planned to identify ways to extend the techniques for anode materials, such as silicon anode.

#### **COLLABORATIONS:**

- Robert Kostecki and Gao Liu (LBNL) – on cathode electrolyte interface diagnosis and anode SEI diagnosis
- Se-Hee Lee (U. of Colorado, Boulder) – on surface coating of cathode materials.
- Michael Sailor (UCSD) – porous Si and carbonization of Si-based anodes.
- Keith Stevenson (UT Austin) – XPS and TOP-SIMS
- Nancy Dudney and Juchuan Li (ORNL) – Si thin film fabrication

#### Milestones

- 1) Establish the initial suite of surface and interface characterization tools, including STEM/EELS, XPS and FP computation (Dec. 13) **Complete**
- 2) Identify the surface coated materials ( $\text{AlF}_3$  and  $\text{Li}_3\text{PO}_4$ ) electrochemical performance matrices, including first cycle irreversible capacity, discharge energy density, voltage stability upon cycling and rate capabilities. (Mar. 14) **Complete/Initiated morphological control**
- 3) Go/No-Go: Stop and change the coating materials if the improvements for rate capability and voltage stability are not significant. Criteria: Characterize coated samples - coating thickness, compositions and morphology before, during and after cycling. (Jun. 14) **Complete**
- 4) Identify ways to extend the STEM/EELS and XPS techniques for anode materials, such as silicon anode. (Sep. 14) **Ongoing**

## Progress Report

**Identification of factors influencing the 1<sup>st</sup> cycle chemical irreversibilities of *a*-Si thin film electrodes.** In order to better understand Si's 1<sup>st</sup> cycle losses, 50 nm thin film sputtered amorphous Si (*a*-Si) electrodes were cycled under a variety of conditions. Thin films were chosen because they have been shown to be mechanically stable during cycling. In this way, chemical degradation mechanisms can be isolated from mechanical degradation mechanisms. An SEM image (Fig. 1a) of an *a*-Si thin film after 100 cycles shows no evidence of delamination or electrical isolation of active material.

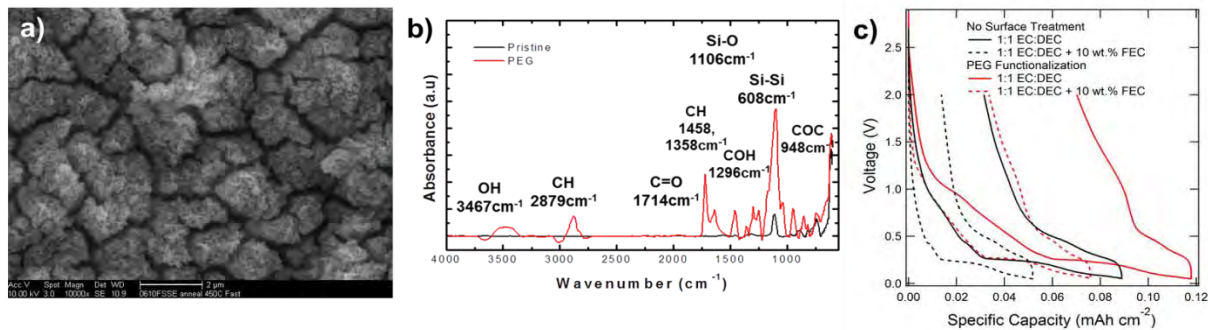


**Figure 1.** a) SEM image of *a*-Si thin film electrode after 100 cycles, b) FTIR spectra of a (100) crystalline Si wafer before (black) and after (red) PEG functionalization, c) 1<sup>st</sup> cycle voltage profiles for *a*-Si thin film electrodes cycled with (dashed) or without (solid) FEC additive and with (red) or without (black) PEG functionalization.

The variables in this study include a 10 wt% FEC electrolyte additive and/or PEG functionalization *via* hydrosilylation. PEG was chosen for its similarity to polymeric electrolyte decomposition products previously identified in Si's SEI. Figure 1b presents the FTIR spectra for (100) crystalline Si wafers before (black) and after (red) PEG functionalization. A variety of organic functionalities confirm a successful hydrosilylation reaction and similar functionalities are assumed on treated *a*-Si thin-films. Without the FEC additive or the PEG functionalization, the initial coulombic efficiency (CE) of an *a*-Si thin film electrode is 63.9%. With the FEC additive, the initial CE increases to its highest value of 73.5%. It is confirmed that FEC imparts chemical stability to the binder-free, additive-free Si electrode/electrolyte interface.

***Li<sub>1.133</sub>Ni<sub>0.3</sub>Mn<sub>0.567</sub>O<sub>2</sub> with crystalline LLTO surface modification.*** The surface of LNMO (Li-excess layered oxide) particles were coated with LLTO (Lithium Lanthanum Titanium Oxides) in order to improve electrochemical performance. A coating of only 1 wt.% was found to improve capacity and voltage retention. Figure 2a presents the XRD of LNMO before and after coating. As the figure indicates, the intensity of the LLTO peak increases as the thickness of the LLTO coating increases (Fig. 2a). Figure 2b compares the 1<sup>st</sup> cycle voltage profile of LNMO and 1% and 2% LLTO-coated LNMO. The CE improved from 73.1% to 79.1% and 91.4%, respectively. This suggests that the LLTO coating holds promise for eliminating LNMO's large initial irreversibility.

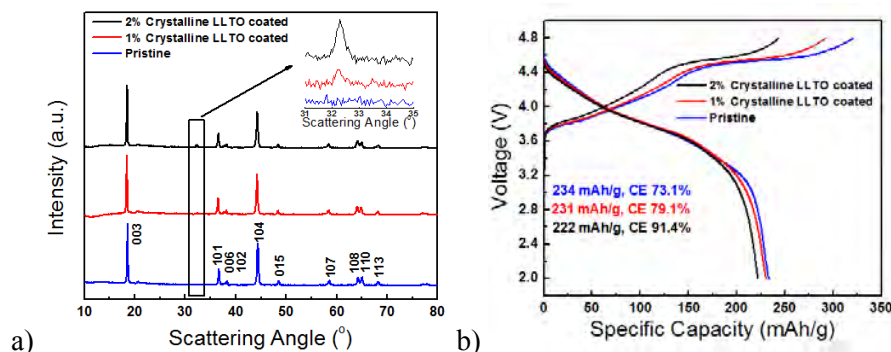


**Figure 2.** a) XRD of  $\text{Li}_{1.133}\text{Ni}_{0.3}\text{Mn}_{0.567}\text{O}_2$  and crystalline LLTO surface modified  $\text{Li}_{1.133}\text{Ni}_{0.3}\text{Mn}_{0.567}\text{O}_2$ . 2) 1<sup>st</sup> cycle electrochemical voltage profiles of  $\text{Li}_{1.133}\text{Ni}_{0.3}\text{Mn}_{0.567}\text{O}_2$  and crystalline LLTO surface modified  $\text{Li}_{1.133}\text{Ni}_{0.3}\text{Mn}_{0.567}\text{O}_2$  at C/20, voltage range is 2.0 to 4.8V.

## Analysis of Film Formation Chemistry on Silicon Anodes by Advanced *In Situ* and *In Operando* Vibrational Spectroscopy

**PROJECT OBJECTIVE:** Understand the composition, structure, and formation/degradation mechanisms of the solid electrolyte interface (SEI) on the surfaces of Si anodes during charge/discharge cycles by applying advanced *in situ* vibrational spectroscopies. Determine how the properties of the SEI contribute to failure of Si anodes in Li-ion batteries in vehicular applications. Use this understanding to develop electrolyte additives and/or surface modification methods to improve Si anode capacity loss and cycling behavior.

**PROJECT IMPACT:** A high capacity alternative to graphitic carbon anodes is Si, which stores 3.75 Li per Si vs. 1 Li per 6 C yielding a theoretical capacity of 4008 mAh/g versus 372 mAh/g for C. But Si anodes suffer from large first cycle irreversible capacity loss and continued parasitic capacity loss upon cycling leading to battery failure. Electrolyte additives and/or surface modification developed from new understanding of failure modes will be applied to reduce irreversible capacity loss, improve long term stability and cyclability of Si anodes for vehicular applications.

**OUT-YEAR GOALS:** Extend the study of interfacial processes with advanced vibrational spectroscopies to high voltage oxide cathode materials. The particular oxide to study will be chosen based on materials of interest at that time and availability of the material in a form suitable for these studies, *e.g.*, sufficiently large crystals or sufficiently smooth/reflective thin films. The effect of electrolyte composition, electrolyte additives, and surface coatings will be determined and new strategies for improving cycle life developed.

### **COLLABORATIONS:**

Chunmei Ban (NREL): Functionalization of Si by Atomic Layer Deposition (ALD) - Effect of functionalization on electrolyte reduction

Gao Liu (LBNL): Surface electrochemistry of electrolyte additives on model Si electrodes

### Milestones

- 1) Develop method to attach Si nanostructures to the electrode substrate used in the spectroelectrochemical cell. (Dec. 13) **Delayed, due Sep. 14**
- 2) Determine the oxidation and reduction potentials and products of at least one electrolyte additive provided by Gao Liu's group. (Mar. 14) **Complete**
- 3) Determine role of the Si nanostructure on the SEI formation structure and properties (Jun. 14) **Ongoing – delayed to Sep. 14**
- 4) Go/No-Go: Feasibility of surface functionalization to improve SEI structure and properties. Criteria: Functionalize a model Si anode surface and determine how SEI formation is changed. (Sep. 14) **Ongoing**

## Progress Report

In Q3, the additive effect (VC, FEC comparison) on the SEI film on a Si (100) single crystal and on Si nanoparticles was investigated. The reference compound poly-VC and Si nanoparticle samples were synthesized and prepared by Hui Zhao, a postdoc scholar in Gao Liu's group (LBNL.) The Si nanoparticles samples were made with CMC-based binder (loading is 50%, with 20% carboxymethyl cellulose and 5% polyvinyl alcohol as binder, 25% additive carbon). All the tests were run in the EC/DEC/LiPF<sub>6</sub> electrolyte (v/v=1:1) with or without 5% additives.

As stated in the previous quarter, the major component formed on the Si anode under various additive conditions is Li<sub>2</sub>CO<sub>3</sub>. The short circuiting of the coin cell during opening deposits Li on the anode, which subsequently reacts with the remaining electrolyte. Thus, a homemade Teflon cell was used to test the Si nanoparticle electrode, which can be opened without shorting the electrodes. A Si single crystal electrode has been used to reveal the role of binder or carbon additive on the electrolyte reactions. As shown in Fig. 1, the typical Li<sub>2</sub>CO<sub>3</sub> peak around 1400-1500 cm<sup>-1</sup> is not found on either the Si (100) or the Si nanoparticle electrode with the Teflon cell. The comparison of *ex situ* IR between Si (100) and nanoparticle surface also shows that the influence of CMC-based binder and/or the carbon black additive on the surface species formed after cycling is negligible.

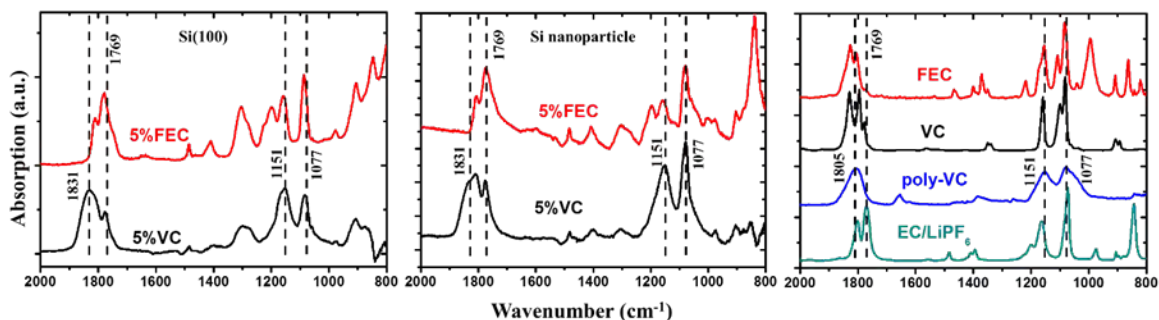


**Figure 1.** *Ex situ* ATR-FTIR spectra of Si (100) p-type wafer and Si nanoparticles with CMC based binder after 3 CV cycles with 0.1mV/s scan rate (2V-0.01V vs. Li/Li<sup>+</sup>), and rinsing with DMC to remove residual electrolyte.

As shown in the *ex situ* IR spectra above, Si electrodes in 5% VC additive show a wide peak at a higher wavenumber (1831 cm<sup>-1</sup>) compared to the EC residual electrolyte peak (1799, 1769 cm<sup>-1</sup>). Based on the synthesized poly-VC standard spectra, the VC additive reduction compound has been assigned to poly-VC or its oligomer, which is consistent with previous reports. However, for Si electrode in FEC additive, the original C=O stretch (1829, 1802 cm<sup>-1</sup>) in FEC disappeared or shifted to a lower wavenumber. The exact reduction product of FEC degradation has not been confirmed yet, due to the lack of significant features except residual electrolyte. However, it is clear that FEC takes a different path as VC: for VC, the path is polymerization and remains a “ring” structure (C=O stretch peak shift to higher wavenumber), while FEC takes an open “ring” pathway like EC. It is noted that if FEC were to react under the same pathway as EC to form LEDC, the fluorine ends up exclusively as difluoroethylene. The solid phase product would thus be identical to that of EC. More experiments are required to explore this further (*i.e.*, concentration dependence, rigorous derivation of reaction path) of VC and FEC reduction with Si nanoparticle electrodes. However, results to date suggest replacing as much linear co-solvent with FEC as possible to be consistent with other needed properties of the electrolyte.

### Electrode Materials Design and Failure Prediction

**PROJECT OBJECTIVE:** The goal of this project is to use continuum-level mathematical models along with controlled experiments on model cells to (i) understand the performance and failure models associated with next-generation battery materials, (ii) design battery materials and electrodes to alleviate these challenges. The focus of the research will be on two systems, silicon-based anodes and Li-sulfur cells. In silicon anodes, the challenges associated with the large volume change and the associated stress effects will be studied. In the Li-S system, the focus will be on the concept of using ceramic single-ion conducting glass layers for lithium protection, along with quantification of the losses associated with such a design and its impact on the performance of the chemistry. A theoretical study of the impact of polarization losses on the energy density will be conducted.

**PROJECT IMPACT:** Si anode-based Li-ion cells and lithium-sulfur cells promise to increase the energy density and decrease the cost of batteries compared to the state-of-the-art. If the performance and cycling challenges can be alleviated, these systems hold the promise for meeting the EV-Everywhere targets.

**OUT-YEAR GOALS:** At the end of this project, a mathematical model will be developed that can address the power and cycling performance of next-generation battery systems. The initial focus will be on silicon anodes and Li-S cells, although the project will adapt to newer systems, if appropriate. The models will serve as a guide for better design of materials, including mechanical properties to reduce stress in silicon anodes, and the kinetics and solubility needed to decrease the morphological changes in sulfur cells and increase the power performance.

**COLLABORATIONS:** None this quarter.

#### Milestones

- 1) Go/No-Go: Stop materials testing. Criteria: Stop materials testing if unsuccessful at obtaining reproducible results for mechanical property values of binder and conductive material composites saturated in electrolyte. (Dec. 13) **Go for materials testing**
- 2) Incorporate material property values and behavior measured for binders saturated with electrolyte into simulations of model systems. (Feb. 14) **Complete**
- 3) Quantify polarization losses at liquid/SIC interface for different electrolytes. (Mar. 14) **Complete**
- 4) Determine possible reasons for dynamic nature of polarization loss in liquid/SIC interface (*e.g.*, interfacial *vs.* bulk). (Jun. 14) **Complete**
- 5) Quantify the impact of the interfacial polarization loss between the liquid/SIC by estimating the energy density of a Li-S cell for a given power to energy ratio. (Sep. 14) **Ongoing**

## Progress Report

**Possible reasons for dynamic nature of polarization loss in liquid/SIC interface.** While the Li-S battery chemistry offers theoretical energy densities that are much higher than those of the present generation of Li-ion batteries, self-discharge due to migration of polysulfides to the Li anode remains a significant challenge in these systems. The use of single ion conductors (SIC) to separate the Li anode from the cathode in Li-S systems has been proposed as a possible solution, as these permit only the transfer of Li-ions. However, this approach introduces interfaces between the electrolyte solution and the SIC. The junction polarization, that is, the drop in potential due to the transfer of Li-ions across such an interface, has implications for cell power.

In the previous quarter, measurements in three different solvents for different concentrations of  $\text{LiPF}_6$  showed substantial polarization losses at the SIC/electrolyte solution interfaces. The values measured, of the order  $0.5 \text{ K}\Omega\text{-cm}^2$ , would significantly decrease the power capability of the system. This quarter, work has focused on determining the source of these losses.

Literature reports suggest that one source of the large resistance is the slow solvation/desolvation kinetics in nonaqueous electrolytes typically used in Li-ion cells. If this hypothesis was correct, then the interfacial polarization losses would be substantial not just across the liquid/SIC interface, but across any liquid/solid interface, including Li metal interfaces. In order to test this hypothesis, experiments were performed using a Li-Li symmetric cell with a Li reference electrode and 1 M  $\text{LiPF}_6$  in EC/DEC (1:1) to compare energies of solvation and desolvation of Li-ions at the Li electrode/electrolyte interfaces. The cells were polarized for two minutes under a range of current densities, then allowed to relax for three minutes, during which potentials were recorded. The measured potentials for the solvation and desolvation processes differ in magnitude by only a few millivolts at  $1 \text{ mA/cm}^2$ , suggesting that differences between the energies of solvation and desolvation of Li-ion are minimal. This is in contrast to voltage drops in the order of 0.5 V in the SIC/electrolyte interface at the same current density.

It is worth noting that a significant difference exists between the surface of the Li metal used in these experiments and those of the SIC. While the SIC interface is planar with minimal roughness, the formation cycles on Li metal leads to high surface area deposits. If the actual area for the Li metal electrode were significantly larger than the cross-sectional area, then the difference would account for the significantly lower polarization losses in the Li metal/liquid interface compared to the SIC/liquid interface.

Conventionally, the Butler-Volmer equation has been used to account for ionic transfer at liquid/liquid interfaces. Using linear kinetics, one can calculate the exchange current density of the ion transfer at the SIC/liquid interface to be  $0.57 \text{ A/m}^2$ , based on the data reported in the previous quarter. Previously the Srinivasan-group has studied the kinetics in the  $\text{LiNi}_{1/3}\text{Co}_{1/3}\text{Mn}_{1/3}\text{O}_2$  cathode using a combined model-experimental approach. In that study, the exchange current density of the porous cathode was estimated to be  $0.6 \text{ A/m}^2$  where the area was based on the total interfacial area available for reaction (estimated *via* a BET experiment on the cathode particles). These results indicate that the value of the exchange current density at the liquid electrolyte/SIC interface is comparable with those reported for liquid electrolyte/composite electrode interfaces, when the difference in area is taken into account. This would suggest that the planar geometry of the SIC interface is a possible cause for the high polarization observed. It also implies that attempts to roughen this interface would help test this hypothesis. This determination fulfills the June 30<sup>th</sup> milestone.

### Predicting and Understanding Novel Electrode Materials from First-Principles

**PROJECT OBJECTIVE:** The aim of the Project is model and predict novel electrode materials from first-principles focusing on 1) understanding the atomistic interactions behind the behavior and performance of the high-capacity lithium excess and related composite cathode materials and 2) predict new materials using the recently developed Materials Project high-throughput computational capabilities at LBNL. More materials and new capabilities will be added to the Materials Project Lithium Battery Explorer App ([www.materialsproject.org/apps/battery\\_explorer/](http://www.materialsproject.org/apps/battery_explorer/)).

**PROJECT IMPACT:** The project will result in a profound understanding of the atomistic mechanisms underlying the behavior and performance of the Li-excess as well as related composite cathode materials. The models of the composite materials will result in prediction of voltage profiles and structural stability – the ultimate goal being to suggest improvements based on the fundamental understanding that will increase the life and safety of these materials. The Materials Project aspect of the work will result in improved data and electrode properties being calculated to aid predictions of new materials for target chemistries relevant for ongoing BATT experimental research.

**OUT-YEAR GOALS:** During year 1-2, the bulk phase diagram will be established – including bulk defect phases in layered  $\text{Li}_2\text{MnO}_3$ , layered  $\text{LiMO}_2$  ( $M = \text{Co}, \text{Ni}, \text{and Mn}$ ) and  $\text{LiMn}_2\text{O}_4$  spinel to map out the stable defect intermediate phases as a function of possible transition metal rearrangements. Modeling of defect materials (mainly  $\text{Li}_2\text{MnO}_3$ ) under stress/strain will be undertaken to simulate effect of composite nano-domains. The composite voltage profiles as function of structural change and Li content will be obtained. In year 2-4, the project will focus on obtaining Li activation barriers for the most favorable TM migration paths as a function of Li content as well as electronic DOS as a function of Li content for the most stable defect structures identified in year 1-2. Furthermore, stable crystal facets of the layered and spinel phases will be explored, as a function of  $\text{O}_2$  release from surface and oxygen chemical potential. Within the Materials Project, hundreds of novel Li intercalation materials will be calculated and made available.

**COLLABORATIONS:** Gerbrand Ceder (MIT), Clare Grey (U Cambridge, UK). Mike Thackeray (ANL), Guoying Chen (LBNL).

#### Milestones

- 1) Finalize low T phase diagram including relevant bulk Li, O and Mn and defect phases in layered  $\text{Li}_x\text{MnO}_2$ , spinel  $\text{Li}_x\text{MnO}_3$  and spinel  $\text{Li}_x\text{Mn}_2\text{O}_4$  (Dec. 13) **Complete**
- 2) Over-charge mechanism processes: oxygen migration paths and activation barriers obtained in lowest energy defect structures; oxygen redox potentials obtained (Mar. 14) **Complete**
- 3) Go/No-Go: On over-charge mechanism. Criteria: Oxygen release, migration or oxygen redox process; process down select based on data. (Jun. 14) **Complete**
- 4) Composite voltage profiles as function of structural change and Li content obtained (Sep. 14) **Complete**

## Progress Report

First-principles calculations to investigate the phase transformation mechanism and its correlation to the voltage profile have continued.

To compare these findings, particularly pertaining to a presumed tendency towards defect layered phase transformation, to the experimental evidence of voltage fade, the evolving voltage profile of bulk  $\text{Li}_x\text{MnO}_3$  was calculated. The voltage profile for the first charge process was obtained based on the intermediate stable structures that were predicted from the previous calculation, assuming that the original layered structure stays intact. To examine the voltage change as a function of the presumed structural evolution, the structure set was explored, as a function of increasing Li content, where all Mn ions belong to a spinel-nuclei (in a defect layered phase). It is noted that it cannot be predicted which of the defect layered structures that would form first, as it may be a continuous degradation of the structure as a function of cycling and increased number of migrated Mn, but that the calculated voltage profile for the defect structures should follow the same discharge trend as found in experiments. The results are shown in Fig. 1, where calculated voltage profiles to recent experimental works are compared. Note that the charge and discharge process corresponds to decreasing and increasing  $x$ , respectively. The blue thick line indicates the voltage profile during the first charge, and clearly indicates that  $\text{Li}_2\text{MnO}_3$  is activated at voltages above 4.5 V, in agreement with experiments. The discharge (red) curve corresponds to a scenario where the original structure has transformed to a defect phase, where a significant amount of Mn resides in the Li layer. This defect structure is substantially more stable at high charge and less stable at high Li content, compared to the original layered structure. It is noted that this structural transition alone (without any presumed oxygen release and/or creation of  $\text{Mn}^{3+}$ ) can give rise to a significant voltage drop – compared to the first charge. At high charge (even locally), the defect migration and subsequent local re-arrangement of Mn is predicted to occur rapidly, and reverting back to the original phase at high Li content is kinetically impeded as the previous computation predicted high Mn activation barriers for the reverse process. Results indicate that the phase transformation can be suppressed if the voltage is maintained under *ca.* 4.7 V and no part of the material reaches high charge or the critical composition  $x < 0.5$ . It is noted that the capacity obtained in experiments is significantly less than the theoretical maximum capacity and one can speculate that an increasing amount of the material becomes inactive.

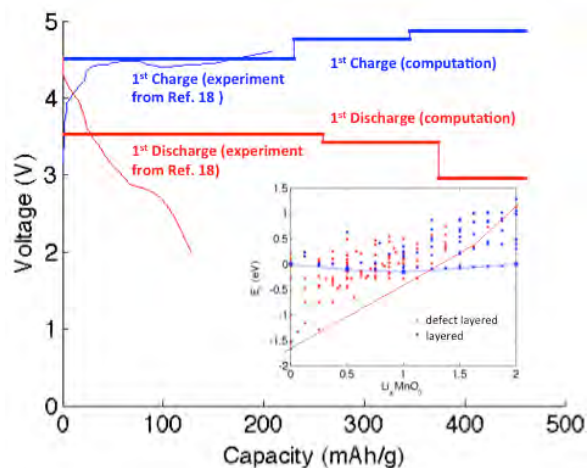


**Figure 1.** Voltage profiles of  $\text{Li}_x\text{MnO}_3$  for the first charge (blue lines) and the discharge process (red lines) assuming a structural transformation, originating from Mn migration.

### First Principles Calculations of Existing and Novel Electrode Materials

**PROJECT OBJECTIVE:** Identify the structure of layered cathodes that leads to high capacity. Clarify the role of the initial structure as well as structural changes upon first charge and discharge. Give insight into the factors that control the capacity and rate of Na-intercalation electrodes, and make suggestions for novel Na-intercalation cathode materials. Generate insight into the behavior of alkali-intercalating electrode materials.

**PROJECT IMPACT:** The project will lead to insight in how Li excess materials work and ultimately to higher capacity cathode materials for Li-ion batteries. The project will also lead to definite conclusions as to whether Na-ion batteries can exceed Li-ion batteries in energy density.

**OUT-YEAR GOALS:** Higher capacity Li-ion cathode materials, and novel chemistries for higher energy density storage devices.

**COLLABORATIONS:** Kristin Persson (LBNL), Clare Grey (Cambridge)

#### Milestones

- 1) Identify at least three ordered states in  $\text{Na}_x\text{MO}_2$  compounds that can be verified with experiments. (Dec. 13) **Complete**
- 2) Obtain computed voltage curve of  $\text{Li}_2\text{MO}_3$  compound where  $\text{M} = \text{Mn}$  or other metal. (Mar. 14) **Complete**
- 3) Go/No-Go: If voltage curves of Na compounds with less than 0.5V error cannot be modeled. Criteria: Obtain voltage curves for all the  $\text{O}_3$   $\text{Na}_x\text{MO}_2$  compounds where M is at least five distinct 3d metals. (Jun. 14) **Complete**
- 4) Complete ground state study in Li-Ni-Mn-O and Li-Co-Mn-O system. (Sep. 14) **Ongoing**

## Progress Report

It was previously reported that excess Li enables macroscopic Li migration in cation-disordered  $\text{Li}_{1+x}\text{M}_{1-x}\text{O}_2$  by activating a percolating network of fast 0-TM Li diffusion channels [1]. To complete the understanding of Li migration through rock salt-type oxides, this percolation analysis has been extended beyond the layered and disordered (DO) rocksalt structures to the other common ordered  $\text{LiMO}_2$  phases: the  $\gamma\text{-LiFeO}_2$  structure and the spinel-like low-temperature  $\text{LiCoO}_2$  structure [2].

The percolation thresholds of the four crystal phases (Fig. 1) are notably different, indicating that the  $\gamma\text{-LiFeO}_2$  structure is not well suited as a Li conductor, since it requires a very large amount of Li excess to become 0-TM percolating. However, the spinel-like structure exhibits excellent percolation properties and is 0-TM percolating even at Li-deficient compositions. In addition, the beneficial properties of the spinel-like structure are robust against some amount of cation disorder, as is evident from the percolation maps in Fig. 2.

As a result of this percolation analysis, the team now possesses a complete map of the Li conduction properties throughout the configurational space of rock salt-type Li transition-metal oxides. Based on the knowledge of the 0-TM accessible Li content, it is now possible to estimate the practical capacity of any rock salt-type Li battery electrode material given its crystal structure and the amount of cation mixing. Thus, the percolation maps (Fig. 2) provide direct guidelines for the design of new battery materials and for the improvement of existing materials.

The predictive power of this model is currently undergoing evaluation.

[1] J. Lee, A. Urban, X. Li, D. Su, G. Hautier, G. Ceder, *Science* **343** (2014) 519-523.

[2] A. Urban, J. Lee, and G. Ceder, *Adv. Energy Mat.* (2014), DOI: 10.1002/aenm.201400478.

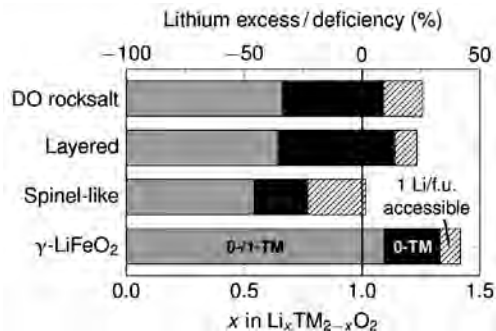


**Figure 1.** Critical Li concentrations in the most common  $\text{LiMO}_2$  crystal phases [2]. The gray region indicates the percolation threshold for 1-TM diffusion (only active in the layered structure), the black region indicates 0-TM percolation, and the hatched region represents the Li content at which 1 Li atom per formula unit becomes 0-TM accessible.

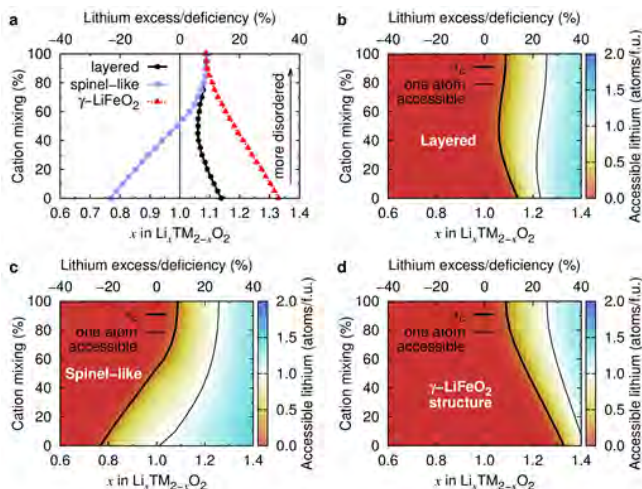


**Figure 2.** (a) 0-TM percolation thresholds and (b)-(d) 0-TM accessible Li content in different  $\text{LiMO}_2$  crystal phases as function of Li content and degree of cation mixing (0%=ordered, 100%=cation-disordered) [2]. The thick and thin black lines in panels (b)-(d) indicate the percolation thresholds and the Li content at which 1 Li atom per formula unit is 0-TM accessible,

### First Principles Modeling of SEI Formation on Bare and Surface/Additive Modified Silicon Anode

**PROJECT OBJECTIVE:** This project aims to develop fundamental understanding of the molecular processes that lead to the formation of a solid electrolyte interphase (SEI) layer due to electrolyte decomposition on Si anodes, and to use such new knowledge in a rational selection of additives and/or coatings. The focus is on SEI layer formation and evolution during cycling and subsequent effects on capacity fade through two concatenated problems: 1) SEI layers formed on lithiated Si surfaces, and 2) SEI layers formed on coated surfaces. Key issues that this project addresses include the dynamic evolution of the system and electron transfer through solid-liquid interfaces.

**PROJECT IMPACT:** Finding the correspondence between electrolyte molecular properties and SEI formation mechanism, structure, and properties will allow the identification of new/improved additives. Studies of SEI layer formation on modified surfaces will allow the identification of effective coatings able to overcome the intrinsic deficiencies of SEI layers on bare surfaces.

**OUT-YEAR GOALS:** Investigating the SEI layer formed on modified Si surfaces involves analysis of the interfacial structure and properties of specific coating(s) deposited over the Si anode surface, characterization of the corresponding surface properties before and after lithiation, especially how such modified surfaces may interact with electrolyte systems (solvent/salt/additive), and what SEI layer structure, composition, and properties may result from such interaction. This study will allow identification of effective additives and coatings able to overcome the intrinsic deficiencies of SEI layers on bare surfaces. Once the SEI layer is formed on bare or modified surfaces, it is exposed to cycling effects that influence its overall structure (including the anode), chemical, and mechanical stability. Elucidating such effects using a molecular level approach will help establish their relationship with capacity fading, which will lead to revisiting additive and/or coating design.

**COLLABORATIONS:** Work with Chunmei Ban (NREL) consists in modelling the deposition-reaction of trimethylaluminum and glycerol on Si surfaces and their reactivity. Work with Brett Lucht (URI) relates to finding the best additives for optimum SEI formation on Si anodes. Reduction of solvents and additives on Si surfaces were studied in collaboration with Kevin Leung and Susan Rempe (SNL).

#### Milestones

- 1) Identify reaction pathways and activation energies for electrolyte reduction on lithiated Si surfaces, both clean and covered with surface oxides and/or with selected SEI products. (Dec. 13) **Complete**
- 2) Quantify electron transfer from a lithiated Si surface covered by a model SEI layer to the electrolyte; develop theory/algorithms accounting for voltage effect on electrolyte reduction reactions. (Sep. 14) **Electron transfer studies completed; voltage effect in progress.**
- 3) Characterize reactivity of additives; identify reaction pathways and interactions of reaction products with electrolyte components; assess aggregation effects. (Jun. 14) **Complete**
- 4) Go/No-Go: Development of a coarse-grained Kinetic Monte-Carlo approach for assessing long-time evolution (order of days) of SEI films. Criteria: Continuation will be based on the demonstrated effectiveness of the technique. (Sep. 14) **Ongoing**

## Progress Report

A  $2e^-$  mechanism was found operative for VC at low/intermediate lithiation stages ( $\text{LiSi}_2$  and  $\text{LiSi}$ ), which results in an adsorbed  $\text{VC}^{2-}$  anion with a broken  $\text{C}_c\text{-O}_c$  bond. Two additional electrons are transferred to  $\text{VC}^{2-}$  at the higher lithiated  $\text{Li}_{13}\text{Si}_4$  surface, yielding  $\text{CO}_2^{2-}(\text{ads})$  and  $\cdot\text{OC}_2\text{H}_2\text{O}^{2-}$ . Although no direct formation of  $\text{CO}_2$  is observed upon VC reduction on  $\text{Li}_x\text{Si}_y$  surfaces, spontaneous reactions between VC and EC reduction species revealed that  $\text{CO}_2$  can be released upon reaction of VC with  $\text{CO}_3^{2-}$ , present in the liquid phase of the electrolyte after reduction of the solvent EC. This is an alternative mechanism to the one proposed recently where  $\text{CO}_2$  is produced *via* reaction of VC with  $\text{EC}^-$ . The simulation results suggest that the  $1e^-$  reduction of EC is much less frequent on Si surfaces at intermediate or high stages of lithiation, where the proposed reaction of VC with  $\text{CO}_3^{2-}$  should be prevalent.

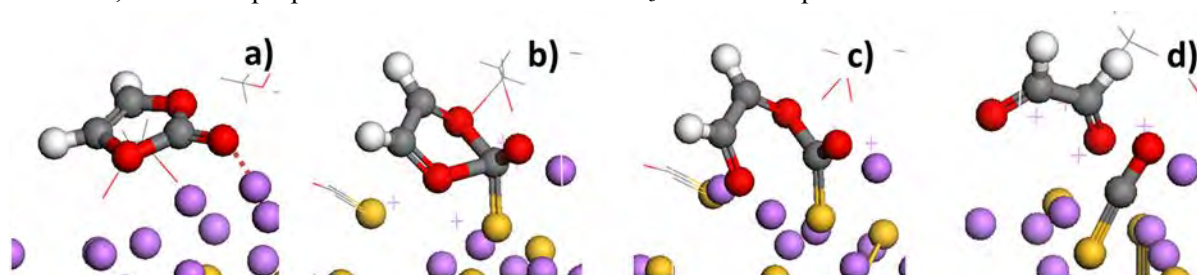


**Figure 1.** Reduction of VC on a  $\text{Li}_{13}\text{Si}_4(010)$  surface. (a) VC adsorption starts with electrostatic interaction between the negatively charged carbonyl oxygen of the molecule and  $\text{Li}^+$  ions on the surface (b) A  $\text{C}_c\text{-Si}$  bond is formed (c) Upon adsorption and transference of two-electrons from the surface to the molecule a  $\text{C}_c\text{-O}_c$  bond is broken. The resultant adsorbed species is an opened VC anion with a double negative charge. (d) The cleavage of a second  $\text{C}_c\text{-O}_c$  bond is observed upon transference of two additional electrons to the adsorbed VC anion. Color code: Li is purple, Si yellow, O red, C black, and H white.

Due to its high reactivity, reduction of FEC on  $\text{Li}_x\text{Si}_y$  surfaces was found to be extremely fast, independent of the degree of lithiation, and able to proceed through three different mechanisms. One of them leads to the adsorbed  $\text{VC}^{2-}$  anion upon release of H and F atoms from the FEC molecule (pathway III in Fig. 2). This is a very interesting finding showing that in some cases the reduction of FEC and VC leads to the exact *same reduction products*, and explaining similarities in SEI layers formed in the presence of these additives. FEC molecules can also be reduced through two other mechanisms, involving the sequential transference of electrons to the molecules that result in formation of  $\text{CO}_2^{2-}$ ,  $\text{F}^-$  (pathway I in Fig. 2), or  $\cdot\text{CH}_2\text{CHO}^-$  or  $\text{CO}_2^-$ ,  $\text{F}^-$ , and  $\cdot\text{OCH}_2\text{CHO}^-$  (pathway II in Fig. 2). These two groups of reduction products, which are different to the ones produced from the VC reduction (pathway III), may oligomerize and form SEI layers with different components to those formed in the presence of VC. Additionally, in every FEC decomposition pathway observed, the fluorine atom leaves the FEC molecule being reduced and forming  $\text{LiF}$  moieties on the anode surface.

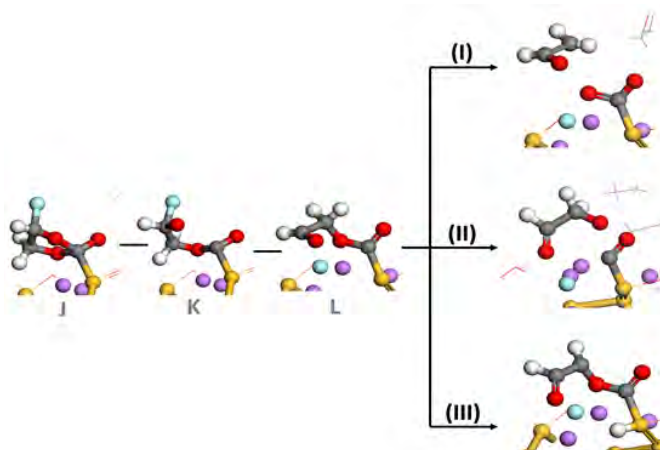


**Figure 2.** Reduction mechanisms of FEC on  $\text{Li}_x\text{Si}_y$  surfaces. Color code for the atoms: light blue (F), red (O), yellow (Si), purple (Li), grey (C) and white (H)

## A Combined Experimental and Modeling Approach for the Design of High Current Efficiency Si Electrodes

**PROJECT OBJECTIVE:** The use of high capacity Si-based electrode has been hampered by its mechanical degradation due to the large volume expansion/contraction during cycling. Nanostructured Si can effectively avoid Si cracking/fracture. Unfortunately, the high surface to volume ratio in nanostructures leads to unacceptable amount of solid-electrolyte interphase (SEI) formation and growth, thereby low current/coulombic efficiency and short life. Based on mechanics models we demonstrate that the artificial SEI coating can be mechanically stable despite the volume change in Si, if the material properties, thickness of the SEI, and the size/shape of Si are optimized. Therefore, the objective of this project is to develop an integrated modeling and experimental approach to understand, design, and make coated Si anode structures with high current efficiency and stability.

**PROJECT IMPACT:** The validated model will ultimately be used to guide the synthesis of surface coatings and the optimization of Si size/geometry that can mitigate SEI breakdown. The optimized structures will eventually enable a negative electrode with a 10x improvement in capacity (compared to graphite) while providing a >99.99% coulombic efficiency, which could significantly improve the energy/power density of current LIB.

**OUT-YEAR GOALS:** Develop a well validated mechanics model that directly import material properties either measured from experiments or computed from atomic simulations. The predicted SEI induced stress evolution and other critical phenomena will be validated against in-situ experiments in a simplified thin-film system. This comparison will also allow fundamental understanding of the mechanical and chemical stability of artificial SEI in electrochemical environments and the correlation between the coulombic efficiency and the dynamic process of SEI evolution. Thus the size and geometry of coated Si nanostructures can be optimized in order to mitigate SEI breakdown, thus provide high current efficiency.

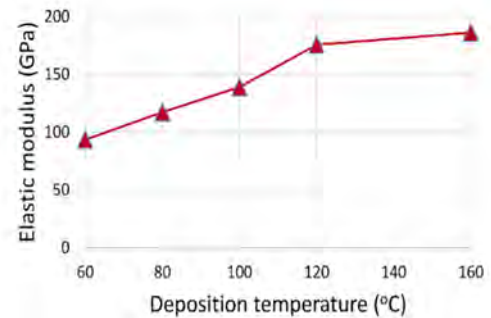
**COLLABORATIONS:** LBNL, PNNL, NREL.

### Milestones

- 1) Compare the basic elastic properties of ALD coatings (*e.g.*, Al<sub>2</sub>O<sub>3</sub>) computed from MD simulations with ReaxFF and measured by AFM and acoustic wave for method validation. (Dec. 13) **Complete**
- 2) Predict the interface strength of given coatings on Si substrate from QM calculations and compare with nanoindentation and scratch tests. (Mar. 14) **Completed calculations, experiments to be completed in Sep. 14.**
- 3) Develop a continuum frame work to model SEI deformation and stability on Si film and compare with *in situ* MOSS measurement. (Jun. 14) **Ongoing – delayed to Sep. 14.**
- 4) Go/No-Go: Stop hard coating core-shell structure design. Criteria: If no mechanically stabled coating can be identified after searching in ALD coating property design space using the continuum model. (Sep. 14) **Ongoing**

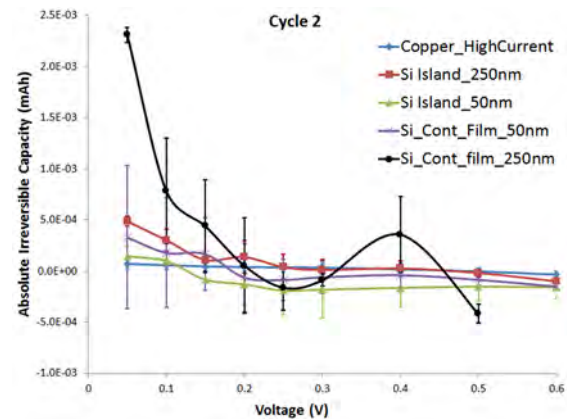
## Progress Report

1) **Tailor the mechanical properties of artificial SEI coatings** *via* changing the atomic layer deposition temperature. Different temperatures (60 to 180°C) were used for ALD deposition and the moduli were measured. The figure to the right shows increasing deposition temperature tends to form denser ALD films, thus increasing the elastic modulus.

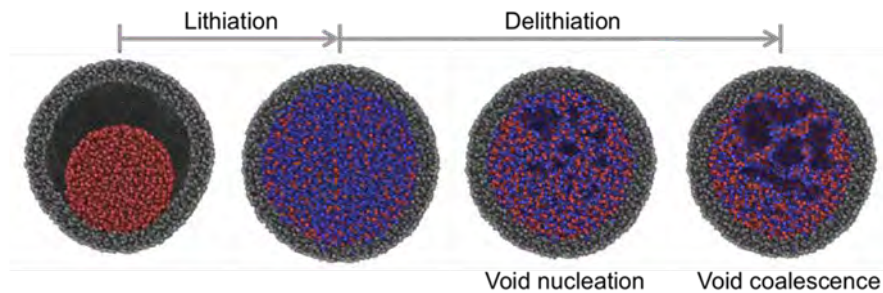


2) **Compare Li transport in SEI components** *via* DFT calculations. Lithium diffusion carriers are Schottky pairs in LiF and Li-ion interstitials in  $\text{Li}_2\text{CO}_3$  on Si electrodes. Lithium conductivity is much lower (18 orders magnitude) in LiF compared to  $\text{Li}_2\text{CO}_3$ . Lithium diffusion is faster in both  $\text{SiO}_2$  and  $\text{Li}_4\text{SiO}_4$ . Even though Li can diffuse more easily in  $\text{LiAlO}_2$  (0.587eV) than  $\text{Al}_2\text{O}_3$  (1.02eV), the diffusion barrier is still higher than those in  $\text{SiO}_2$  (0.16eV) and  $\text{Li}_4\text{SiO}_2$  (0.22eV).

3) **Reveal SEI failure mechanism** by correlating the irreversible capacity loss with expansion strain in the underlying Si. It was observed that thicker islands exhibit a lot of in-plane expansion and contraction compared to thin islands which can be used to study the SEI stability. The figure to the right shows preliminary data on irreversible capacity loss for various model samples. It can be clearly seen that thick islands (25  $\mu\text{m}$  x 25  $\mu\text{m}$  x 250 nm) show a higher irreversible capacity compared to thin islands (25  $\mu\text{m}$  x 25  $\mu\text{m}$  x 50 nm). Along with these results, *in situ* MOSS measurements have also been planned to gauge the strain to stress ratio to estimate mechanical properties of the SEI layer.



4) Molecular dynamics simulations rely on ReaxFF for a proper description of bond-making and bond-breaking reactions. Currently, Li-Si, Li-Si-O, Li-Al-O have been developed separately. Preliminary MD simulations were performed to investigate the failure mechanism in the yolk-shell structure. This study suggests that the fracture of the Li-Si system during delithiation is governed by nanoscale void nucleation and coalescence, instead of interfacial delamination between Si core and shell, as shown below.



## Predicting Microstructure and Performance for Optimal Cell Fabrication

**PROJECT OBJECTIVE:** This work uses microstructural modeling coupled with extensive experimental validation and diagnostics to understand and optimize fabrication processes for composite particle-based electrodes. The first main outcome will be revolutionary methods to assess electronic and ionic conductivities of porous electrodes attached to current collectors, including heterogeneities and anisotropic effects. The second main outcome is a particle-dynamics model parameterized with fundamental physical properties that can predict electrode morphology and transport pathways resulting from particular fabrication steps. These two outcomes will enable the third, which is an understanding of the effects of processing conditions on microscopic and macroscopic properties of electrodes.

**PROJECT IMPACT:** This work will result in new diagnostic tools for rapidly and conveniently interrogating electronic and ionic pathways in porous electrodes. A new mesoscale 3D microstructure prediction model, validated by experimental structures and electrode-performance metrics, will be developed. The model will enable virtual exploration of process improvements that currently can only be explored empirically.

**OUT-YEAR GOALS:** This project was initiated April 2013 and concludes March 2017. Goals by fiscal year are as follows.

1. Fabricate first-generation micro-four-line probe and complete associated computer model.
2. Assess conductivity variability in electrodes; characterize microstructures of multiple electrodes.
3. Fabricate four-line ionic conductivity probe; complete first-gen dynamic particle packing (DPP) model.
4. Fabricate N-line probe for anisotropic film conductivity; validate DPP model; assess effect of processing variables.
5. Use conductivity predictions in full electrochemical model; evaluate effect of innovative processing conditions.

**COLLABORATIONS:** Karen Thomas-Alyea of A123 and Andrew Jansen of ANL both provided battery materials. Transfer of our technology to A123 to improve their electrode production process is in process. A modeling collaboration with Simon Thiele of University of Freiburg was continued.

### Milestones

- 1) Measure variability and average electronic conductivity for five candidate electrode compositions using four-line probe. (Dec. 13) **Complete**
- 2) Measure microstructure of three candidate electrodes using SEM/FIB. (Mar. 14) **Complete**
- 3) Determine appropriate set of descriptors or metrics that effectively characterize previously observed microstructures. (Jun. 14) **Complete**
- 4) Go/No-Go: Discontinue current four-line probe geometry. Criteria: If measurement variability is not significantly less than sample-to-sample variability. (Sep. 14) **Ongoing**

## Progress Report

**Completion of Milestone 3.** Metrics capable of describing relevant information from the electrode structure were developed. This will allow for validation of the fabrication microstructure model that is under development (part of milestones for FY 2015) by comparing model results to experimental structures. To date, cathodes containing Toda 523 and Toda 5050 active materials have been examined by means of these metrics.

An image processing algorithm is used to segment the images (obtained from FIB/SEM sequential cross-sections of real composite electrodes) into three phases: active material, nonporous carbon/binder domains, and macroscopic pores. These segmented images can then be analyzed. Figure 1 shows representative 2D segmented structures created from this algorithm. Table 1 lists the primary metrics that are computed from the segmented images and also lists the key structural features associated with those metrics. Table 2 gives example values for two cathode samples. When these values are compared between the two samples, they allow one to discriminate the structures on the basis of the key metrics.

**Table 1.** Metrics selected to analyze the electrode structure.

Metric	Purpose
Volume fraction	Provide abundance of each phase
Voxel contact probability	Describe short-range arrangement of adjacent phases including surface area
Fourier spectrum	Provide the long-range periodicity and size of domains
Ionic and electronic conductivities	Provide the long-range connectivity of phases and gauge electrochemical performance

**Table 2.** Volume and surface fraction for two sample cathodes.

Sample 523		Sample 5050	
Volume Fraction:		Volume Fraction:	
Active	52.7%	Active	84.2%
Carbon	35.7%	Carbon	11.1%
Pore	11.6%	Pore	4.7%
Surface Area Fraction:		Surface Area Fraction:	
Active	26.1%	Active	40.3%
Carbon	40.2%	Carbon	89.8%
Pore	57.6%	Pore	92.8%

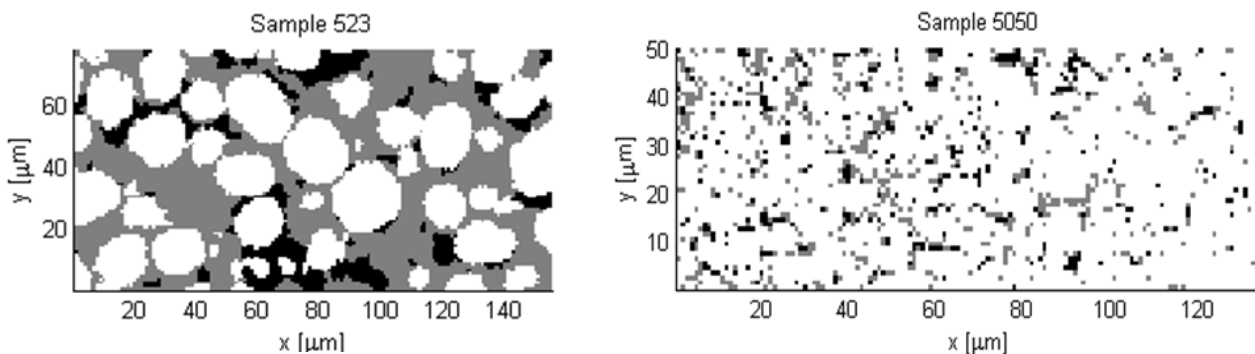


**Figure 1.** (a) Segmented FIB/SEM image of Toda 523 NMC cathode (size: 77.5  $\mu\text{m}$  x 39  $\mu\text{m}$ ); (b) Segmented FIB/SEM image of Toda 5050 NMC cathode (size: 69.5  $\mu\text{m}$  x 25.0  $\mu\text{m}$ ). White shows active material, gray shows nanoporous carbon/binder domains, and black shows macro-size pores. Sample 5050 shows smaller nonspherical active particles that occupy more of the volume than for Sample 523.